Impact of voltage waveform quality on distribution network planning

C Lombard

 orcid.org 0000-0002-8843-6778

Dissertation submitted in fulfilment of the requirements for the degree *Master of Engineering in Electrical and Electronic Engineering* at the North-West University

Supervisor: Prof APJ Rens

Graduation May 2018

Student number: 21157014

For Liandri – without you, these pages would be empty.

ABSTRACT

The present study investigated the power losses in a specific portion of the MV distribution network in Potchefstroom, South Africa. This was done in an attempt to assess and predict the impact of harmonic distortion on distribution network planning. In addition, the newly developed concept of prevailing harmonic current phase angles was used to determine the impact of distributed generation (DG) on distribution networks. With the current drive towards alternative energy sources DG will play a major role in the planning of future distribution networks.

Potchefstroom local authorities gave permission for power quality recorders to be installed on their active network. The area isolated for this study traces the power along one feeder from the distribution substation, Gamma, up to the end-user, North-West University. This feeder supplies a load mix of small businesses, housing and classrooms. Applying mathematical models, derived from literature, to collect data allowed for the calculation of the impact of harmonic distortion on distribution network power losses.

For the DG analysis, data was collected at three different sites before and after the installation of a solar PV system. This data was used to calculate the prevailing harmonic current phasors for the fundamental, third, fifth and seventh harmonic. Calcaulations were done for pre-installation, PV only and post-installation scenarios to allow for thorough evaluation and estimation of results.

The main study allowed for the development of a quick reference guide for the impact of harmonic distoriton in distribution networks. This guide can be used by city electrical engineers when planning future distribution networks. Using the phase angle study as a basis, future research would allow for a similar tool to be developed in order to estimate the impact of DG on the harmonic distortion in distribution networks.

Keywords: *Power quality, harmonics, distributed generation, prevailing harmonic phase angles, network planning*

Table of contents

LIST OF FIGURES

LIST OF TABLES

ABBREVIATIONS

AC	Alternating current
CEER	Council of European Energy Regulators
DC	Direct current
DG	Distributed generation
DSM	Demand-side management
EHV	Extra-high voltage
HV	High voltage
IEC	International Electrotechnical Commission
IEEE	Institute of Electrical and Electronic Engineers
IPPs	Independent power producers
LPU	Large power users
LV	Low voltage
MV	Medium voltage
NERSA	National Energy Regulator
NRS	National Rationalized Standard
PAR	Prevailing angle ratio
PCC	Point of common coupling
PF	Power factor
PQ	Power quality
PV	Photovoltaic
QoS	Quality of supply
R^2	Coefficient of determination
rms	Root mean square
TDD	Total demand distortion
THD	Total harmonic distortion
THDF	Transformer harmonic de-rating factor
TRF	Transformer

CHAPTER 1: INTRODUCTION

The first chapter provides an overview of power quality and the rationale behind selecting the field of study. The main focus of the present study is defined in the problem statement, which flows into secondary research objectives and a definition of the scope of the study. A summary of the research methodology is provided, followed by the limitations of the present research. This chapter concludes with a discussion of the document structure.

1.1 Background

The National Energy Regulator of South Africa (NERSA) published a directive on power quality (PQ) in 2002 [4], in order to provide guidelines for the regulation of PQ in South Africa. The South African electrical network is expanding rapidly and will reach a total capacity of 80 000 MW in 2026. This raises the question: How effectively is all this power managed through the distribution channels and what capacity reaches the end-user? Considering the sporadic implementation of load shedding since 2008, the matter of network efficiency becomes even more acute. According to Fin24 [1] South Africa experienced 99 days of load shedding in 2015. This number could potentially have been less if the electrical networks were operating at maximum efficiency. PQ is often overlooked as a factor contributing to network efficiency. Medium-voltage (MV) distribution networks form the heart of the South African power grid. Therefore, these networks will be the focus of this study. Every unit of energy sold to end-users flows through MV distribution networks. For the purpose of the present study, MV refers to a voltage level between 1 kV and 44 kV [2] (in South Africa 11 kV is the most commonly used distribution voltage).

A survey done by Magnet Communication [3] indicated that 24% of South Africa's professional engineers are employed in the electrical engineering sector. This sector is divided further into specialist fields such as quality of supply, protection and several others. NERSA launched the national PQ directive in 2002 [4] with the goal to introduce regulatory requirements into the South African power system environment. The PQ directive is based on a report by the Council of European Energy Regulators (CEER) on PQ regulation in Europe. The directive stipulates that the PQ delivered by the licensed reseller should meet the expectations of the customer. However, the potential of PQ to improve energy efficiency is still relatively unknown.

In 2005, the Department of Minerals and Energy published the Energy Efficiency (EE) Strategy of the Republic of South Africa [5]. This document confirms that the South African government recognises the fact that energy efficiency is one of the most cost-effective ways to meet the demands of sustainable development. As a result, the South African national electricity utility,

Eskom, has embarked on a demand-side management (DSM) program to reduce the need for additional generation capacity.

South Africa has a unique power-system environment in which Eskom functions as the largest power supplier and sole owner of the entire transmission network. Since 1994, the South African electrical network infrastructure has been expanding rapidly. The aim was to supply power to previously disadvantaged communities and to cater for continuous economic growth. According to Eskom [6], two coal-fired power plants are under construction as well as one pumped storage facility. These projects form part of Eskom's new build programme that commenced in 2005 in order to increase Eskom's generation capacity to 52 589 MW by 2021. Since the start of the program, 7 000 MW was added to the grid, which increased the current generation capacity to 44 087 MW.

This mentioned additional power, therefore, needs to be distributed throughout the country to the end-users. The power will flow from the point of generation through transmission networks to sub-transmission networks and thereafter through reticulation networks. The sub-transmission and reticulation networks are collectively termed distribution systems. In other words, every unit of electricity consumed in South Africa flows through a distribution system before it reaches the end customer. It is, therefore, paramount that the health of the country's distribution systems should not be neglected.

The PQ delivered by power plants is assumed to be of an acceptable standard. The low-voltage (LV, typically less than 1 kV) networks are connected directly to the medium-voltage (MV, typically between 1 kV and 44 kV) [2] network. As a result, their power quality depends on that which is provided by the MV network. Although the LV network may influence the power quality in the MV network, cleaning up the MV network will isolate LV networks with poor PQ. PQ pollution from the medium voltage (MV) networks can influence PQ in high-voltage (HV, typically above 44 kV) transmission networks. This further emphasises the importance of effective PQ in distribution networks.

Distribution networks in South Africa have a twofold character:

- private, large power users (LPUs) that buy directly from Eskom;
- public, owned by Eskom or local municipalities.

LPUs will have a contract with Eskom regarding, amongst other matters, the PQ that is delivered. Local municipalities are licensed by NERSA to buy and resell electricity within their boundaries. These local authorities must report to NERSA on the PQ they deliver to their customers in terms of the NRS 048 standard.

Various international studies have been conducted on power quality and energy losses:

- A study in the Netherlands on the losses in cables and transformers (both distribution system components), [7] examined losses due to harmonics, unbalance and the power factor in a single-load power system. The research found a relationship between PQ and energy losses in the power system. However, the study did not consider the losses in a power system that have multiple feeders and loads.
- A similar study in Brazil [8] confirmed significant losses in cables and transformers that should be compensated for depending on financial feasability. A further study in the Netherlands, investigated the possibility to increase energy efficiency by improving PQ [9]. The mentioned study did not only focus on harmonics, unbalance and power factor, but also on the impact that voltage regulation holds. The research furthermore [9] found a relation between efficient usage of energy and certain PQ phenomena.
- A study in Estonia [10] investigated the relation between the quality of supply voltage, and the consumption and losses of power. These researchers found that losses of and demand for power in consumer networks are affected by characteristics of power consumption and supply-voltage quality.

In a study on the costs due to poor quality [11] it was found that there is insufficient focus on the financial aspects of PQ. Both the financial and technical aspects should be considered when attempting to solve problems of power quality.

Recent research [12] by a team at the Technische Universitaet Dresden, Germany showed that 'prevailing' harmonic phase angles can be used to characterise the harmonic emissions of electronic equipment. These include light bulbs, solar photovoltaic (PV) inverters and electric vehicle chargers. In certain cases, it is possible to define this harmonic characterisation as prevailing phasors, which potentially can be used to estimate the influence equipment exerts on an electrical network.

1.2 Problem statement

No formal study could be found on the electrical losses that can be attributed to poor PQ, specifically on MV distribution networks in South Africa. Thus, it is important to conduct a study to calculate the losses in a MV distribution network due to harmonic distortion, and to assess the potential impact of these losses on distribution network planning. Furthermore, no formal study

was done to assess the potential impact the installation of distributed generation (DG) may have on the harmonic levels within a distribution network.

The primary problem statement for the present study can be defined as follows: *How much do harmonics influence the losses in a MV distribution system?*

Two secondary statements can be formulated to support the primary problem statement:

a. What is the potential impact of these losses on planning a distribution network?
b. Can the introduction of renewable DG influence the harmonic levels in a distribution network, and can this impact be estimated?

1.3 Research objectives

The following objectives are defined in order to answer the questions implied by the problem statement.

1.3.1 Primary objective

The main purpose of the research will be to record, calculate and estimate the losses in a typical South African distribution system, which occurs due to distortion in both the current and voltage waveforms. The study will include cases where voltage THD is not compliant to the NRS 048 requirement.

1.3.2 Secondary objectives

Derived from the primary objective, the secondary objectives for the research were:

a. Establish a method to estimate the impact of losses within a distribution network on planning a distribution network.

b. Determine whether “prevailing” harmonic-phase angles makes it possible to estimate the impact of renewable DG on the voltage THD levels in a distribution network.

1.3.3 Basic hypothesis

The presence of harmonic distortion causes losses in a distribution network, particularly losses of capacity. If these deficiencies are not taken into consideration, they will have a negative influence on the planning of a distribution network. It should, therefore, be possible to generate a quick reference tool that could estimate the impact of harmonics when planning such a network.

It should also be possible to assess the potential impact of DG on a distribution network by application of the “prevailing” phasors concept.

1.4 Research methodology

The research methodology was structured as follows:

- Literature review: Provides an overview of the current literature on the research topic.
- Research design: Describes how the practical research was conducted as well as the process of verification and validation.
- Data analysis: Undertaking a detailed analysis of the field data, including calculations of the losses.
- Planning tool: Using the collected data and established relationships during the data-analysis phase, a network planning tool was developed.

1.5 Restrictions of the study

Even though the present research provides new understanding in the research field, the study still has to factor in certain limitations. The results aim to present a pragmatic approach to consulting engineers when planning for network capacity where non-sinusoidal voltages and currents are expected. Restrictions are:

a. The study is based on a dynamic network in an uncontrolled environment.
b. The study examines the MV network in isolation and does not include the possible influence of either the LV or HV network.

1.6 Dissertation structure

The dissertation document is divided into the following six chapters:

- **Chapter 1: Introduction**
  This chapter provides the background on the research topic and explains the research objective.
- **Chapter 2: Literature review**
  The literature review aims to describe the current progress on the research topic and identify potential shortcomings within the current body of knowledge.
- **Chapter 3: Research design**
  In the research design, the scope of the study is defined along with the processes used in the following chapter to analyse the data. The validation and verification process is also described in this chapter.

- **Chapter 4: Distribution network analysis**
  Building on the research design and using the methods described in the previous chapter, the various parameters are calculated and compared as proposed in chapter 3.
- **Chapter 5: Phase-angle analysis**
  In this chapter, using the method described in Chapter 3, the data of the phase angle is analysed according to the availability of valid prevailing phasors.
- **Chapter 6: Network-planning tool**
  Using the results from Chapter 4, a new network planning tool is developed and explained with a practical example.
- **Chapter 7: Conclusions and recommendations**
  In this chapter, the success of the research is discussed regarding answers to the problem statement and proving or disproving the hypothesis in Chapter 1. In addition, recommendations are made to improve on the shortcomings identified during the research process.

1.7 Summary

This chapter presented a well-defined problem statement and documented restrictions to the study. The chapter concluded by providing the research structure. This lays the foundation for the literature review in chapter 2.

CHAPTER 2: LITERATURE REVIEW

The literature review analyses PQ concepts, parameters and the applicable technical standards, particularly within the South African power-system regulatory environment.

Energy losses occur not only at the fundamental frequency as harmonic voltages and currents increase the apparent power loading of a power system. In order to define energy losses under non-sinusoidal voltage and current waveform conditions, asymmetry between phase voltages and unbalance in loading, the IEEE 1459-2010 [13] approach to power definitions is presented.

The impact of PQ on distribution network planning is then derived and analysed.

2.1 Sources of harmonics in power systems

DG that injects energy by means of solid-state electronics (grid-connected inverters) will not only inject currents at the fundamental frequency, but also at harmonic frequencies due to the non-linear principle of operation. It is expected that DG will mostly be from renewable energy (RE) sources with a major portion of this, variable renewable energy (VRE).

Wind and photo-voltaic (PV) energy sources are examples of VRE as both are variable in principle and connect to the electrical grid by means of a grid-connected inverter.

Other known sources of harmonics in distribution systems are voltage harmonics resulting from energy-efficient appliances at LV level (solid-state lighting and variable speed drives for example). These harmonics are transferred over the windings of a MV/LV transformers and could be amplified at MV level due to a resonant condition between the system inductance and a capacitor bank installation.

2.2 An introduction to power quality

PQ has enjoyed increasing popularity ever since the late 1980s and is a concept that covers a broad scope of power system disturbances. In engineering terms, electrical power is described as the rate at which energy is delivered and it is proportional to the product of voltage and current. The *Handbook for Electrical Engineers* [14] states that PQ can be viewed as the compatibility between the quality of the voltage supplied by the utility, and the operation of end-use equipment.

The NRS 048 [15] standard on minimum levels in PQ elaborates that PQ entails a specific group of electromagnetic compatibility levels that are used to set minimum standards. These

compatibility levels should be chosen in such a way that the equipment connected to the electrical network has a high probability of operating correctly.

The concept of compatibility is visualised in Figure 2-1 below. This depiction is derived from the NRS 048 [15] on the basis of voltage harmonics that display a normal distribution. Throughout the literature, the terms PQ and quality of supply (QoS) are used interchangeably.

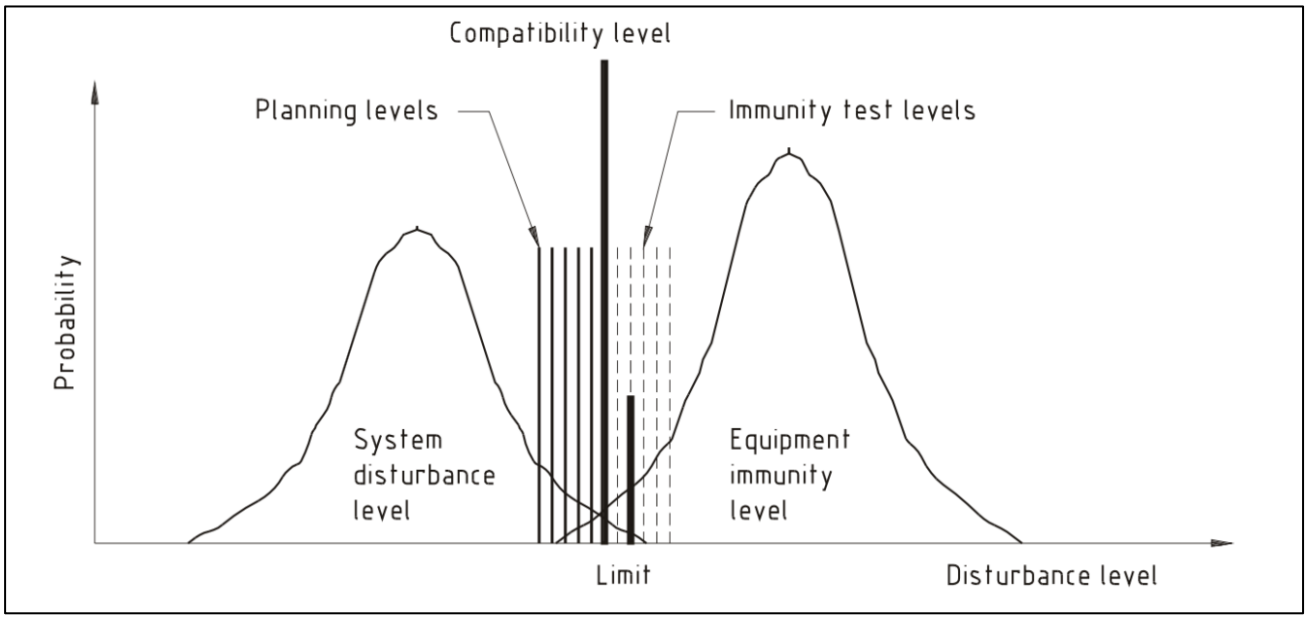

Figure 2-1: PQ compatibility level [14]

The scope of PQ can be divided into two main categories: steady-state PQ and PQ waveform events (or waveform disturbances). Steady-state PQ is qualified by regulating voltage magnitude, voltage total harmonic distortion, voltage asymmetry (also termed voltage unbalance), frequency and voltage flicker. Compatibility levels are defined in terms of steady-state characteristics with additional limit values for voltage magnitude and frequency.

Voltage waveform events (disturbances) are a different challenge as viewed from the perspective of the utility. The utility has no control over, for example, lightning induced short-circuit currents flowing and causing large enough voltage drops over network impedances to be recorded as a voltage sag (or dip) condition. This can occur at even more than one location in the power system. Voltage sags are managed by benchmarking the dip performance of a network against a norm, for example, the characteristic dip numbers as published in the NRS 048 part 2 document (latest version NRS 048 part 2 of 2015) [15].

In *Electrical Power Systems Quality* [16] Santoso et al. state that electric utilities, resellers and end customers are becoming increasingly concerned about the quality of electric power. Each of

these stakeholders has different requirements for PQ. The customer wants to buy the best product for maximum profitability, while for the utility and reseller PQ plays a major role in customers' satisfaction.

There are several reasons for the increasing concern about PQ among stakeholders :

a. The increased use of microprocessor-based electronic devices are far more sensitive to the quality of supplied power than the older technologies [16].
b. The average harmonic distortion levels from the power system are increasing. This is due to the constant drive towards energy efficiency, which is often achieved by using power electronics. Most of the new generation energy-efficient technologies contribute to the harmonic distortion levels of the power system [16].
c. Customers are becoming more aware of PQ issues and are challenging the utilities to improve the QoS [16].
d. Power systems are much more interconnected than before, between cities and even countries. Therefore, the failure of one component can cause a significant ripple-effect throughout the whole power system [16].
e. The increasing numbers of DG plants that are being installed throughout the power system also play a role. This takes place from transmission level in the form of independent power producers (IPPs) to smale scale solar PV on residential LV networks. In this regard, the South African Department of Energy [18] aims to install 3 725 MW of renewable energy by 2016, 3 200 MW by 2021, and 6 300 MW by 2025, down to LV distribution level with residential homeowners installing rooftop photovoltaic (PV) systems. According to a Solar PV Industry Report [19], by November 2016, there was an estimated 280 MW of privately owned PV capacity, excluding IPPs, in South Africa.

Power quality is ultimately a consumer-driven issue, and the end-user's point of reference takes precedence. A common PQ problem in distribution networks and industrial factories is harmonic distortion [17], particularly that of a current. A major source of harmonic distortion is nonlinear loads, which have been increasing in recent years.

There are numerous existing solutions for the various PQ problems. The issues range from a simple solution such as balancing the loads on a transformer, to costlier and more complex mitigation such as installing active harmonic filters. However, the economics should clearly be considered when attempting to solve PQ problems. In certain instances, it is simpler and more cost-effective to desensitise the equipment to the existing PQ issues, rather than attempting to correct the PQ.

2.3 Power quality in South Africa

In South Africa, it is the role of NERSA to regulate the energy landscape, which includes electrical energy. The goal is to protect both the customer and the utility with regard to the price and quality of the delivered product. In this regard, NERSA published a PQ directive in March 2002 [4] to help establish a PQ management system in the country. From this document, it is possible to describe the PQ management framework that is currently implemented in South Africa.

2.3.1 PQ management framework

The framework is based on the two most important PQ categories, namely steady state and disturbances, each with its own unique management strategy:

- ***Steady-state PQ:*** Network operators need to plan according to the compatibility and planning levels set by the NRS 048 standard [15].
- ***PQ disturbances:*** The position of the customer in relation to the distribution network and exposure to the weather is important in this regard. It determines the potential number and severity of PQ disturbances that the customer may experience. Disturbances should be managed on a case-by-case basis and acknowledge the potential limitations due to the network configuration.

Within the mentioned PQ management framework, the various stakeholders have certain responsibilities in order for the system to be successful. The relationship between the various stakeholders as well as examples of typical stakeholders in a South African context are illustrated in Figure 2-2 below. Other configurations are possible, such as large companies as customers that are supplied directly by Eskom, however these examples fall outside the scope of the present study.

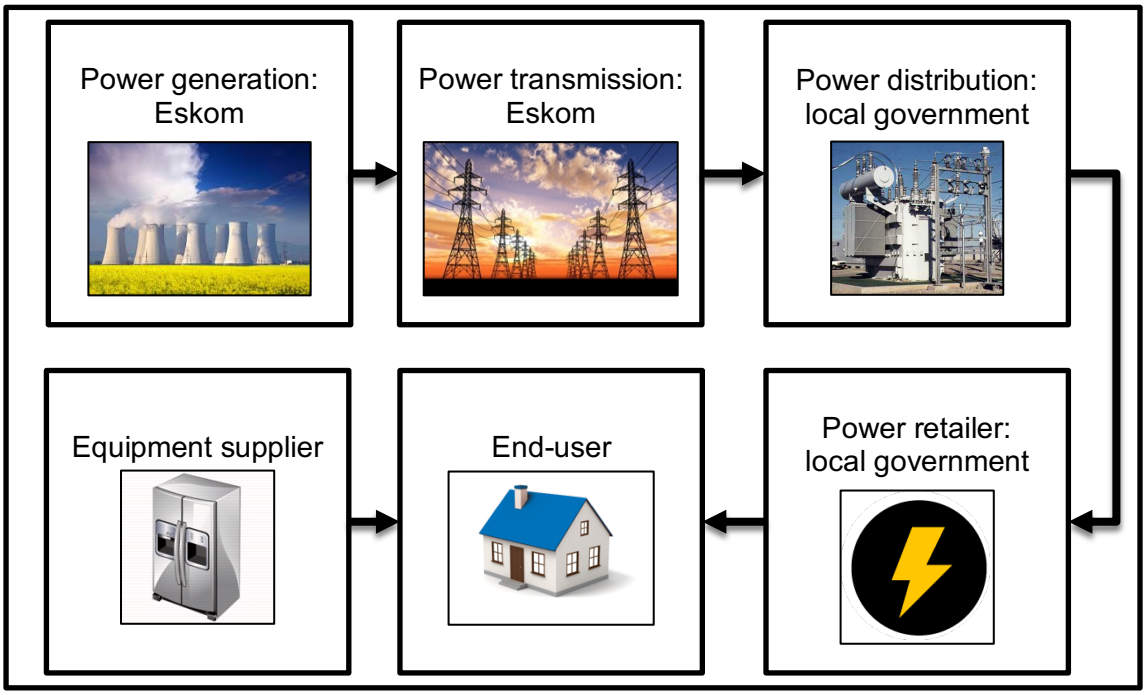

Figure 2-2: Power-system stakeholders

2.3.2 Responsibilities of the transmission service provider

The transmission service provider refers to the owner of the national transmission network and operator of the national power system, which is Eskom. Eskom is responsible for the quality of power delivered to all its customers. In most instances, these are municipalities or large industrial sites, both of which operate their own distribution networks.

2.3.3 Responsibilities of the distribution company

The distribution utility is responsible for the PQ in the distribution system. Thus, these companies are required to manage the PQ received from the transmission service provider as well as DG installed in the distribution network. The distribution company is also responsible for managing network incidents and quality degradation by customers that are connected to the network.

2.3.4 Responsibilities of the retailer

In South Africa, the distribution company is usually also the retailer. The retailer has an obligation towards the customer regarding QoS as well as to avoid impacting the PQ of the distribution company negatively.

2.3.5 Consumer rights

The selling and purchasing of electrical energy can be classified as the sale of consumer goods and products. Therefore, this process is regulated by the Consumer Protection Act, no 68 of 2008 [20], which was signed into law on 24 April 2009. The Act aims to support a fair market for consumer goods and products such as electrical energy. This is achieved by establishing national standards to protect the customer and simultaneously promote responsible consumer behaviour.

According to the Act, a consumer is defined as any person to whom goods or services are marketed, who have entered into transactions with suppliers, or are users of specific goods or services.

The right to fair value, good quality and safety, is highly relevant to the sale of electrical energy and specifically PQ. This right implies that the producer, distributor and retailer warrant the compliance of the goods with the requirements of safety and high quality. This applies to any transaction or agreement in South Africa involving the supplying of goods to a consumer.

The above-mentioned right is supported by the requirements from a NERSA electricity distribution license, as documented in the Electricity Regulation Act 4, 2006 [21]. In the Act, it is stated specifically that licensees (i.e., operators of distribution networks) should comply with all directives that govern relations between a licensee and its end-users in accordance with the NER PQ directive. It is also stated that the quality of electrical energy, supply and service, should comply with national standards such as NRS 048 [15].

2.3.6 Responsibilities of the consumer

It is the responsibility of the consumer to ensure that all electrical and electronic devices connected to the electrical network comply with the relevant national standards for safety and compatibility. There is a possibility that the consumer can cause pollution in the electrical network. Therefore, the consumer is responsible for managing the emissions of electrical pollution according to the emission levels agreed on with the network operator.

2.3.7 Responsibilities of the equipment supplier

All electrical and electronic equipment suppliers must be able to provide data of technical performance regarding the PQ characteristics of their equipment. This data should be sufficient for the customer to evaluate whether the equipment is suitable for the conditions of their local electrical network.

2.4 Types of power quality problems

Numerous types of PQ problems are found in power systems throughout the world with definitions and terminologies depending on the region. Therefore, the present study defines and discusses types of PQ problems based on NRS 048 as the accepted standard for South Africa.

The NRS 048 has been developed specifically for South Africa and is based on standards drawn up by the Institute of Electrical and Electronic Engineers (IEEE) and IEC in Europe. These standards are relevant since the IEEE is the leading international professional organisation for electrical engineers. Furthermore, the IEC aims to improve international trade by ensuring compatibility between equipment and the power system.

The latest official release of the NRS 048 is: NRS 048-2:2007 Edition 3.1: Electrical Supply – Quality of Supply Part 2: Voltage Characteristics, Compatibility Levels, Limits and Assessment Methods [15]. This latest edition is aligned with NERSA's PQ directive and is used widely throughout Southern Africa by power system stakeholders.

Work on a fourth edition is already in an advanced stage since the third edition was withdrawn on 18 August 2016 [22]. This revised edition will include new developments in SANS 1816 (Electricity Supply – Quality of Supply: Power Quality Monitoring Instruments Specification) [23] and SANS 61000-4-30 (Electromagnetic Compatibility – Testing and Measurement Techniques – Power Quality Measurement Methods) [24]. Based on Cigre TB261 of 2004 [25], compatibility levels have been introduced for HV and extra-high voltage (EHV) applications. This new edition also aligns with the latest revision of NRS 048-4 (Application Guidelines for Utilities) [26], which addresses the selection and use of planning levels. As a result, indicative planning levels have been removed from NRS 048-2 [27]. An official release of this revised edition of NRS 048 is imminent.

2.4.1 Power quality recording

PQ parameters and events can be recorded by various instruments that are available on the market. Historically instruments were classified as Class A (investigation) or Class B (statistical). In the latest release of IEC 61000-4-30 Ed 3 [28], these parameters have been revised to Class A (advanced), Class S (surveys) and Class B (information). In the South African context, in terms of SANS 1816 [23], the classifications were updated to Class I (investigation) and Class M (monitoring) with Class B being declared obsolete.

2.4.2 Steady-state PQ

2.4.2.1 Frequency variations

The power system frequency is one of the most important parameters to consider when assessing a power system's operational characteristics. In South Africa, the primary responsibility for the system frequency lies with Eskom as the main generator and operator of the transmission network [29]. In South Africa, the standard system frequency is 50 Hz.

2.4.2.2 Voltage unbalance

In three-phase systems, voltage unbalance is experienced when voltages indicate unequal magnitudes [30]. The system is viewed as unsymmetrical when the displacement between the three-phase voltages does not reach 120°. Achieving a perfectly balanced and symmetrical three-phase system is unattainable. This is due to the unbalanced connection of single-phase loads and differing self- and mutual impedances of components within the power system.

Voltage unbalance is commonly calculated by using the symmetrical component method. In this approach, a three-phase unsymmetrical phasor system is replaced by the sum of the positive, negative, and zero sequence symmetrical [30]. The voltages of the respective phase can thus be calculated as follows:

$$\underline{U_A} = \underline{U_{1A}} + \underline{U_{2A}} + \underline{U_{0A}} \tag{2-1}$$

$$\underline{U_B} = \underline{U_{1B}} + \underline{U_{2B}} + \underline{U_{0B}} = a^2\underline{U_{1A}} + a\underline{U_{2A}} + \underline{U_{0A}}. \tag{2-2}$$

$$\underline{U_C} = \underline{U_{1C}} + \underline{U_{2C}} + \underline{U_{0C}} = a\underline{U_{1A}} + a^2\underline{U_{2A}} + \underline{U_{0A}} \tag{2-3}$$

where *a* is the rotational operator defined by:

$$a = e^{j\frac{2}{3}\pi} = -\frac{1}{2} + j\frac{\sqrt{3}}{2} \tag{2-4}$$

The relationship between the unsymmetrical phasor set and the sum of the symmetrical phasors are presented in Figure 2-3 taken from [30].

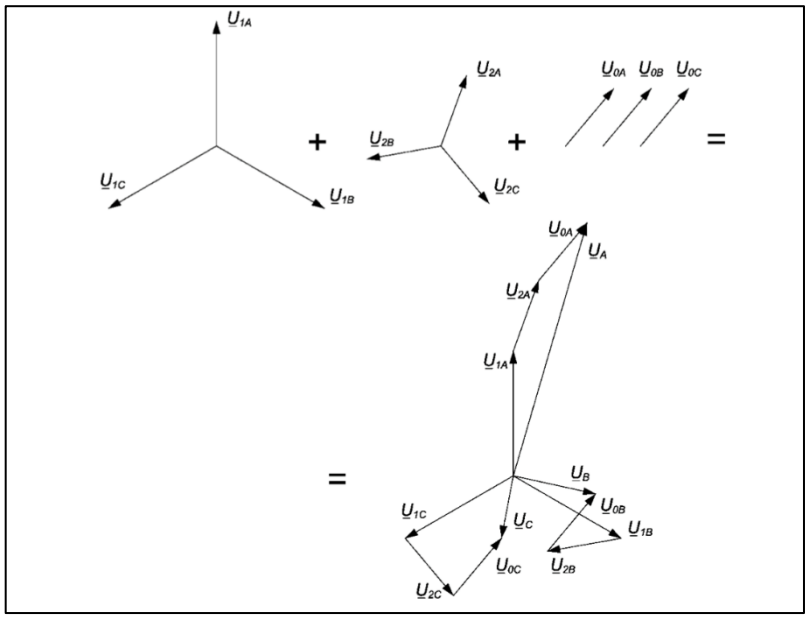

Figure 2-3: Unsymmetrical phasor sum and its symmetrical components [30]

According to NRS 048 [15], the negative sequence components are used to calculate the voltage unbalance. Thus, the unbalance K-factor regarding negative-sequence components can be calculated by using:

$$K_{2U} = \frac{U_{2(1)}}{U_{1(1)}}.100\% = \left[\frac{(\underline{U_A}+a^2\underline{U_B}+a\underline{U_C})}{\underline{U_A}+a\underline{U_B}+a^2\underline{U_C}}\right].100\% \quad (2\text{-}5)$$

where

$$\underline{U_2} = \frac{1}{3}\left(\underline{U_A} + a^2\underline{U_B} + a\underline{U_C}\right) \quad (2\text{-}6)$$

and

$$\underline{U_1} = \frac{1}{3}\left(\underline{U_A} + a\underline{U_B} + a^2\underline{U_C}\right) \quad (2\text{-}7)$$

The most basic calculation of voltage unbalance can be described as the maximum deviation from the average of the three-phase values, divided by the average of the three-phase values, which is expressed in percentage [31]. It can be calculated in terms of the following equation:

$$U_{UB} = \frac{(U_{max}-U_{min})}{U_{avg}} \quad (2\text{-}8)$$

According to NRS 048 [15] under normal operating conditions, the unbalance compatibility of the voltage shall be 2%.

2.4.2.3 Harmonics

Harmonics is an unwanted feature in power systems. Only since the widespread use of power electronics, harmonics have been viewed as a key issue. Harmonics are produced by equipment that show a non-linear voltage or current characteristic. Harmonic distortion can be regarded as pollution within the power system that could lead to problems if certain limits are exceeded.

According to NRS 048 [15] and the Handbook of Power Quality [32], the term 'harmonic' can be described as a component of voltage or a current with a frequency that is an integer multiple of the fundamental frequency. This concept is illustrated in Figure 2-4 below, derived from the Handbook of Power Quality [32].

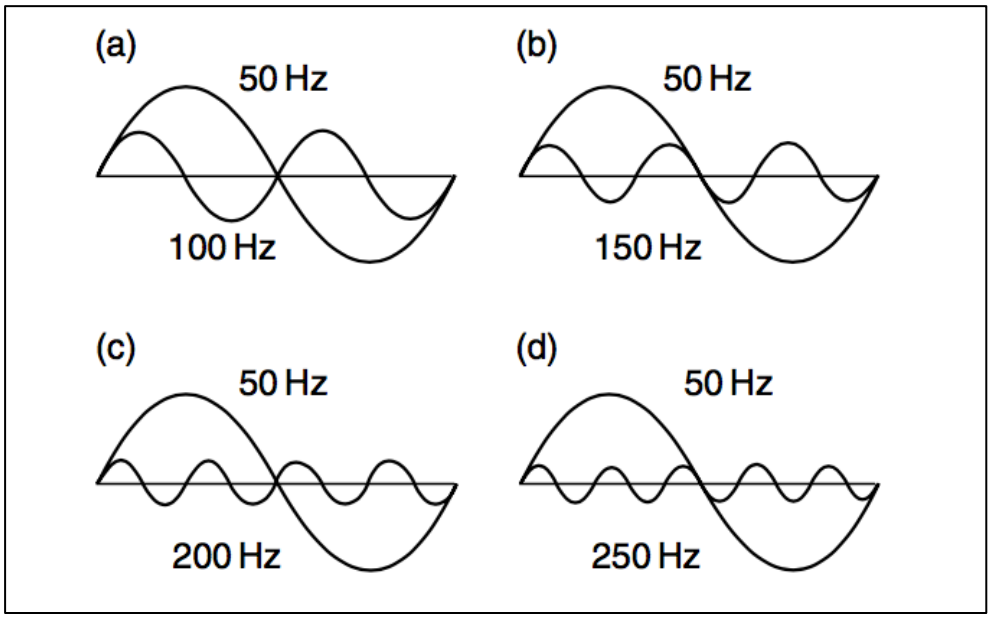

Figure 2-4: A 50 Hz waveform and its harmonics

The term 'harmonics' is often used without sufficient clarification, for example, "The induction furnace cannot operate properly because of harmonics". This statement could refer to any number of problems:

a. The voltage distortion could be so significant that the power produced by the control system, which is based on the firing angles, is below ideal conditions.
b. The harmonic currents are so extensive that certain sections of the power system such as a transformer, should be rated at a lower power to prevent damage.

Harmonic currents are caused by non-linear loads since they do not draw current in a sinusoidal wave. This is depicted in Figure 2-5 below, derived from the *Handbook of Power Quality* [32], indicating the typical current waveform of a single-phase rectifier.

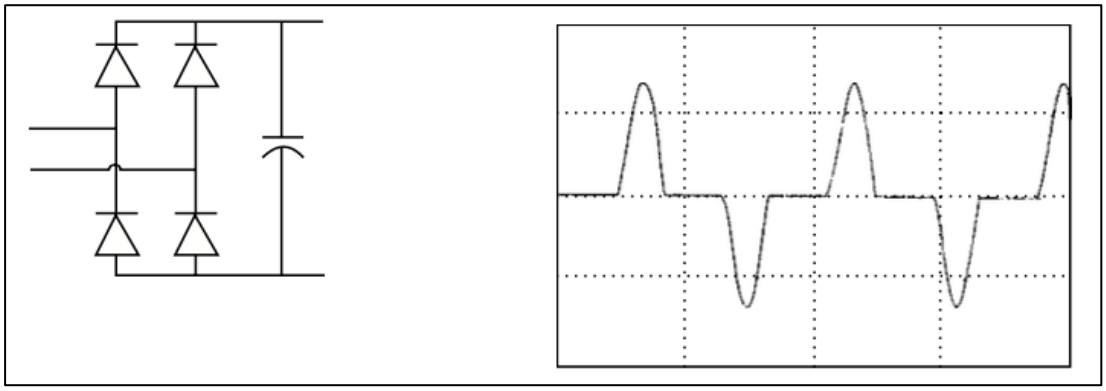

Figure 2-5: Single-phase rectifier's current [32]

Harmonic voltages are a result of the interaction between harmonic currents and the impedance of the power system, as explained by Ohm's law:

$$V = \frac{I}{Z} \quad (2\text{-}9)$$

where

V = voltage

I = current

Z = impedance

Figure 2-6 on the following page represents a sample a network, in order to explain voltage distortion. The diagram is derived from Fundamentals of Harmonics [34].

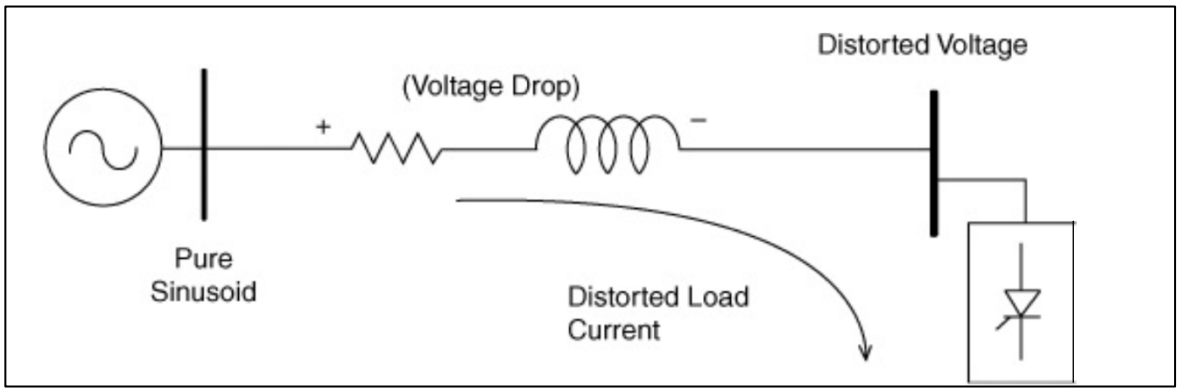

Figure 2-6: Harmonic currents causing harmonic voltages [34]

In the following example, the load is a single-phase rectifier with a non-sinusoidal current as depicted in Figure 2-7 below. The voltage source produces a perfect sinusoidal voltage waveform.

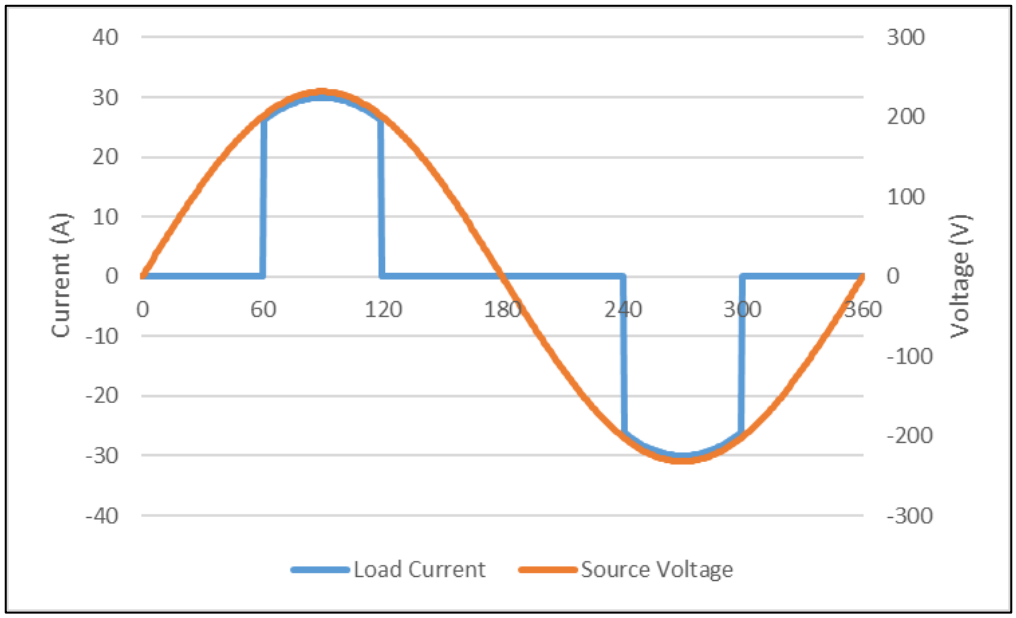

Figure 2-7: Load current and source voltage

As the non-sinusoidal current travels through the network from the load, it causes a voltage drop across the transmission line, due to the impedance of the latter. This voltage drop is a function of the current that flows through the system, based on equation 2-9. Therefore, the voltage drop across the transmission line would also be non-sinusoidal. The resulting distorted voltage is depicted in Figure 2-8 on page 19.

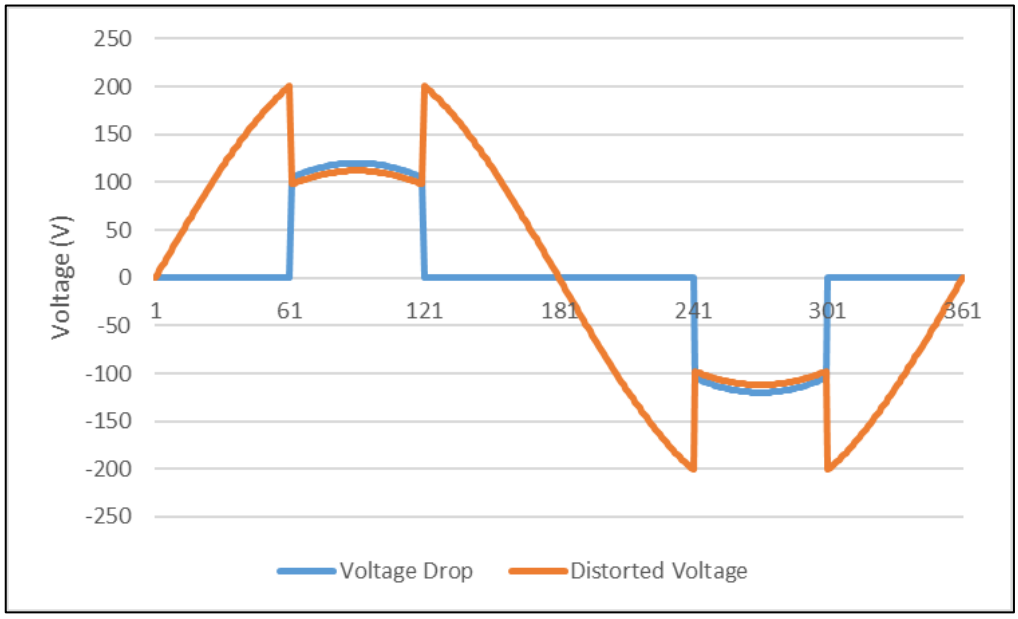

Figure 2-8: Non-sinusoidal voltage drop and resulting distorted voltage

Although the distorted current causes the voltage distortion, it exerts limited control over the voltage distortion. This is because the voltage distortion depends on the load current, system impedance, and other devices connected to the system. Therefore, identical loads in different positions in the power system will indicate different voltage distortion values. This serves as the basis for the division of responsibilities for harmonic control as documented in IEEE 519 [33]. It is assumed that a certain level of voltage distortion is acceptable. Thus, network operators and end-users must work together to keep the actual voltage distortion below the compatibility levels. By limiting the harmonic currents the users inject, the voltage distortion can be kept below objectionable levels. When attempts to limit the harmonic currents cannot maintain a low enough voltage distortion, it is the responsibility of the network operator to modify the network characteristics and bring the voltage distortion back to compliant levels.

In the United States [34], the total voltage distortion limit in the transmission system is less than 1%. However, the harmonic distortion increases closer to the load. It is common practice to neglect higher order harmonics, from 40 and higher, when analysing power systems.

A Harmonic indices

The Fundamentals of Harmonics [34] mentions two most commonly used indices to measure the content of a harmonic waveform. These indices are total harmonic distortion (THD) and total demand distortion (TDD). Both can be applied to either voltage or current.

In South Africa, PQ is evaluated from the QoS perspective. Therefore, the THD is measured at the PCC (point of common coupling) between the utility and the end-user and is considered the responsibility of the utility. The effects of voltage distortion caused by harmonic currents in the power system are evaluated by calculating the voltage THD at a specific PCC:

$$V_{THD} = \frac{\sqrt{\sum_{h=2}^{50}}}{V_1} = \sqrt{\left(\frac{V_2}{V_1}\right)^2 + \left(\frac{V_3}{V_1}\right)^2 + \cdots \left(\frac{V_N}{V_1}\right)^2} \quad (2\text{-}10)$$

where:

V_1 = rms (root mean square) fundamental voltage in volt

V_N = V_2, V_3, V_4, etc., = rms harmonic voltage values in volt

THD can be used to characterise the distortion in both current and voltage waveforms even though it is most commonly applied to the latter.

Characterising distortion levels of a current by using current THD can often be misleading. This is because THD is a relative value and a current with a small magnitude may have an extremely high THD. In this case, it does not affect the power system since the current does not have a large enough magnitude to create an impact. Certain analysts [34] have attempted to avoid this difficulty by referring THD to the fundamental of the peak demand for the load current rather than the fundamental of the current sample. This is called TDD, and is used to evaluate the current distortions caused by harmonic currents drawn by the end-user. The TDD of the current can be calculated by applying the following equation:

$$TDD = \frac{\sqrt{\sum_{h=1}^{h=\infty}(I_h)^2}}{I_L} \quad (2\text{-}11)$$

Where:

I_L = rms value of the current at maximum demand

h = harmonic order (1, 2, 3, 4, etc.)

I_h = rms current at the harmonic order of h

B Harmonic standards

The NRS 048-2 [15] states that the voltage THD in LV and MV networks may not exceed 8%. This THD should be calculated to include all harmonics up to the 40th order. In addition to THD, there are also compatibility levels for each harmonic present in LV and MV power systems. These compatibility levels are shown in Table 2-1 below, derived from NRS 048 [15].

Table 2-1: Harmonic voltage compatibility levels [15]

Odd harmonics				Even harmonics	
Not multiples of 3		Multiples of 3 (See NOTE)			
Harmonic order *h*	Magnitude %	Harmonic order *h*	Magnitude %	Harmonic order *h*	Magnitude %
5	6	3	5	2	2
7	5	9	1,5	4	1
11	3,5	15	0,5	6	0,5
13	3	21	0,3	8	0,5
$17 \leq h \leq 49$	{2,27 x (17/*h*)} – 0,27	$21 \leq h \leq 45$	0,2	$10 \leq h \leq 50$	{0,25 x (10/*h*)} + 0,25
NOTE The levels given for odd harmonics that are multiples of 3 apply to zero sequence harmonics. Also on a three-phase network without a neutral conductor or without load connected between phase and earth, the actual values of the third and ninth harmonics might be much lower than the compatibility levels, depending on the voltage unbalance of the system.					

2.4.2.4 Power factor

In the business of selling electrical energy, the main goal is to deliver active energy to the customer with the minimum amount of losses incurred along the way. Establishing electrical distribution networks requires capital investment and the investors expect to see a return on their investment. Lost energy translates into forfeited income and a reduction in the return on investment for the investor. Furthermore, these losses lead to additional heat, which causes premature ageing of the distribution system's components. Electrical supply lines are built to operate at a rated current-carrying capacity, also referred to as ampacity. When the load requires large amounts of reactive power, the line is not utilised optimally. This is because although the line may operate close to its rated ampacity, extremely limited active energy (kWh) is delivered to the customer [35].

Power factor (PF) is used as an indicator for line utilisation. This factor can be defined as the ratio of active power to the apparent power transmitted through the line. PF can also be calculated as the phase difference between the voltage and current, and is represented by the cosine of the phase shift angle (also known as the power-factor angle).

$$\mathrm{P}F = \frac{P}{S} = cos\theta \qquad (2\text{-}12)$$

where

P = active power measured in watt

S = apparent power measured in VA

PF can either be leading, i.e. the current leading the voltage, or lagging, i.e. the current lagging the voltage. A *lagging* PF is the result of inductive loads that "absorbs" reactive power, whereas a *leading* PF is the result of a capacitive load that "supplies" reactive power. With only resistive load connected to the system, the PF would be one (also known as unity PF). When the power system is operating at unity PF, the line loss for a given total active power is at a minimum. However, this is rarely the case since both inductive and capacitive loads are present throughout the network. By using the principles of leading and lagging power factors, it is possible to improve the PF in a system closer to unity by installing the correct reactive power supplying or absorbing equipment [36]. The concept of unity PF, as well as leading and lagging PF, are illustrated in three sections of Figure 2-9 below.

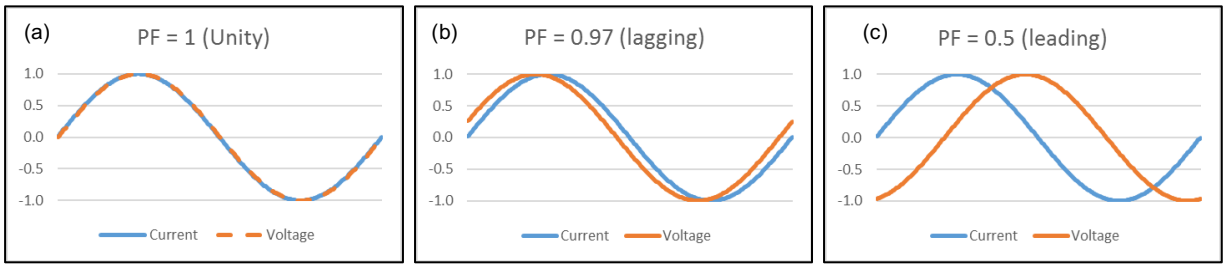

Figure 2-9: Power-factor concept: (a) unity power factor, (b) 0.97 lagging, (c) 0.5 leading

The term PF can also be illustrated by way of a power triangle, which indicates the power factor angle, active power, reactive power and apparent power. The power triangles for the above cases are shown in the three sections of Figure 2-10 below.

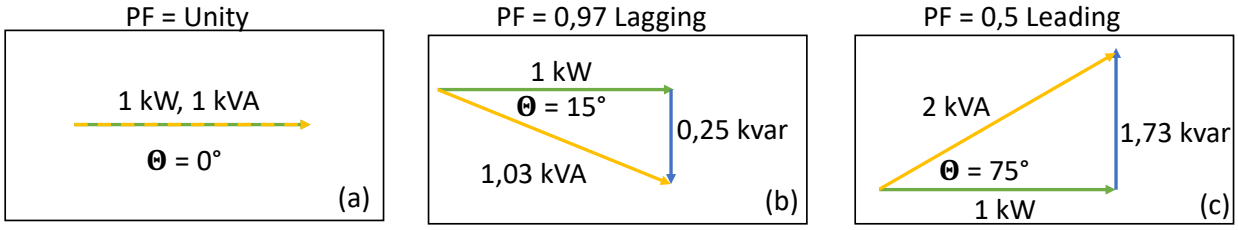

Figure 2-10: Power-factor triangles: (a) unity, (b) 0.97 lagging, (0.5) leading

There are different PF definitions due to the various elements present in the power system. The most common are fundamental power factor, also known as displacement power factor, which

only considers the fundamental active and apparent powers. Effective power factor considers the total active power and the effective apparent power that are present in the system, thus including the effects of distortion powers within the power system. The effective power factor is illustrated in Figure 2-11 below, derived from [31].

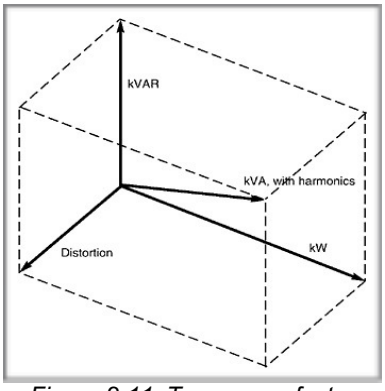

Figure 2-11: True power factor

To protect the return on their investment, operators from the distribution network apply penalties to consumers with poor power factors, forcing them to keep their utilisation of the line at a reasonable level.

2.4.3 Problems with NRS 048

Seeing that the NRS 048 [15] focuses primarily on the QoS principle, it contains no limits or criteria for the current harmonics in the power system. As stated previously, end-users are expected to operate their equipment in such a way as to avoid impacting the voltage distortion in the network negatively. Based on the previous explanation of the cause and effect relationship between non-linear current and voltage distortion, a high level of current harmonics contributes to increased levels of voltage distortion in the network. Without proper compatibility levels for current harmonics, this could prove difficult to for the system operators to manage.

In this regard, the IEEE 519 [33] can be utilised as a valuable reference tool. The reason is that it views the management of harmonics in a power system as a joint responsibility between the end-users and system operators. Therefore, harmonic limits are recommended for both currents and voltages. These recommended values consider as acceptable a certain level of voltage distortion. The limits for the harmonic current that are presented in Table 2-2 below, apply to networks that operate between 120 V and 69 kV, thus covering both LV and MV networks, which are the focus of the present study [33].

Table 2-2: Harmonic current's limits [33]

Maximum harmonic current distortion in percent of I_L						
Individual harmonic order (odd harmonics)[a, b]						
I_{SC}/I_L	$3 \le h < 11$	$11 \le h < 17$	$17 \le h < 23$	$23 \le h < 35$	$35 \le h \le 50$	TDD
< 20[c]	4.0	2.0	1.5	0.6	0.3	5.0
$20 < 50$	7.0	3.5	2.5	1.0	0.5	8.0
$50 < 100$	10.0	4.5	4.0	1.5	0.7	12.0
$100 < 1000$	12.0	5.5	5.0	2.0	1.0	15.0
> 1000	15.0	7.0	6.0	2.5	1.4	20.0

2.5 Sources of power quality problems

The common source of PQ problems can be divided into two categories depending on the location of the source in relation to the power meter [31]; these are:

a. utility side of the meter, which include network switching, power system faults and lightning;
b. customer side of the meter, which include non-linear loads, poor grounding, electromagnetic interference and static electricity.

2.5.1 Utility side

PQ problems on the utility side can be caused by human activities or natural events, but all involve interference with the current or voltage. Examples of such events are switching and lightning strikes.

2.5.2 Customer side

PQ problems on the clients' side usually involve a disturbance in the current or voltage that is delivered to the end-user. These disturbances may damage sensitive equipment in the end-user's facilities as well as the other users that are electrically connected. For example, harmonic distortion could cause the current magnitude to be higher than planned, and thus exceeding equipment ratings. A further example is voltage transients that could exceed equipment ratings, in both instances damaging vital components from the system [39]. PQ problems caused by customers are usually due to various occurrences, which are discussed under the following subheadings.

2.5.2.1 Non-linear loads

The numerous types of non-linear loads include those of electronic equipment that use the following: switched-mode power supplies, variable speed drives, rectifiers, inverters, arc welders and arc furnaces. It also includes electronic and magnetic ballasts in fluorescent lighting and medical equipment such as x-ray machines. These mentioned devices distort the smooth sinusoidal waveform into irregular forms that then produce harmonics. Most non-linear loads not only generate harmonics, but also cause a poor power factor.

2.5.2.2 Power factor improvement capacitors

Capacitors improve the power factor by providing the reactive power that is required in the system, thus, freeing up additional capacity on the lines and transformers that feed power to the customer. This also reduces the difference in phase shifts between the voltage and the current – the concept is illustrated in Figure 2-12 below. When planned carefully, the capacitors can match the lag in the system and thus eliminate the need for the power system to supply reactive power.

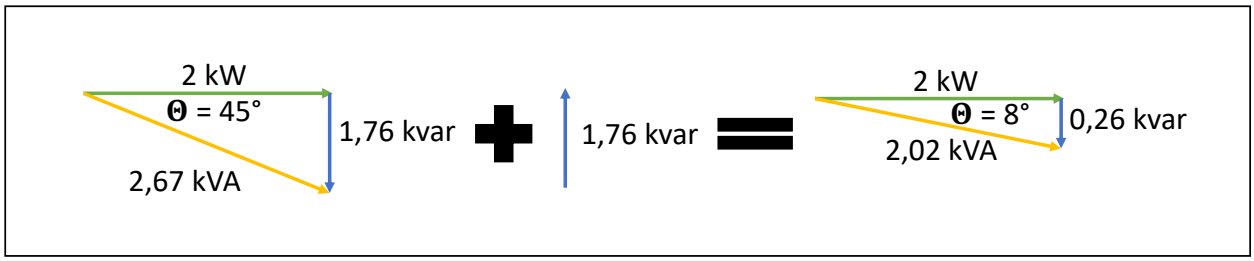

Figure 2-12: Power-factor improvement through installation of capacitor

The capacitors introduce a current into the system that is leading the voltage by 90°. The net result of this leading current and the actual lagging current is a reduced power-factor angle.

The downside of capacitors is that these can amplify the harmonics that are present in the system. This occurs according to the concept of harmonic resonance, which is explained subsequently.

2.5.2.3 Harmonic resonance

Harmonic resonance occurs when the inductive reactance matches the capacitive reactance in a power system [31]. This may be caused by the installation of capacitors to correct the power factor. Resonance at the fundamental frequency causes the current and voltage to be in phase, leading to a unity power factor. However, when resonance occurs at a harmonic frequency, the harmonic current will reach a maximum magnitude. When this happens, it may damage the equipment and cause incorrect meter readings.

Both the inductive and capacitive reactance depend on the frequency of the current and voltage. It is, therefore, possible for resonance to occur at specific frequencies. Inductive and capacitive reactance are calculated by applying the following equations:

$$X_L = 2\pi f L \tag{2-13}$$

where:

X_L = inductive reactance in ohm

f = frequency in hertz

L = induction in henry

$$X_c = \frac{1}{2\pi f C} \tag{2-14}$$

where:

X_C = capacitive reactance in ohm

f = frequency

C = capacitance in farad

In power systems, both parallel and series resonance can occur. Furthermore, since most PF correction capacitors are installed in parallel, parallel resonance is encountered most often. In the case of parallel resonance, the total reactance can be calculated through equation 2-15 below.

$$Z_T = \sqrt{R^2 + (X_L - X_C)^2} \tag{2-15}$$

where:

X_T = total reactance in ohm

R = resistance in ohm

When the capacitive and inductive reactance are equal ($X_C = X_L$) during resonance, the total reactance is equal to the resistance ($Z_T = R$). According to Ohm's law ($I = \frac{V}{X_T}$), the harmonic

current is at a maximum magnitude during resonance. The resonant frequency can be calculated by applying equation 2-16 below.

$$f_{resonant} = \frac{1}{2\pi}\frac{1}{\sqrt{LC}} \quad (2\text{-}16)$$

It is possible to prevent resonance by sizing and locating the capacitors to avoid the resonant frequency, or by installing detuning filters alongside the capacitors.

2.5.2.4 Distributed generation

Distributed generation (DG) is a term used to describe technology that produces electric power, which can be integrated within distribution systems. It can be categorised as renewable DG such as wind, photovoltaic (PV) panels and geothermal energy; or fossil fuel-based DG such as diesel engines and fuel cells. DG should not be confused with renewable generation although various forms of DG are renewable. DG uses smaller-sized generators than typical central power stations do. These reduced generators are distributed throughout the power system closer to the loads. With a focus on distribution networks, the DG's size can be capped at 10 MW. Generators larger than 10 MW are usually connected at transmission voltage levels and are no longer considered to be DG, but rather centralised generation [43].

Several engineers who are involved in ensuring power quality have also focused on DG due to the considerable overlap in the two technologies. This overlap occurs through the potentially significant variances in DG outputs, which affects the load connected to the distribution network and, by implication, the voltage and current in the distribution system [40].

Owing to the recent advances in renewable energy – and specifically solar photovoltaics – (PV) the possibility of high DG penetration has become a reality. As a result, all the utilities, network operators, and power generators are rushing to introduce regulations in a rapidly changing market. The expansion of solar PV as DG in South Africa is confirmed by a survey [19], which found that South Africa had 280 MW of privately owned PV plants in November 2016, and there are new installations taking place constantly. In addition, more than 2.8 GW of generation capacity that was procured through the South African IPP Program is operational already, according to their website [41]. The question arises why network operators are concerned with regulating DG, and what the potential impact of a high penetration of DG technologies would entail [42].

DG does pose several risks to the network operator. These risks occur mainly since historically, DG was not considered during the planning, design, or implementation of distribution networks. Traditional distribution systems are considered passive with power flowing only in one direction,

namely from the secondary winding of the transformer to the end of the feeders. After the introduction of DG, distribution systems experience both consumption and generation at previously exclusive consumption nodes. This change should be incorporated into criteria for planning and operation. Although DG introduces numerous potential problems, the present study only focused on the possible PQ problems that DG may introduce into the network.

According to IEEE 1547 [44], the potential PQ problems are:

- Traditional methodology on voltage control assumes that the load and voltage decrease as the distance from the substation increases. When DG is introduced into the network, this assumption is no longer valid since the voltage may increase at the point of connection of a DG unit, which may be at any point along the feeder.
- Harmonics were limited to known sources that were larger and smaller distributed ones.
- PV and several small wind generators are DC machines that rely on inverters to produce an AC waveform, and thus are able to produce high harmonic content.

It is apparent that PQ problems begin to appear when DG approaches 15% of the feeder capacity, where problems with voltage regulation are often those visible first [40]. The network can be upgraded to accommodate higher levels of DG penetration, but this will come at a cost. Ultimately, the end-user will pay for this upgrade through higher electricity tariffs or increased basic charges.

2.6 Distribution systems

Distribution substations serve a variety of private and public customers by distributing electric power. Such systems can be owned by private companies, Eskom or local municipalities.

A typical distribution system consists of the following components [45]:

- three-phase primary circuits, also called feeders – supplying load in designated areas;
- distribution transformers – converting primary voltage to useful voltages for practical applications.

In South Africa, the electrical network planning horizon is up to 20 years, seeing that several components of power systems have extended lead times, such as generation plants. The expansion of distribution networks falls within a five to 10-year planning horizon [46].

Planning of distribution networks can be described as the selection of a system configuration, or a sequence of system configurations for successive years, which allows compliance to the requirements of the load while considering its future growth. The goal is to minimise the system costs while satisfying the operational constraints [47].

2.6.1 MV distribution systems in South Africa

The South African power network is supplied by only one utility (Eskom) that has grouped the power system into four levels: generation, transmission, sub-transmission and reticulation. These levels can be defined further as described in Table 2-3 below.

Table 2-3: Eskom voltage levels [43]

Level	Description
Generation	Is the plant where the energy is generated. This can be coal-fired, nuclear or hydro power plants.
Transmission	These networks distribute the power from the power plants throughout the country at between 220 kV and 765 kV.
Sub-Transmission	These networks range between 44 kV and 132 kV.
Reticulation	This would typically be an MV network with transformers delivering LV to customers.

The sub-transmission and reticulation levels collectively are termed distribution networks and supply below 132 kV [48].

The major components of a power distribution system are transformers and overhead lines or underground cables. In more established urban settings throughout South Africa, underground cables are the preferred method of power distribution, whereas overhead lines are used in lower-income and informal areas.

The operating temperature of a cable is determined by heat produced due to the flow of current. This heat is directly proportional to the power loss in the cable. Harmonics is one of the leading causes of premature failures in underground cables, according to [49]. This threat of harmonics to underground cables increases as the cable's size increases.

Considering the large number of customers that are served by underground cables, the threat caused by harmonics cannot be ignored.

2.6.2 MV cable planning

In South Africa, most underground MV distribution networks are operated at 11 kV. This is due to the higher overall costs of systems that operate at higher voltage levels [48].

Eskom recommends cable sizes for the distribution system as indicated in Table 2-4 below [50].

Table 2-4: Recommended cable sizes for distribution systems [45]

MV feeder Type	Cable conductor (Cu) size (mm^2)
Substation	630/1 core
Primary	185 or 300/3 core
Secondary	95 or 185/3 core
Mini-substation	Not exceeding 185/3 core
Radial (spur)	Not exceeding 50/3 core

Eskom [50] provides the following guidelines that should be considered when choosing MV cables:

- 11 kV primary feeder cables should have copper conductors and may not exceed 300 mm^2, which can carry 437 A equating to 8.3 MVA load on the cable.
- Secondary feeder cables should also have copper conductors and may not exceed 185 mm^2, which can carry 342 A on 11 kV that equates to 6.5 MVA.
- Mini-substation feeder cables should be copper and may not exceed 185 mm^2.

In Figure 2-13 below, derived from [50], the roles of the various cable types are clearly illustrated as follows:

- Primary feeder cables are used to bridge long distances where there are no load points present, and it is not economical to use a higher voltage.
- Secondary feeder cables are used to supply mini-substations and sub-switching stations directly. These cables are usually interconnected at Type B mini-substations and sub-switching stations. The cables normally begin and end at main HV/MV substations or switching stations equipped with protective functions.

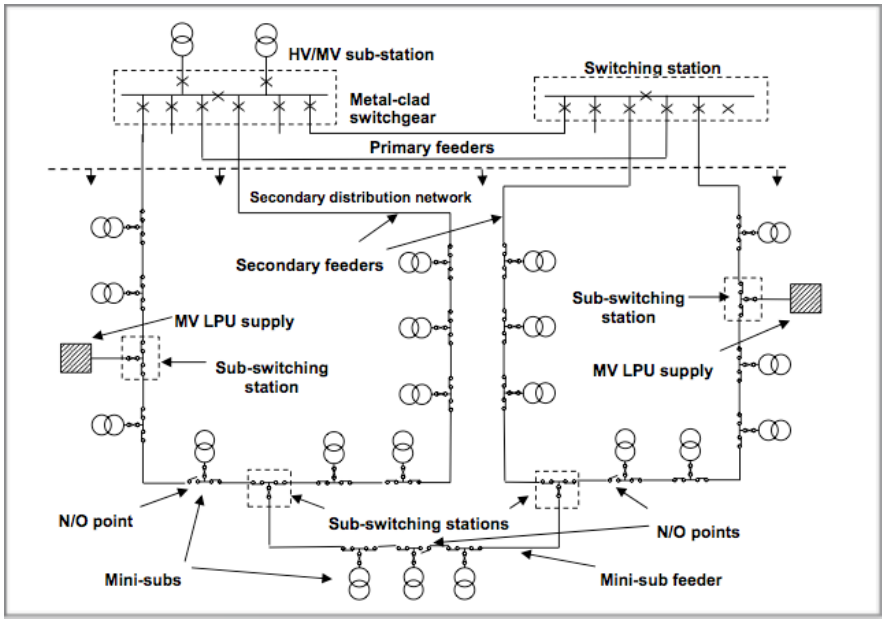

Figure 2-13: Generic MV distribution network [50]

2.7 Impact of power quality problems

A power system may incur two types of losses: technical and non-technical [51]. Technical losses occur naturally within the power system, such as dissipation of power within a transmission line. Non-technical losses are caused by external factors such as theft, maladministration and non-payment by customers.

The general impact of harmonics in a power system have been discussed previously. This section examines the specific impact of harmonics on both transformers and cables.

2.7.1 Losses in transformers

Distribution transformers are designed and built to supply linear loads at a rated frequency. When harmonics are present in the network, this could lead to additional losses in the transformers. The harmonics causes the transformer temperature to increase, which results in a reduced lifetime for the transformer. Considering the significant initial capital investment required for transformers and the potential disruption of supply during their replacement it is essential to ensure the transformer's lifetime is maintained at its maximum [52].

The presence of harmonic currents contributes significantly to additional heating in the transformer, which leads to higher losses. Eddy current losses especially increase with the square of the harmonic number. This leads to a reduction in the useful life of a transformer and a decrease in its insulation [53]. Eddy current losses in non-sinusoidal conditions are calculated by applying equation 2-17.

$$P_{Ec} = P_{EC1} \sum_{h=1}^{h=max} \left(\frac{I_h}{I_1}\right)^2 n^2 \quad (2.17)$$

where

P_{EC1} = fundamental eddy current loss

n = harmonic order

I_h = hth order harmonic current

In the case of a fully loaded transformer that supplies power to IT equipment, the total transformer losses would be twice as high as for the equivalent linear load. This results in higher operating temperatures and shorter lifetimes for the equipment. In essence, these circumstances would reduce the transformer's lifetime from 40 years to approximately 40 days. Fortunately, few transformers are loaded fully, but the effect must be considered when selecting the equipment [54].

Two commonly used methods to calculate the harmonic losses in transformers are the improved-parameter and the measurement method [55].

The improved parameter is simplified to the point where harmonic losses easily can be estimated in practice. This parameter only calculates the losses related to a current, and provides an accurate estimation of the phase shift between voltage and current. As the harmonic distortion increases, the error margin of the improved parameter method decreases. Therefore, this method is useful to estimate voltage distortion levels above 5%.

$$P_{th} = K.\sum_{h=2}^{h_{max}} I_h^2 R_{DC} \quad (2\text{-}18)$$

where:

$$R_{DC} = R_q\left(c_0 + c_1 h^b + c_2 h^2\right) \quad (2\text{-}19)$$

R_1 = fundamental DC resistance

I_h = rms current at harmonic h with non-sinusoidal AC current (A)

h = harmonic order

h_{max} = highest significant harmonic order

Typical values for the coefficients of equation 2-19 are presented in Table 2-5 below [55].

Table 2-5: Typical R_{DC} coefficients [55]

	c_0	c_1	c_2	b
Distribution transformer	0.85-0.90	0.05-0.08	0.05-0.08	0.9-1.4
Power transformer	0.75-0.80	0.10-0.13	0.10-0.13	0.9-1.4

When the distortion of the load voltage is less than 5%, the measurement method would be best suited to determine the harmonic losses using equation 2-20.

$$P_{th} = 3.\sum_{h=2}^{h_{max}} U_h I_h \cos\varphi_1 \quad (2\text{-}20)$$

where

U_h = phase voltage at harmonic h

I_h = phase current at harmonic h

Φ_h = phase between voltage and current at harmonic h

However, when the THD is too large, for example, above 20%, the error will be significant for both methods [55].

When triplen harmonics enter the wye side of a wye-delta transformer, they add up in the neutral conductor, as the harmonics are all in phase. The delta winding provides ampere-turn balance so that the currents can flow, however, they remain trapped in the delta windings. Effectively the triplen harmonics are absorbed in the winding and do not propagate onto the supply. This makes delta-wound transformers useful to harmonically isolate different networks. All other harmonics pass through. Therefore, the circulating current must be considered when rating the transformer [54]. This concept of triplen blocking is only valid under balanced network conditions. When these conditions become unbalanced, it is possible for some triplen harmonics to pass through the transformer. The concept of triplen blocking is illustrated in Figure 2-14 below, as derived from [34].

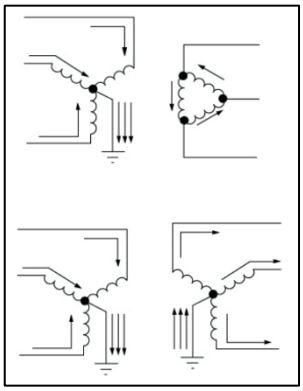

Figure 2-14: Flow of triplen current in three-phase transformers [34]

2.7.2 Effect on transformer's lifetime

As mentioned previously, the higher transformer losses lead to the generation of additional heat which increases the transformer's operating temperature. This leads to a degradation of the transformer's insulation, and possibly a reduced lifetime. To compensate for this condition, the transformer should be de-rated, a process where the maximum load of the transformer is reduced [56].

The de-rating can be undertaken in two different ways [57]:

a. The "K-factor", developed in the United States, calculates a factor increase in the eddy current loss. This factor specifies the appropriate transformer design.
b. The "Factor K", used in Europe, estimates the extent to which a standard-design transformer should be de-rated to ensure the total loss during harmonic load does not exceed the loss of the fundamental design.

2.7.3 K-rated or de-rated?

The advantage of using a K-rated transformer is that it is designed to operate in a power system with harmonic loads. Therefore, the transformers are designed to reduce eddy current losses by using low-loss steels. Additionally, the neutral-point connections are brought out individually, which gives the star point a current rating of 300%.

On the other hand, de-rating a transformer has several disadvantages. Firstly, due to the oversizing, the protection level of the primary current may be too high to protect the secondary. Secondly, reducing the protection level may cause nuisance tripping. Thirdly, a de-rated transformer is less efficient and holds the risk of future overloading when the initial de-rating is no longer available [57].

2.7.4 Diversity

Each non-linear load generates harmonics independently with a magnitude and phase angle that depends on the circuit design and immediate loading. When several loads are connected in parallel, for example all the computers on an office floor, the overall sum of each harmonic will be less than the sum of the individual magnitudes. In other words, the K-factor of the overall load would be less than what would be expected from the measurement of the individual items. Similarly, when there are linear loads present, the overall K-factor is reduced, seeing that the harmonic load makes up only a portion of the full load.

It is difficult to successfully predict the overall K-factor of an installation. The worst-case figure can be obtained by taking the harmonic spectrum of each load and summing it, including the fundamental for all linear loads. In practice, the K-factor will be less than this value, but it is impossible to predict by what margin. It should be also emphasised that the worst case may not correspond to full-load conditions [57].

2.7.5 Losses in cables

The losses that can be incurred in cables are expounded below.

2.7.5.1 Harmonic distortion

Cables and lines incur similar heating effects to transformers when harmonics are present. The losses due to distorted currents are proportional to the square of the rms current. Furthermore, the increase in resistance with frequency due to the skin and proximity effects should be considered.

Skin effect refers to the tendency of AC current to flow where the impedance is the lowest, namely on the outer surface of a conductor. However, this effect has a limited impact at power system frequencies and only becomes significant from the seventh harmonic onward (350 Hz) [54]. The AC to DC resistance ratio depends on the ratio of r/δ with r as the conductor radius, and δ as the current penetration thickness. Where δ can be calculated in terms of:

$$\delta = \sqrt{\frac{2\rho}{\omega\mu}} \tag{2-21}$$

with:

μ = magnetic permeability (H/m)

ω = frequency (rad/s)

ρ = resistivity ($\Omega m/m^2$)

This clearly indicates that δ depends on frequencies and thus decreases as the frequency increases. For a typical round-copper conductor with a 20 mm diameter, the R_{ac}/R ratio at 350 Hz is 1.6.

The resistance may increase due to the neglecting of the frequency. This may cause a slight underestimation in the envisaged losses. In such a case, the I^2R losses in a cable can be separated into the following two parts:

a. Losses caused by the fundamental active current, which is inherent to load operation and cannot be compensated for.
b. Losses resulting from the fundamental reactive current and by the harmonic current, both of which are undesirable and can be compensated for.

A study [7] found a definite relation between the current THD and the harmonic losses in the power system. The network for the mentioned study consisted of a three-phase 400 kVA transformer, a 100 m three-phase LV cable with R = 0.059 Ω/km, and a constant 240 kW load. Under non-sinusoidal conditions, the total losses in a cable with m conductors can be calculated in terms of:

$$P_{cable} = \sum_{m=1}^{m} \sum_{n=1}^{40} R_{m,n} I_{m,n}^2 = \sum_{m=1}^{m} R_{m,1} I_{m,1}^2 + \sum_{m=1}^{m} \sum_{n=2}^{40} R_{m,n} I_{m,n}^2 \quad (2\text{-}22)$$

where:

P_{cable} = active power losses per unit length

m = number of conductors in the cable

n = harmonic order

$R_{m,n}$ = resistance of the m^{th} conductor per unit length for the n^{th} order harmonic

$I_{m,n}$ = rms value of the n^{th} harmonic current in the m^{th} conductor

The results for the harmonic losses are shown in Table 2-6 below.

Table 2-6: Estimation of harmonic losses, [6]

Current THD %	% Harmonic losses
0	0
5	0,04
10	0,2
20	1,08
30	3,01
50	3,54

2.7.5.2 Impact of DG on harmonic phase angles in distribution systems

The harmonic phase angle is a useful tool for a variety of applications such as harmonic power calculations and assessing harmonic emissions [58]. The harmonic phase angle can either be 'relative' or 'absolute' based on the following definitions:

- ***Relative*** harmonic phase angle refers to the angle between the current harmonic and the voltage harmonic, and is used to evaluate harmonic power flows and calculate electric power under distorted conditions.
- ***Absolute*** harmonic phase angle refers to the angle between the current harmonic and the voltage fundamental. It is used to assess harmonic currents at different points in the network, study the summation of various harmonic currents from various loads, model harmonic loads and their effects, and to design counter measures for harmonic loads.

Harmonic phasors are used to simplify the analysis of the distortion of the waveform from the voltage and current in the frequency domain. To reduce the volume of data, the harmonic phasors are aggregated by retaining a single representative value of the harmonic voltage during the aggregation period. The aggregation is necessary since it is impractical to track the harmonic phasors continuously. The reason is that the IEC 61000-4-30 [60] calculates the harmonic phasors from a 10/12 cycle block of data. This process produces a significant amount of data when tracking the specific harmonic phasor over an extended period.

During the calculation of the harmonic phasor according to the IEC 61000-4-30 [60] method, aspects of the phasor's information is lost. This is because only the rms values are retained during aggregation. The IEC 6100-4-30 aggregation is calculated as follows:

$$V_{3s,h} = \sqrt{\frac{1}{15}\sum_{i=1}^{15} V_{200ms,h,i}^2} \quad (2\text{-}23)$$

where $V_{3s,\,h}$ is the aggregated 3-second value calculated from the magnitude of 15 consecutive 10/12 cycle block phasors (50 Hz system) at harmonic number h.

$$V_{10min,h} = \sqrt{\frac{1}{200}\sum_{i=1}^{200} V_{3s,h,i}^2} \quad (2\text{-}24)$$

where $V_{10min,\,h}$ is the aggregated 10-minute value calculated from 200 consecutive $V_{3s,\,h}$ values at harmonic number h.

This calculation is proposed [59] to compensate for the loss of phasor information during IEC 61000-4-30 phasor aggregation. This is done by aggregating the harmonic phase angles to attain a “prevailing” phase angle. The aggregated harmonic phasor $Y_{agg,\,h}$ at harmonic order h would be calculated from the 10/12 cycle block values over an aggregation interval.

$$Y_{agg,h} = Y_{agg,h}\angle\varphi_{agg,h} \quad (2\text{-}25)$$

where

$Y_{agg,\,h}$ = the rms value of the aggregated harmonic voltage or current phasor at harmonic h, based on the principles of (2.25), but with the number of samples used that reflect a suitable time interval such as 1 minute.

$\varphi_{agg,\,h}$ = the aggregated harmonic voltage or current phase angle with harmonic order h.

Both values can be calculated as:

$$Y_{agg,h} = \sqrt{\frac{1}{N}\sum_{i=1}^{N} Y_{200ms,h,i}^2} \quad (2\text{-}26)$$

$$\varphi_{agg,h} = arg\left(\sum_{i=1}^{N} Y_{N,h,i}\right) \quad (2\text{-}27)$$

where:

$Y_{200ms,\,h}$ = the rms value of the harmonic voltage or current phasor.

The aggregated harmonic phasor is also referred to as the prevailing harmonic phasor when it is aggregated over an extended period such as a week. This is also called the "phasor-sum method" to aggregate the time of harmonic phase angles, and is used in the absence of a standard definition. This is done by adding the harmonic phasors within a time interval and using the phase angle of the phasor sum.

When there are strong variations amongst the individual phasors, the aggregated harmonic phasor loses its relevance. This relevance can be calculated as the prevailing angle ratio (PAR), which quantifies the variation between the harmonic phasors in the aggregated value for a single time interval. The PAR can be calculated in terms of:

$$PAR^h = \left(\frac{\left| \sum_{i=1}^{h} \underline{I}_i^{(h)} \right|}{\sum_{i=1}^{h} \left| \underline{I}_i^{(h)} \right|} \right) \tag{2-28}$$

The PAR value should be evaluated as follows [61]:

- ***High prevalence:*** PAR ≥ 0.95, then the aggregated phasors show a high similarity, and there is a low uncertainty about the calculated prevailing phasor.
- ***Medium prevalence:*** 0.95 > PAR ≥ 0.89, then the aggregated phasors show good similarity, and there is a low uncertainty about the calculated prevailing phasor.
- ***Low prevalence:*** 0.89 > PAR ≥ 0.8, then the aggregated phasors are dispersed but a general tendency can be identified, and an acceptable uncertainty regarding the prevailing phasor.
- ***No prevalence:*** PAR < 0.8, then the aggregated phasors are dispersed widely and show no prevalence; thus, the calculated prevailing phasor becomes meaningless.

The prevailing harmonic phase angle makes it possible to evaluate new equipment's potential to cancel out existing harmonics [62]. Harmonic currents caused by different circuit topologies indicate diverse prevailing directions – this provides an inherent potential for cancellation. Knowledge of prevailing harmonic phase angles can also be used to assess the potential impact new equipment such as electric vehicle chargers or PV inverters have on the total harmonic emissions in the distribution grid [63].

Due to varying conditions of the supply network, individual equipment show significant variations in its harmonic emission levels (magnitudes). As the harmonic order increases the phase angles diversify further and do not show any prevailing direction. It was found by [64] that the impedance of the supply network has less impact on harmonic magnitudes than the distortion of the supply voltage. In the mentioned study, the following effects were observed:

- Harmonics for the same equipment types add up arithmetically.
- The cancellation effect is better between different equipment types.
- The various harmonic orders can have differing levels of harmonic cancellation, depending on the diversity of phase angles and the harmonic magnitude.

Harmonic cancellation effects have a substantial impact on the total harmonic voltages in the grid and cannot be neglected for realistic simulations. The cancellation effect depends on changes in technology and may improve or worsen in the future [65], [66].

2.8 Summary of literature study

Beginning with the impact of PQ on the various levels of power systems, it became evident throughout the reviewed literature that PQ issues are even more prevalent closer to the loads. Therefore, generation and transmission systems are viewed as areas of the power system with better PQ. On the other end of the spectrum, LV reticulation networks are perceived as having the worst PQ. Due to these reasons, most of the current literature has studied the PQ of LV networks.

Due to these reasons, limited research has been done on the PQ in MV networks. Although the general level of PQ is better at distribution levels, it is influenced directly by the PQ levels of the LV network. Distribution systems can be viewed as a buffer that protects the transmission system from the poor PQ found in LV networks.

In South Africa, most distribution systems are operated by the local governments or city councils responsible for managing the PQ within the distribution networks. PQ can also influence the revenue of these city councils. Given that 52% of the income of the operational budget of the Tlokwe City Council [67] is relying on revenue from electricity, the potential impact of PQ on distribution networks also implies a potential impact of PQ on their available revenue.

However, the general theme throughout the literature was that the main PQ problem impacting the network efficiency and lifetime of equipment, is the presence of harmonics. Not only is it a highly prevalent PQ problem, but harmonics has potentially devastating effects on power systems and electronic equipment. Combined with the fact that the general levels of harmonics in power systems are increasing, it becomes clear that the study of harmonics and its influence on planning a distribution network will contribute to the current body of knowledge in this field. Several studies have been undertaken on the impact of harmonics on individual system components. However, almost no studies examine the impact that harmonics have on an entire distribution network.

Add to this the already complex scenario, namely increasing penetration of renewable DG, particularly in power distribution systems. As a result, an interesting future lies ahead for harmonics in the modern power system. The International Energy Agency's Energy Outlook 2015 [68] anticipates that the world's electrical demand will increase by 70% in 2040, with a determined effort to reduce the environmental impact of power generation. This confirms the future increase in renewable generation, which is largely DG. The rise of renewable DG poses new challenges to the current distribution systems. This raises crucial questions on the impact of DG on already known issues surrounding distribution system, one of which is harmonics. The issue is whether DG will contribute to the levels of harmonic distortion, or whether there is a potential for DG to improve the levels of harmonic distortion in distribution networks.

To summarise: There is potential for new research on the effects of harmonics when planning distribution networks in South Africa. Therefore, the present research study focused on calculating, estimating and predicting the harmonic distortion levels and its impact on South African distribution systems. The design of the research to answer these questions is presented and discussed in chapter 3.

CHAPTER 3: Research design

The literature review (Chapter 2) indicated that the present study should focus especially on the impact harmonics have on planning distribution networks within the South African context. This led to the secondary objective of assessing the potential impact renewable DG has on the expected levels of harmonic distortion.

Therefore, the first step in the research methodology was to identify the study area for the distribution network and studies on renewable DG. The area of research was a sample of an existing distribution network within a South African urban setting while the renewable DG study was based on measurements taken at specific sites before and after the installation of renewable DG applications, especially in the form of solar photovoltaic systems.

After the data was collected, it was verified and processed to deliver the required results. All the calculations are based on the IEEE 1459 [13] power definitions under non-sinusoidal conditions. For the purpose of the present study, it is assumed that the impact of all other PQ issues can be ignored. This is because it was found to have limited potential impact and are found extremely rarely in significant levels within modern distribution networks.

The aim was to combine the losses of individual components into a single system-loss figure, which was extrapolated to include the entire distribution system of the particular area of research, namely Potchefstroom. Thereafter, the system loss was used to assess the potential impact these losses could have on the network planning that the city has put in place.

The results from the above-mentioned assessment were used to design an estimator measuring the loss in distribution systems for future distribution networks. This was done to ensure the networks are capable of functioning throughout their planned lifetime, even if there is a certain level of harmonic distortion.

For the renewable DG analysis, the present study focuses on applying the principles of prevailing harmonic phasors to determine how renewable DG contributes to the levels of harmonic distortion within the distribution system. Even though there are other potential renewable DG problems, these fall outside the intended scope of the present study.

3.1 Study network and field data

The following subsection describes and defines the scope of the network that was studied.

3.1.1 Distribution system analysis

The study network is a portion of a ring-based distribution network in Potchefstroom, South Africa. This network utilises primary distribution substations that supply various switching substations. These switching substations can either supply directly to customers or to secondary switching substations. Secondary switching substations in turn supply direct to the customers.

The network diagram in Figure 3-1 below indicates the elements that are present in the network under investigation.

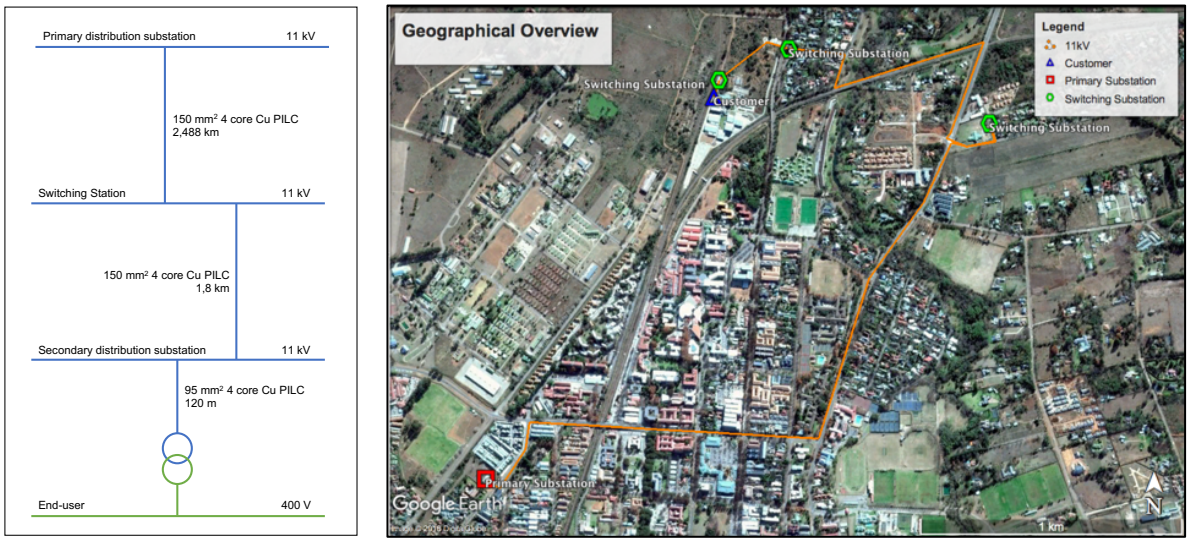

Figure 3-1: Study network overview

The primary substation, Gamma, comprises two 20 MVA 66/11 kV transformers. The present study followed one feeder from the substation to the end-user, collecting data along the way. From the Gamma substation, the next point on the route is Makou switching substation that feeds several rings throughout the area. After Makou, the cable passes directly through Reiger switching substation into the NWU Engineering main switching substation. Here the load is again split into two legs with the one feeding directly to the main administration building, which is the customer depicted in Figure 3-1 above. The total route length from the primary substation to the customer is 4 408 km and covers different cable sizes as well as voltage levels, starting at 11 kV and ending on 400 V. Therefore, this section of the network would provide an accurate representation of the entire network for the city of Potchefstroom.

To analyse the network, IEC 61000-4-30 class A power quality recorders, CT Lab ImpedoDuo, were installed at each point where the line branched off to isolate the power flow from the primary substation to the end-user.

3.1.2 Phase-angle study

The second part of the study focused on the impact of renewable DG on distribution networks, especially the impact on the harmonics present in the network. Again, class A power quality recorders were used for the data collection. Several sites have been identified that have no DG installed, in order to establish a baseline, as well as a few sites where measurements were taken before and after the renewable DG was installed. Lastly, measurements were taken on a renewable DG plant only as a control dataset.

The sites investigated in the current study are:

a. DG only
    i. Silwerjare Old-age Home solar plant: measures the power produced by a three-phase 60 kWp solar photovoltaic plant at 400 V in the town of Schweizer-Reneke.
    ii. NWU solar plant: measures the power produced by three single-phase 3 kWp solar photovoltaic plants at 230/400 V at the North-West University in the city of Potchefstroom.
b. Before and after DG
    i. BDB auditors: had measurements taken before and after the installation of a three-phase 17 kWp solar photovoltaic plant at 400 V in the city of Klerksdorp. The site consists of an office building and indoor swimming school.
    ii. Silwerjare Old-age Home: had measurements taken before and after the installation of a three-phase 60 kWp solar photovoltaic plant at 400 V in the town of Schweizer-Reneke. The site contains an Old-age home and several small residential units.

3.2 Non-sinusoidal quantities of power flow

The traditional instrumentation designed for the sinusoidal 50 Hz waveform is prone to significant errors when the current and voltage waveforms become distorted. Therefore, the IEEE 1459 sets a practical approach to the definition of power under non-sinusoidal conditions [69]. The IEEE 1459 uses the principle of effective apparent power in a three-phase system, as indicated in the following equation:

$$S_e = 3V_e I_e \tag{3-1}$$

where V_e and I_e are the equivalent voltage and currents. In a sinusoidal and balanced power system, S_e would be equal to conventional apparent power.

S_e can be divided into active and non-active power as follows:

$$S_e^2 = P^2 + N^2 \tag{3-2}$$

where P represents active power and N the non-active powers.

This concept assumes a virtual balanced circuit that has the same linear power losses as the actual unbalanced circuit. Such an equivalence leads to the definition of an effective line current I_e [13]. The IEEE 1459 power definitions are outlined in Table 3-1 below.

Table 3-1: IEEE 1459 Summary of three-phase quantities for non-sinusoidal waveforms [13]

Quantity or indicator	**Combined**	**Fundamental powers**	**Nonfundamental powers**
Apparent	S_e (VA)	S_{e1} S_1^+ (VA) S_{1U}	S_{eN} (VA) S_{eH}
Active	P (W)	P_1^+ (W)	P_H (W)
Non-active	N (var)	Q_1^+ (var)	D_{eI} D_{eV} (var) D_{eH}
Line utilization	$PF = P / S_e$	$PF_1^+ = P_1^+ / S_1^+$	—
Harmonic pollution	—	—	S_{eN} / S_{e1}
Load unbalance	—	S_{1U} / S_1^+	—

To calculate the effective apparent power, the effective voltage and current are required. For three-wire power systems (delta connection, as is the case in most 11 kV networks in South Africa) the effective currents and voltages can be calculated as follows:

$$I_e = \sqrt{\frac{I_a^2 + I_b^2 + I_c^2}{3}} \tag{3-3}$$

where I_a, I_b and I_c are the rms values of the phase currents and I_e is the equivalent current. Similar to with the apparent power, the effective rms current can be separated into a fundamental and non-fundamental (harmonic) component.

$$I_{e1} = \sqrt{\frac{I_{a1}^2 + I_{b1}^2 + I_{c1}^2}{3}} \tag{3-4}$$

where I_{e1} is the fundamental equivalent current and I_a, I_b and I_c are the rms values of the fundamental phase currents;

$$I_{eH} = \sqrt{I_e^2 - I_{e1}^2} \quad (3\text{-}5)$$

where I_{eH} is the equivalent harmonic current.

$$V_e = \sqrt{\frac{V_{ab}^2 + V_{bc}^2 + V_{ca}^2}{9}} \quad (3\text{-}6)$$

where V_e is the equivalent voltage and V_{ab}, V_{bc} and V_{ca} are the rms values of the phase-phase voltages.

Again, the effective rms voltage can be separated into a fundamental and non-fundamental (harmonic) component;

$$V_{e1} = \sqrt{\frac{V_{ab1}^2 + V_{bc1}^2 + V_{ca1}^1}{9}} \quad (3\text{-}7)$$

where V_{e1} is the equivalent fundamental voltage and V_{ab1}, V_{bc1} and V_{ca1} are the rms values of the phase-phase voltages

$$V_{eH} = \sqrt{V_e^2 - V_{e1}^2} \quad (3\text{-}8)$$

where V_{eH} is the equivalent harmonic voltage.

Similarly, the effective apparent power can be stated in terms of active and non-active power, it can also be explained in terms of fundamental and non-fundamental power as seen in equation 3.9 below. This confirms that, in the case of zero distortion, the effective apparent power would be similar to the fundamental apparent power, which in turn is similar to the conventional apparent power

$$S_e^2 = S_{e1}^2 + S_{eN}^2 \quad (3\text{-}9)$$

where S_e is the conventional apparent power.

The non-fundamental apparent power can be reduced further into three components of distortion power: current, voltage, and harmonic. These quantities are calculated with the effective currents and voltages in equations 3-10 through 3.13.

$$S_{eN}^2 = D_{eI}^2 + D_{ev}^2 + S_{eH}^2 \quad (3\text{-}10)$$

where D_{eI} is the current distortion power, D_{eV} is voltage distortion power and S_{eH} is harmonic apparent power.

$$D_{eI} = 3V_{e1}I_{eH} \quad (3\text{-}11)$$

$$D_{eV} = 3V_{eH}I_{e1} \quad (3\text{-}12)$$

$$S_{eH} = 3V_{eH}I_{eH} \quad (3\text{-}13)$$

$$P_{eH} = P_{total} - P_1 \quad (3\text{-}14)$$

where P_{eH} is the total harmonic active power, P_{total} is the total active power and P_1 is the fundamental active power.

The harmonic distortion power can be calculated by applying equation 3-15 below:

$$D_{eH} = \sqrt{S_{eH}^2 - P_{eH}^2} \quad (3\text{-}15)$$

Accompanying the new definition for the power quantities are new definitions for the well-known harmonic indices. Voltage and current THD are also calculated in terms of effective harmonic and fundamental values, as is clear from equations 3-16 and 3-17:

$$THD_{eV} = \frac{V_{eH}}{V_{e1}} \quad (3\text{-}16)$$

where THD_{eV} is the equivalent total harmonic voltage distortion.

$$THD_{eI} = \frac{I_{eH}}{I_{e1}} \quad (3\text{-}17)$$

where THD_{eI} is the equivalent total harmonic current distortion.

A new index, Harmonic Pollution, is calculated as the ratio of the non-fundamental effective apparent power to the fundamental effective apparent power, as explained in equation 3.18. This indicates the overall levels of harmonic pollution, both voltage and current, present in the power system.

$$\mathrm{H}armonic\ Pollution = \frac{S_{eN}}{S_{e1}} \quad (3\text{-}18)$$

Lastly, the power factor is calculated by using the total active power and the total effective apparent power, as shown in equation 3-19 below:

$$PF_e = \frac{P_{\Sigma,3\emptyset}}{S_e} \tag{3-19}$$

3.3 Statistical tools

In statistical terms [70], bivariate data refers to datasets with two variables, *x* and *y*, which are particularly relevant when determining the relationship between two parameters. When both *x* and *y* are numerical values, each "data point" is made up of a pair of numbers. An unorganised list of the data reveals limited information about its distribution or relationship to each other.

The data can be organised by employing a scatter plot where each pair of numbers is represented by a point on a rectangular coordinate system. The horizontal axis represents the *x* values and the vertical axis the *y* values. A point is placed where a vertical line from the value on the *x*-axis intersects a horizontal line from the value on the *y*-axis.

To determine the relationship between the two variables, the present study performed a regression analysis on the dataset. It is standard practice for the *y* dataset to be defined as the dependent variable, and the *x* dataset to be defined as the independent variable.

The coefficient of determination (R^2) multiplied by 100 provides the percentage of *y* values that are attributable to the relative relationship, determined by the regression line. The closer this percentage is to 100%, the more successful the relationship explains the variation in *y* for changes in *x*.

In the case of linear relationships, Pearson's sample correlation (*r*) can be used as a quantitative assessment of the strength of the relationship between two datasets.

$$r = \frac{\sum(x_i-\overline{x})(y_i-\overline{y})}{\sqrt{\sum(x_i-\overline{x})^2}\sqrt{\sum(y_i-\overline{y})^2}} = \frac{S_{xy}}{\sqrt{S_{xx}}\sqrt{S_{yy}}} \tag{3-20}$$

$$S_{xx} = \sum x_i^2 - \frac{(\sum x_i)^2}{n} \tag{3-21}$$

$$S_{yy} = \sum y_i^2 - \frac{(\sum y_i)^2}{n} \tag{3-22}$$

$$S_{xy} = \sum x_i y_i - \frac{(\sum x_i)(\sum y_i)}{n} \tag{3-23}$$

r does not depend on the unit of measurement of either variable.

r does not depend on which of the two variables is labelled *x.*

If the value of r is between -1 and +1, near +1, this indicates a substantial positive relationship. When r is near -1, this indicates a strong negative correlation. If r is between -0.5 and +0.5, the relationship is weak [70].

In the data analysis, Microsoft Excel was used to calculate trend lines (regression lines), which help determine the relationship between two parameters. For each data group, several trend lines were evaluated according to their least squares values, and the best fit line was chosen to represent the relationship. The different types of trend lines as defined by Microsoft [71] are listed below:

- ***Linear:*** a straight line that is used with simple datasets, and shows a steady decrease or increase.
- ***Logarithmic:*** a curved line where the rate of change in the data occurs rapidly and then stabilises.
- ***Polynomial****:* a curved line used on fluctuating data. The order of the polynomial is determined by the number of fluctuations that appear in the curve.
- ***Power:*** a cured lined that best fits data which increase at a specific rate.
- ***Exponential:*** a curved line that is used when data values rise or fall with increasingly higher rates.

3.4 Distribution network analysis

The data for the network under investigation along with the non-sinusoidal power flow quantities were used in the distribution network analysis, which followed these steps:

- Calculate the active power losses for cables and transformers.
- Calculate the apparent power losses for cables and transformers.
- Calculate transformer de-rating if applicable.

3.4.1 Active power losses

3.4.1.1 Cable

According to [8], a conductor can be represented by an equivalent Pi model as illustrated in Figure 3-2 below.

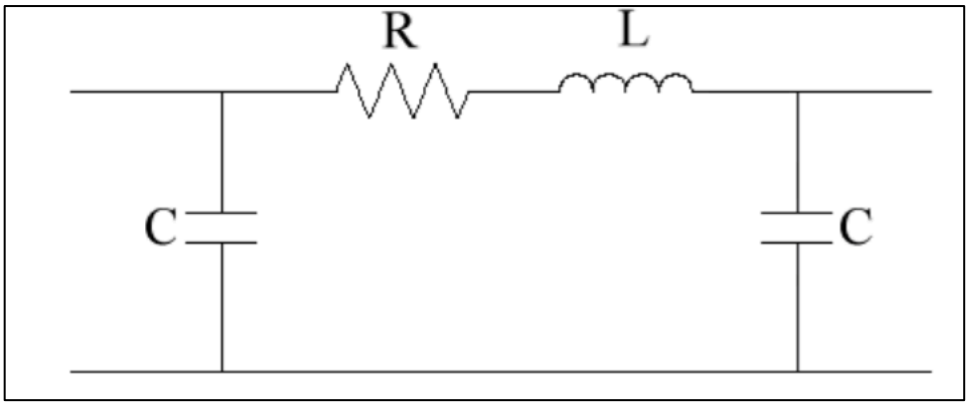

Figure 3-2: Pi equivalent model of a cable

This model can be simplified to a point where it can be represented by a pure resistance, which is adequate for the present study, as depicted in Figure 3-3 below.

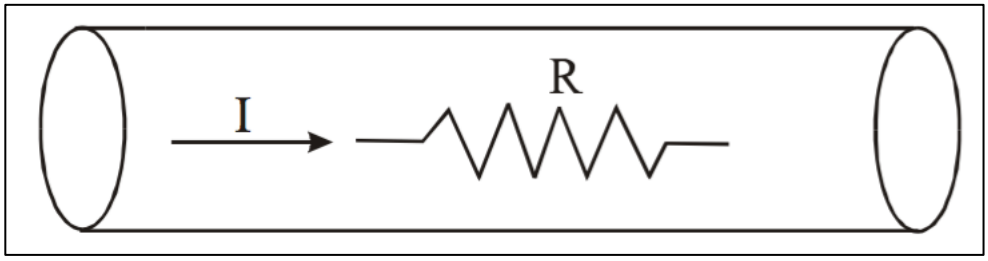

Figure 3-3: Resistive cable model

The AC resistance of a cable is determined by its DC resistance value plus skin and proximity effects. Both these mentioned effects depend on the power system's frequency, conductor's size, as well as the resistivity and permeability of the material. The total losses in a cable consisting of "m" conductors can be calculated by:

$$P_{cable} = \sum_{m=1}^{m} \sum_{n=1}^{40} R_{m,n} I_{m,n}^2 \quad (3\text{-}24)$$

where

P_{cable} = active power losses in a cable per unit length

m = number of conductors on the cable

n = harmonic number

$R_{m,n}$ = resistance of the m^{th} conductor per unit length for the n^{th} order harmonic

$I_{m,n}$ = rms value of the n^{th} harmonic current in the m^{th} conductor.

Assuming the resistance increase due to frequency is neglected and that a slight underestimation of the loss calculation is acceptable, the I^2R losses can be separated into two parts:

a) I^2R losses caused by the fundamental current, which are fundamental to the load operation and cannot be compensated for.

b) I^2R losses resulting from the fundamental reactive and harmonic currents, which are undesirable and can be compensated.

In light of the knowledge above, it is possible to rewrite equation 3-24 as follows:

$$P_{cable} = \sum_{m=1}^{m} R_m I_m^2 + \sum_{m=1}^{m} \sum_{n=2}^{n} R_{m,n} I_{m,n}^2 = P_{cable,50Hz} + P_{cable,harm} \quad (3\text{-}25)$$

3.4.1.2 Transformer

The presence of harmonic currents increases the losses and the demand of apparent power in the network. The reason is that the factor-K is calculating the de-rating of the transformer due to the extra thermal effect of harmonics. According to [7], the factor-K can be used to estimate the additional fundamental losses by applying the following formula:

$$P_T = K(I_1^2 R) \quad (3\text{-}26)$$

where I_1 is the fundamental current and R the resistance of the transformer [7].

According to [72] the transformer load loss can be calculated by the following formula:

$$L_L = I_R^2 R \quad (3\text{-}27)$$

This equation can be rewritten to calculate the transformer resistance as follows:

$$R = \frac{L_L}{I_R^2} \quad (3\text{-}28)$$

The load losses of a Schneider Electric 20 MVA distribution transformer [73] is 120 kW. Therefore, the resistance can be calculated as 0.1089 Ω by applying equation 3-28. This resistance will be

utilised for the additional loss calculations of the main distribution transformer. In the case of an 800 kVA distribution transformer, the load loss amounts to 7 kW [74], which equates to a resistance of 3.97 Ω. This resistance value was be used for all additional loss calculations of the secondary transformer.

3.4.2 Apparent power losses

An increase in the distortion levels of the power system's voltage or current will lead to an increase in the total effective apparent power, as was demonstrated in section 3.2. This increase reduces the potential maximum fundamental apparent power that the power system components can deliver. The resolution of apparent power due to distorted and asymmetrical supply voltages, non-linear and unbalanced loading, is presented graphically in Figure 3-4 below.

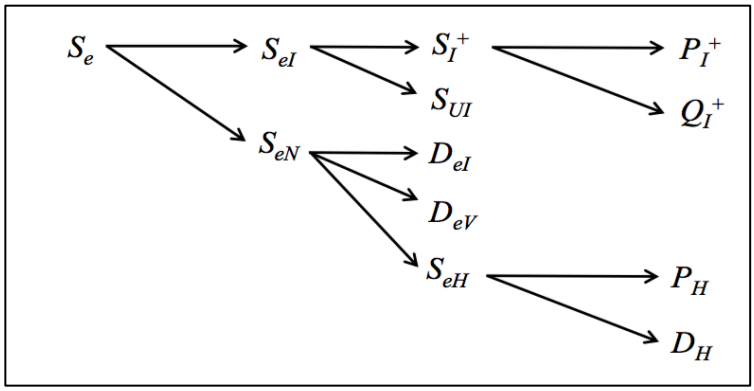

Figure 3-4: Resolution of effective apparent power [13]

The fundamental apparent, active and reactive powers are the quintessence of the power flow in electrical networks. These powers define what is generated, transmitted and sold by the electricity utilities, and bought by the end-users. Therefore, a loss of the system's capacity to deliver any of these fundamental quantities means lower efficiency and usability of the power system. It would, therefore, be functional to define apparent power loss as lost capacity due to the presence of non-fundamental apparent power in the system. This loss will be defined as the ratio of non-fundamental apparent power to the total effective apparent power, calculated as follows:

$$Capacity\ Loss = \frac{S_{eN}}{S_e} \times 100\% \quad (3\text{-}29)$$

3.4.3 Transformer de-rating

The European factor-K quantifies the effects of harmonic currents on transformer loading and is a suitable method to estimate transformer de-rating. This effect can be calculated in terms of:

$$K = \frac{\sum_{h=1}^{hmax} I_h^2 h^2}{\sum_{h=1}^{hmax} I_h^2} \quad (3\text{-}30)$$

where I_h denotes the rms of the h^{th} harmonic current [75].

An alternative method is using the crest factor obtained during the harmonic analysis, as proposed by Henderson and Rose in [76]. According to this method, the transformer harmonic de-rating factor (THDF) is calculated by applying equation 3-31 below:

$$THDF = \frac{\sqrt{2}}{CF} \quad (3\text{-}31)$$

In [32] crest factor (CF) is defined as the ratio of the rms value to the average value of a sine wave. For a pure sine wave, this value is 1.11. Other values indicate the presence of distortion in the waveform. Crest factor applies to both current and voltage waveforms.

3.5 Phase-angle analysis

According to Meyer in [62], phase angles are commonly used in analysing power systems either for studies on harmonic load flow, or to determine the location of the harmonic phase angle on a polar coordinate system. In the present study, the focus was on ascertaining the harmonic phase angle's location. This is achieved by studying the angle between the harmonic current and the voltage fundamental of each respective phase. From this basis, a prevailing phase angle can be derived, and conclusions made about the harmonic cancellation potential of different equipment types.

With regard to calculating the prevailing harmonic phase angle, the first step was to determine the prevailing angle ratio (PAR), as explained in section 2.6.5.2. If the PAR is valid according to the set criteria, then the prevailing harmonic phasor can be calculated as follows:

$$\underline{I_{VEC}^{(h)}} = \sum_{i=1}^{h} \underline{I_i^{(h)}} = I_{VEC}^{h} \angle \emptyset_{VEC}^{(h)} \quad (3\text{-}32)$$

$$I_v^{(h)} = \sqrt{\frac{\sum_{i=1}^{h} \left(I_i^h\right)^2}{h}} \quad (3\text{-}33)$$

$$\theta_v^{(h)} = \emptyset_{VEC}^{(h)} \quad (3\text{-}34)$$

3.6 Verification and validation

Throughout the data analysis in the present study, the researcher followed the prescribed processes of validation and verification. According to the Systems Engineering body of knowledge [77], these mentioned terms can be defined as:

- ***Validation:*** Confirmation, through the presentation of impartial evidence, that the specified requirements have been met.
- ***Verification:*** Confirmation, through the presentation of impartial evidence, that the requirements for a specific application have been met.

3.6.1 Validation

The validation of the research entailed a multistep process, the first of which was the initial colloquium held for the title registration where the research topic was discussed at a peer-reviewed forum. This discussion validated the relevance of the research topic.

Once the research was in progress, continuous discussions took place with senior academics and industry experts to guide the direction of the study. The literature review also helped validate the methods that were employed throughout this study.

Further validation came from the acceptance of an extract from the research presented as a paper at an IEEE conference.

The final validation would occur when answering the original problem statement and demonstrating the relevance of the research findings to prove or disprove the hypothesis stated in section 1.3.3.

3.6.2 Distribution analysis – verification

The first step in the verification of the distribution data analysis was to verify that the collected meter data were valid and that the instrument configuration was correct with regard to CT ratios and time synchronisation. Calculating Pearson's correlation coefficient, confirmed the time synchronisation, and calculating the output/input ratio confirmed that the CT ratios of both instruments were correct.

Throughout the data analysis, calculations were performed by using both the collected meter data and applying standard mathematical formulas populated with data from the datasheets for the equipment, cable, and transformer.

Furthermore, the repetitive nature of the investigated network segments allowed for cross-verification between cable sections.

3.6.3 Phase-angle analysis – verification

For an analysis of the phase angle, the first step was to validate the calculated prevailing phasor by using the PAR value. Once the prevailing phasor has been validated, it was plotted on a polar axis and visually compared with a plot of the aggregated data of the phase angle. The prevailing phasor and shape of the aggregated phase-angle data should have been similar.

3.7 Way forward

In this section, the geographical and electrical scope was documented along with additional calculations and analysis tools that will be used throughout the study. This was followed by an explanation of the validation and verification process that was followed during the writing of this report. Based on the information at hand, the data analysis will be discussed in the following chapter (Chapter 4).

CHAPTER 4: Data analysis

Based on the methodology presented in the previous chapter, Chapter 4 focused on the process of data analysis for the study area. The detailed results of the calculations for each parameter are discussed in this chapter along with the validation and verification processes mentioned in chapter 3.

4.1 Distribution network analysis

Section 4.1 presents and discusses the results obtained from the analysis of the three cable sections comprising the selected section of the distribution system. These three sections are:

- **Cable 1:** Gamma substation to Makou switching substation;
- **Cable 2:** Makou switching substation through Reiger switching substation to NWU Engineering switching substation; and
- **Cable 3:** NWU Engineering switching substation to the NWU admin building.

An overview of the above-mentioned sections are depicted graphically in Figure 4-1 below.

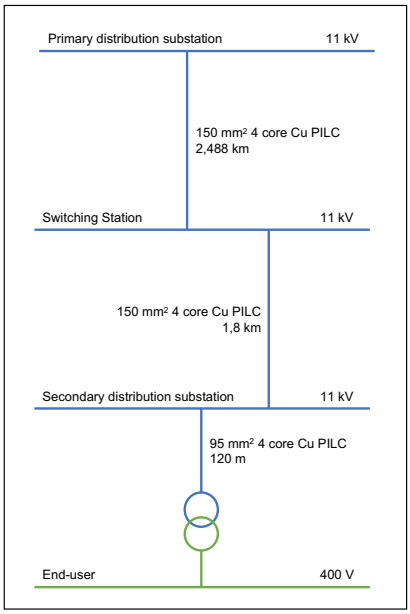

Figure 4-1: Distribution network overview

4.1.1 Cable 1

For Cable 1, between the primary and switching stations, a seven-day data set was selected consisting of 1 008 ten minute samples, from 28 January 2015 to 3 February 2015. To verify the time settings on both instruments, Pearson's correlation factor was calculated as 1 and the output/input relationship as 99.56%. This is confirmed in Figure 4-2 below, where the two load

profiles are plotted on the same axis. Thus, the data collected for Cable 1 is deemed valid for use in the calculations.

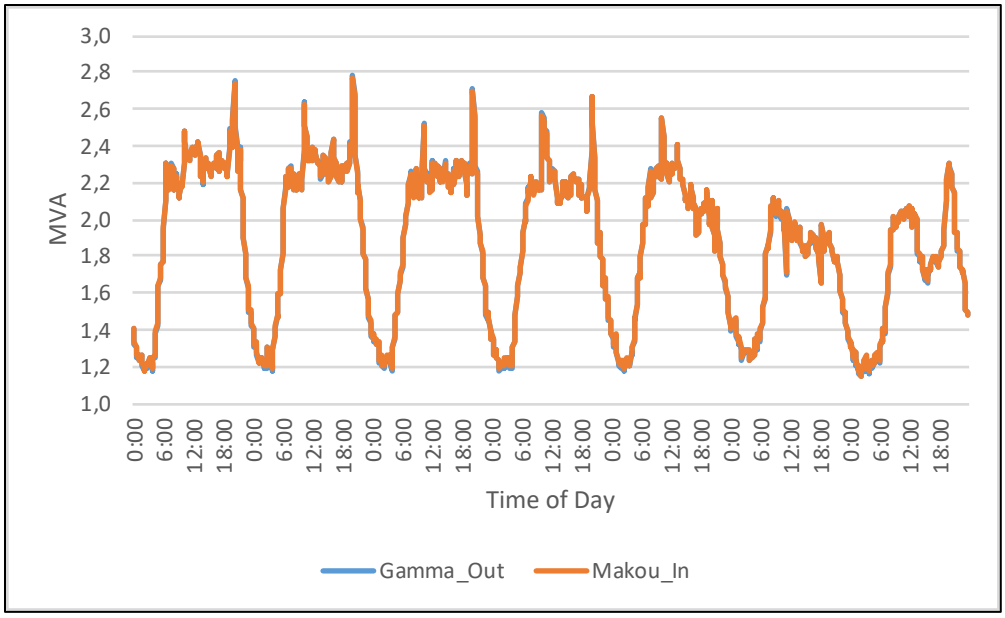

Figure 4-2: Cable 1 – Load profile

4.1.1.1 Active power losses in Cable 1

The active power loss in Cable 1 was calculated in two ways:

- ***Method 1:*** using the collected meter data and subtracting the output from the input.
- ***Method 2:*** calculating the fundamental component of equation 3.25 and using a standard resistance of 0.1494 Ω/km, as stated in the Aberdare brochure [78].

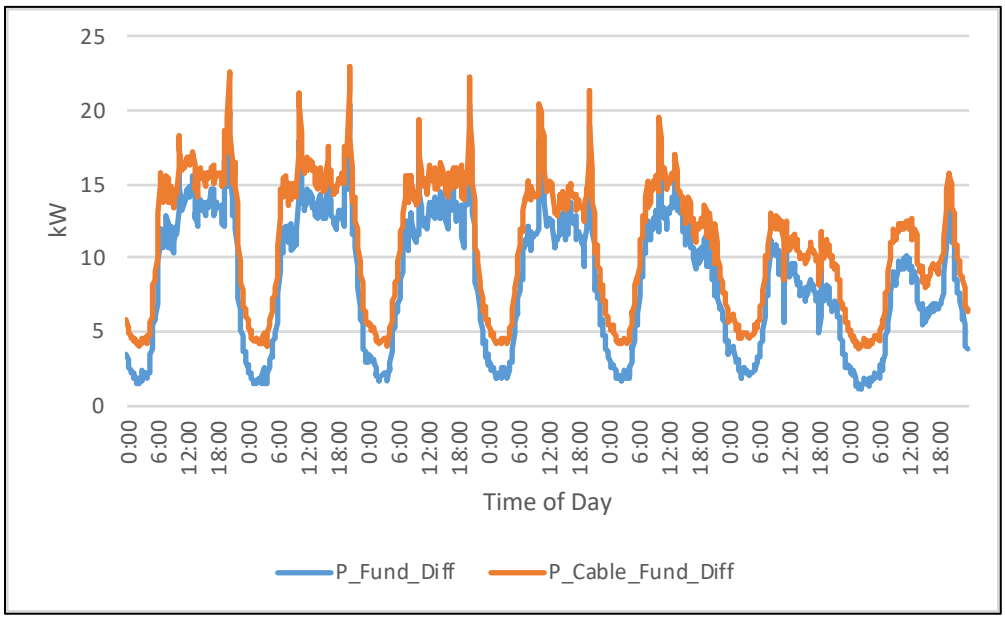

Figure 4-3: Cable 1 – active power losses

Figure 4-3 above indicates that the result between the two methods is extremely close and both follow the same pattern as the load changes throughout the day. It was found that the maximum

loss according to the first method was 22.96 kW, and the highest loss according to the second method was 20.48 kW, which is a difference of 12.1%. During the lower loading period, the difference between the two methods increased, as is evident from Table 4-1 below.

Table 4-1: Cable 1 – compare methods to calculate active power loss

Calculation	Method 1 result (kW)	Method 2 result (kW)	% Difference
Minimum	1.08	3.79	250.4
Average	8.52	10.94	28.5
Maximum	20.48	22.96	12.1

The increase mentioned above may have been caused by differences between the actual environmental and loading conditions of the cable, compared to the test conditions during which the resistance as stated in the brochure was calculated. The resistance stated in the brochure was calculated at an operating temperature of 70°C and at rated current. Figure 4-4 below clearly shows this fluctuation in the actual cable resistance, demonstrating that the test conditions were much closer to the maximum load conditions the cable incurred, than the minimum ones. This can be attributed to the fact that the maximum load current is much closer to the cable's rated current. The pattern followed by the actual resistance is related extremely close to the load profile of the cable.

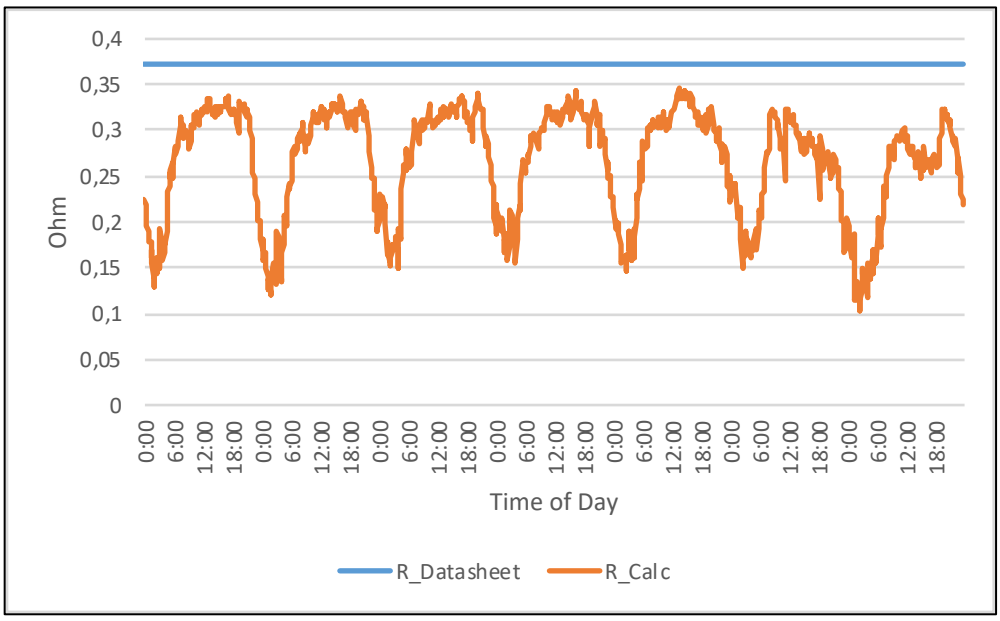

Figure 4-4: Cable 1 – simplified cable resistance

This relationship is confirmed by the direct relationship between the active power loss and the effective current in the cable, as depicted in Figure 4-5 below. This relationship is defined by the 2nd order polynomial trend line (cf. red-dash curve in the illustration) with a coefficient of determination (R^2) value of 0.9902.

$$y = 1.4555x^2 - 60.427x \quad (4\text{-}1)$$

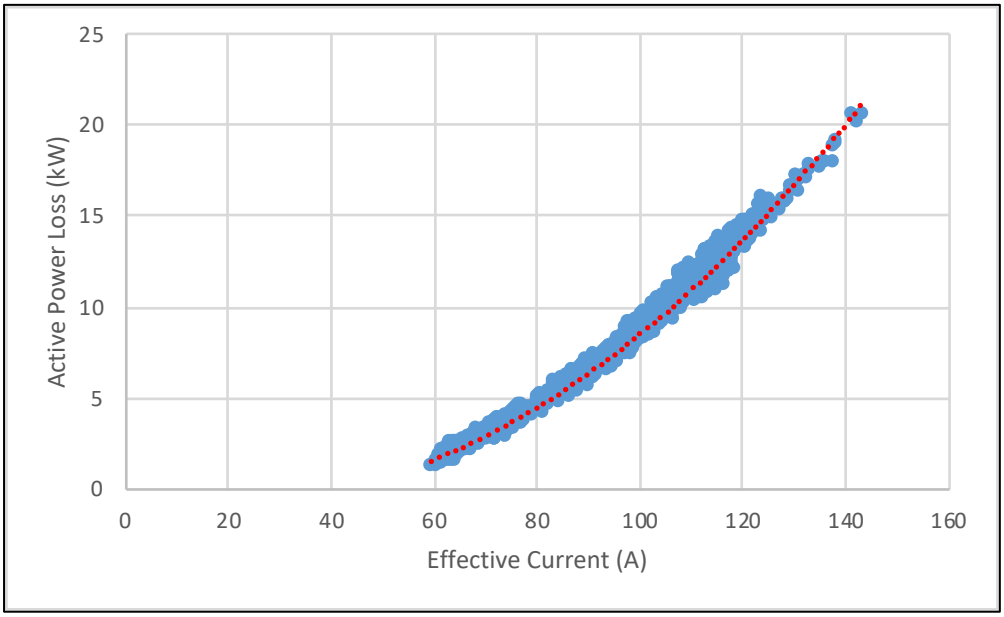

Figure 4-5: Cable 1 – active power loss vs. effective current

In contrast, the active power loss decreases as the harmonic current increases (*see* Fig 4-6 below). This relationship is defined by an exponential trend line (cf. the red-dash curve in the illustration) with an R^2 value of 0.6735.

$$y = 216658e^{-0.402x} \quad (4\text{-}2)$$

The relationship between the active power loss and harmonic current in cable 1 can be seen in figure 4-6.

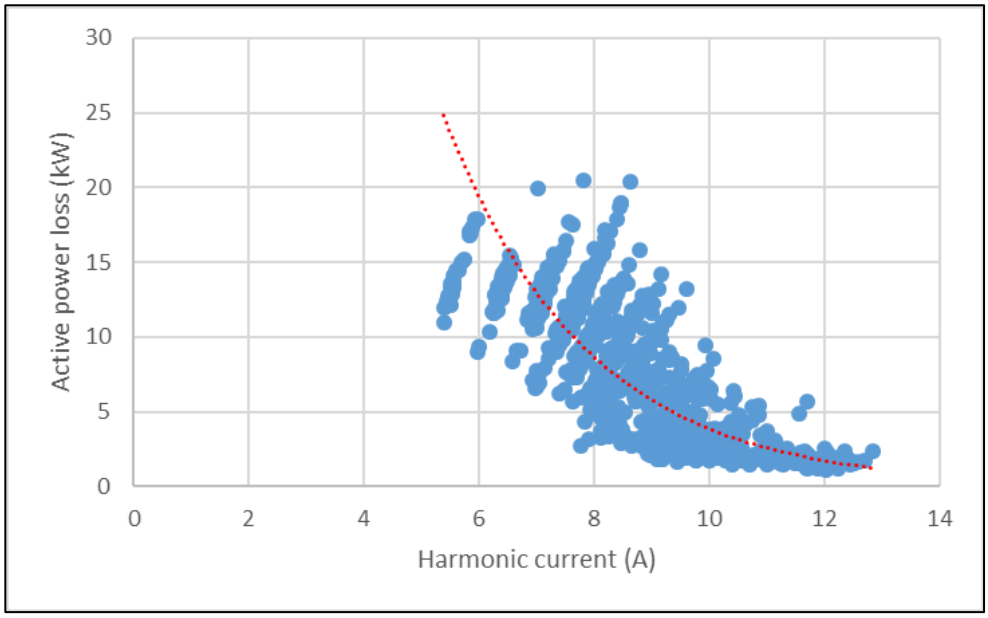

Figure 4-6: Cable 1 – active power loss vs. harmonic current

Therefore, it can be argued that the fundamental active power loss that the cable incurs is influenced primarily by the cable loading and not by the current harmonic levels within the cable.

The active power loss as a percentage of the input power can be calculated for Cable 1, with the results presented in Table 4-2 below. These results indicate that the active power loss percentage is so minimal that it can be viewed as negligible.

Table 4-2: Cable 1 – active power losses

Calculation	Method 1 (%)	Method 2 (%)
Minimum	0.1	0.3
Average	0.5	0.6
Maximum	0.7	0.8

4.1.1.2 Active power losses in the transformer at Cable 1

The transformer, refers to the HV/MV transformer that is feeding power into the busbar at the primary distribution substation, refer to figure 4-1. As is the case with the active power losses in a cable, a formula also calculates the additional active power losses in a transformer due to the presence of harmonics, as indicated by equation 3.25 above. By using the methodology described in subsection 3.4.1.2, the additional active power losses for the transformer at the Gamma substation was calculated. The results of this calculation is presented in Table 4-3 below.

Table 4-3: Transformer 1 – additional active power losses

Calculation	Result (%)
Minimum	0.16
Average	0.20
Maximum	0.26

A comparison between the additional active power loss and the total power loss (*see* Fig 4-7 below), reveals a direct relation between the two parameters defined by the trend line with an R^2 value of 0.9908.

$$y = 1 \times 10^{-6}x^2 - 0.0013x + 2.0939 \quad (4\text{-}3)$$

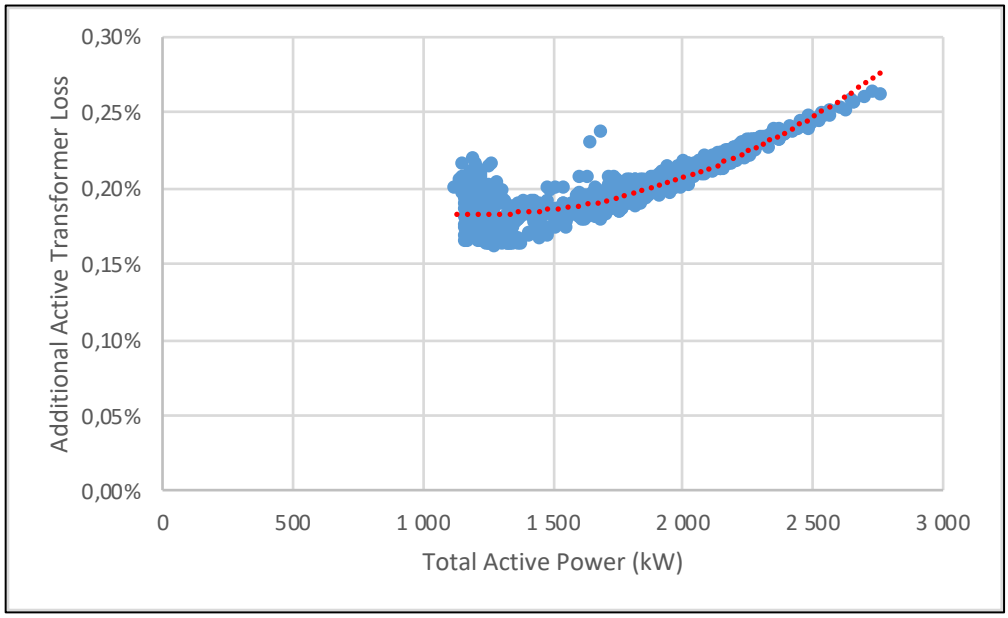

Figure 4-7: Transformer 1 – additional active power losses vs. total active power

Again, as is evident from Figure 4-8 below, the harmonic current does not have a decisive impact on the active power losses. This is confirmed by the 5th order polynomial trend line (cf. the red-dash curve) with an R^2 value of 0.4087.

$$y = -1\text{x}10^{-6}x^5 + 5\text{x}10^{-5}x^4 - 0.0008x^3 + 0.0064x^2 - 0.00254x + 0.042 \quad (4\text{-}4)$$

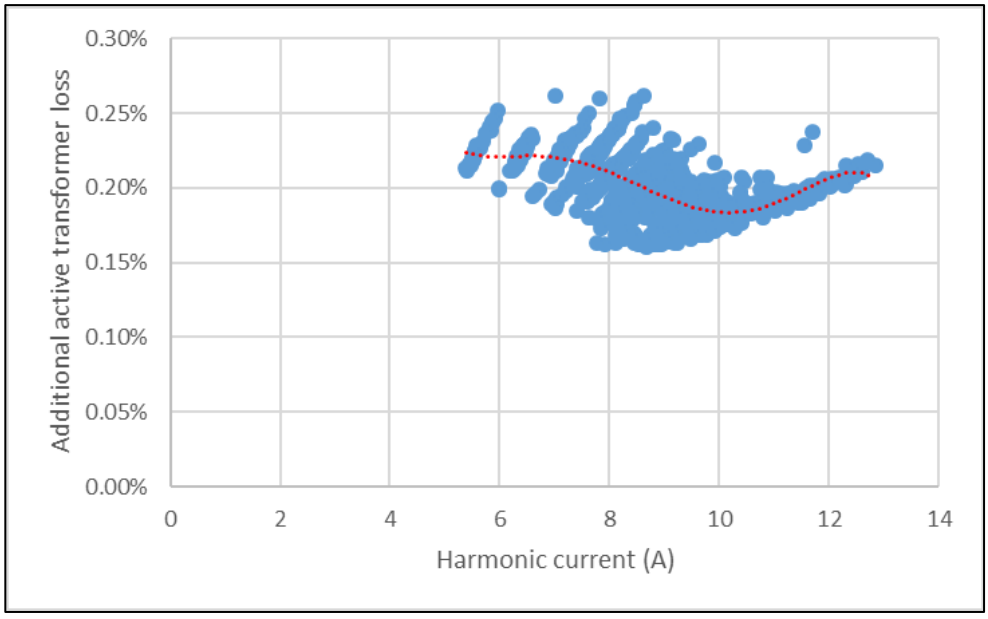

Figure 4-8: Transformer 1 – additional active power loss vs. harmonic current

4.1.1.3 Apparent power losses in Cable 1

The findings for the apparent power losses in Cable 1, plotted against harmonic current in Figure 4-9 below, indicate a definite relation between the apparent power (capacity) loss and the level of current distortion that is present in the cable. This relationship can be represented by a 4th order polynomial trend line (red-dash curve) with an R^2 value of 0.8978.

$$y = 0.001x^2 - 0.011x + 0.0344 \quad (4\text{-}5)$$

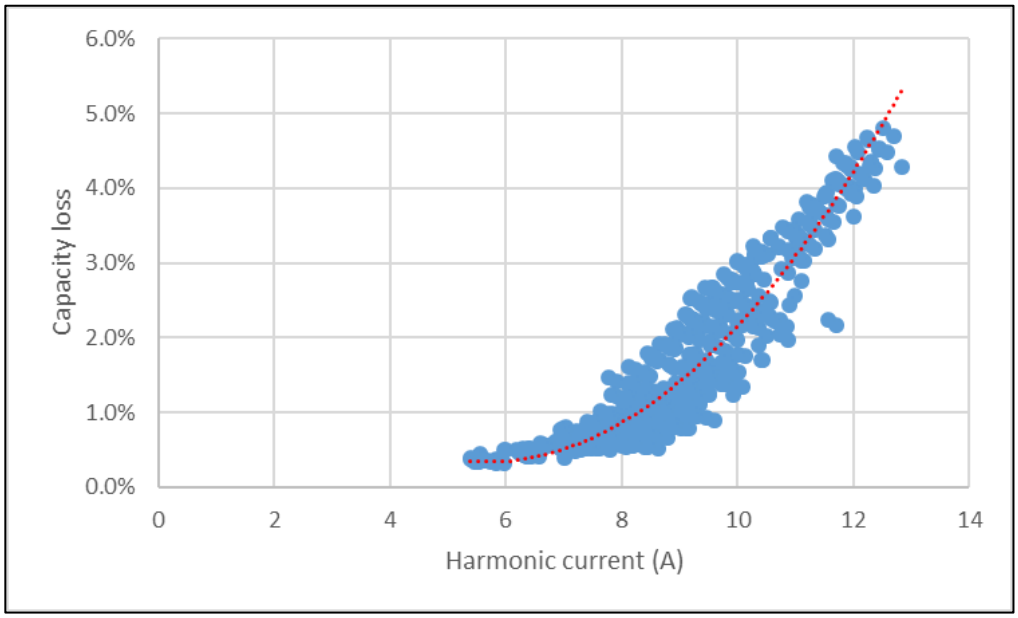

Figure 4-9: Cable 1 – capacity loss vs. harmonic current

Being cognisant of the relationship between the capacity loss and current distortion, the capacity loss was also plotted against voltage distortion in Figure 4-10 below to search for a possible relation. Although a certain relation was found, it did not seem as definitive as the case was with distortion of the current. This fact is confirmed by the lower R^2 value, 0.7588 of the exponential trend line (red-dash curve).

$$y = 0.0002e^{86.378x} \quad (4\text{-}6)$$

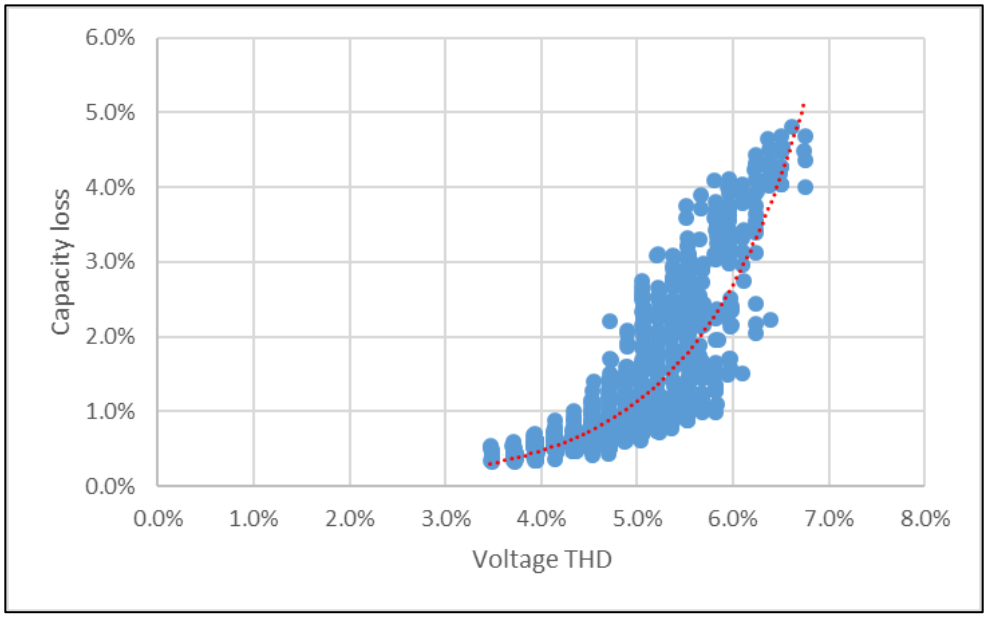

Figure 4-10: Cable 1 – capacity loss vs. voltage THD

The QoS parameters in South Africa are driven from the voltage perspective. Therefore, knowledge of the relationship between the harmonic current and voltage distortion would make it possible to determine capacity loss based on an estimated voltage distortion. This relation is depicted clearly in Figure 4-11 below, according to which the 2nd order polynomial trend line (red-dash curve) has an R^2 value of 0.7712 and is defined by the following equation:

$$y = 3451.3x^2 - 154.12\text{x} + 7.6144 \quad (4\text{-}7)$$

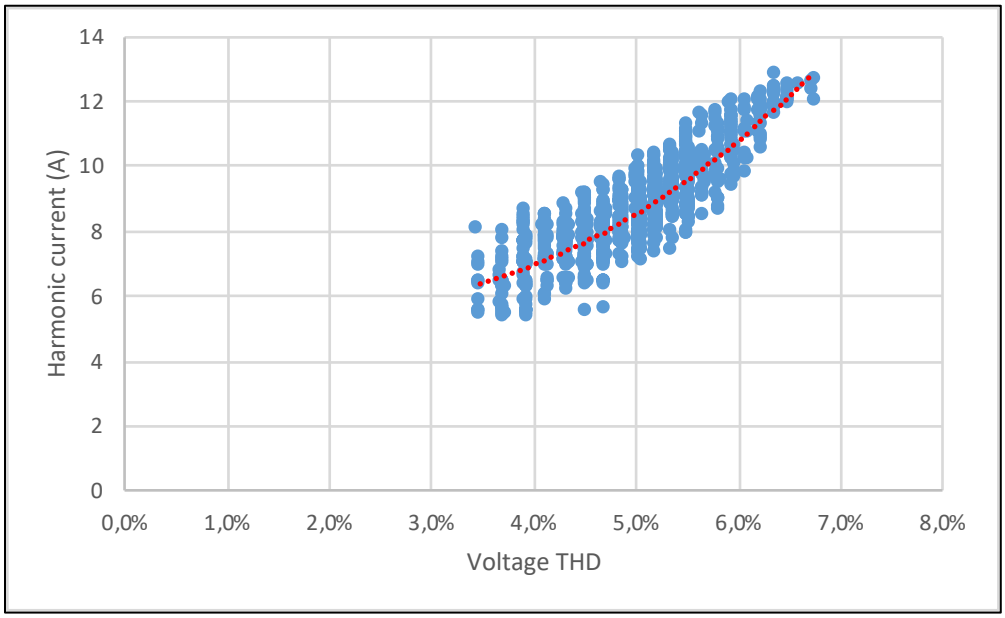

Figure 4-11: Cable 1 – harmonic current vs. voltage THD

The final parameter with which to compare the capacity loss is the effective apparent power, as depicted in Figure 4-12 below. An R^2 value of 0.912 for a power trend line suggests a sound relationship between the two parameters, defined by the following equation:

$$y = 7 \times 10^{14} x^{-2.681} \quad (4\text{-}8)$$

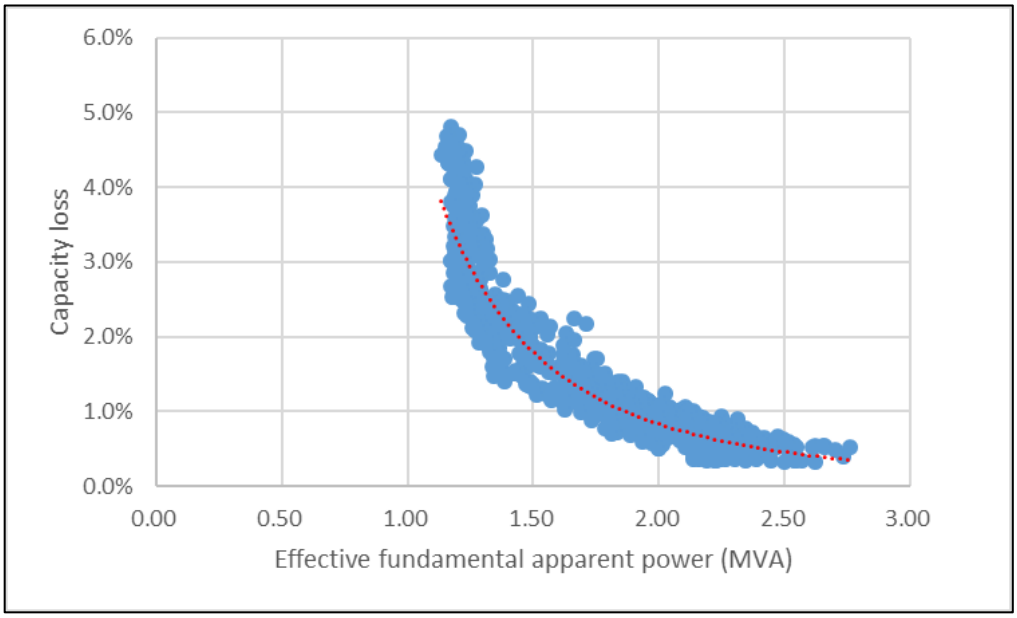

Figure 4-12: Cable 1 – capacity loss vs. effective fundamental apparent power

The steady decline in the capacity loss as the effective apparent power increases suggests that the current distortion decreases as the effective apparent power increases.

Comparing the capacity loss versus effective apparent power (Fig 4-12), and harmonic current versus effective fundamental apparent power (Fig 4-13 below), the expected similarity can clearly be seen with a decline in harmonic current. This occurs as the effective apparent power increases, just as with the capacity loss. Current distortion can be related to effective fundamental apparent power by the 3rd order polynomial trend line (red-dash curve) in equation 4-9, with an R^2 value of 0.652.

$$y = 7 \times 10^{-19} x^3 - 2 \times 10^{-12} x^2 - 1 \times 10^{-6} + 14.472 \quad (4\text{-}9)$$

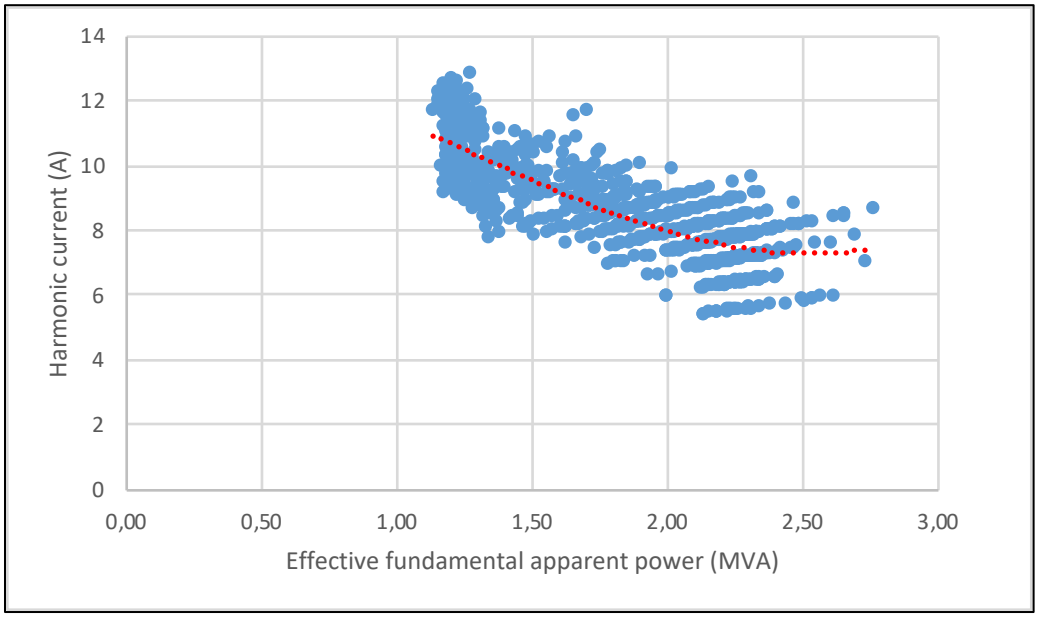

Figure 4-13: Cable 1 – Harmonic current vs. effective fundamental apparent power

The contribution that each component of non-fundamental apparent power makes to the total non-fundamental apparent power is depicted in Figure 4-14 below. The finding show that these contributions are dominated by that of the current distortion power. This finding concurs with the previous finding on the relationship between capacity loss and current distortion, which indicated that the capacity loss is related closely to the current distortion.

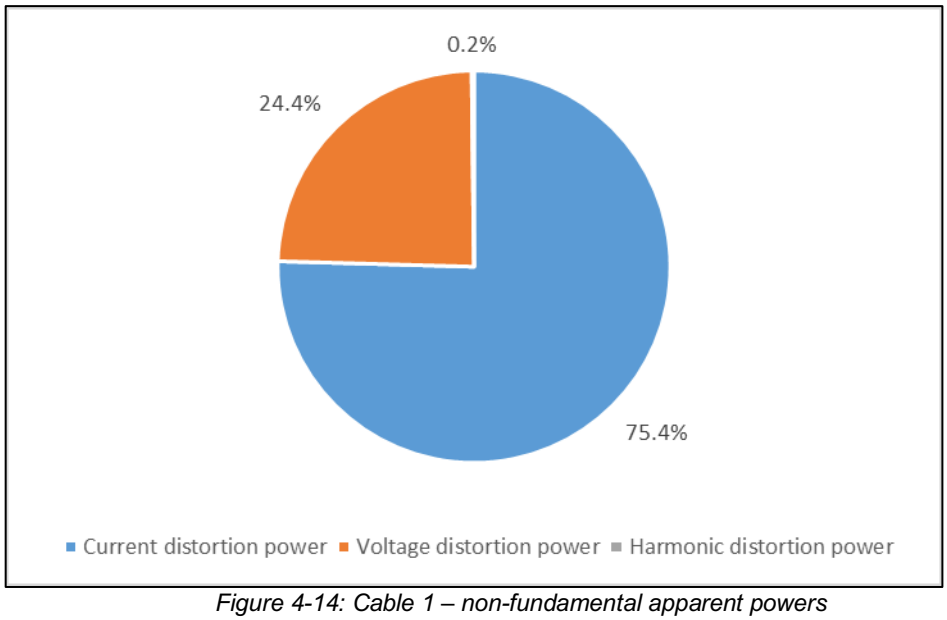

Figure 4-14: Cable 1 – non-fundamental apparent powers

4.1.1.4 Transformer's harmonic de-rating factor

The ‚HV/MV, transformer's harmonic de-rating factor was calculated by applying equation 3-31. This factor was found to be related directly to the crest factor of the current waveform. This finding created the expectation of a clear relationship between the crest factor and level of harmonic current present in the cable. The finding was also confirmed by the visible relation as is evident

in Figure 4-15 below, and is defined by the 3rd order polynomial trend line (red-dash curve) with an R^2 value of 0.7085 and defined by the following equation:

$$y = 0.0029x^2 - 0.0248x + 1.4671 \quad (4\text{-}10)$$

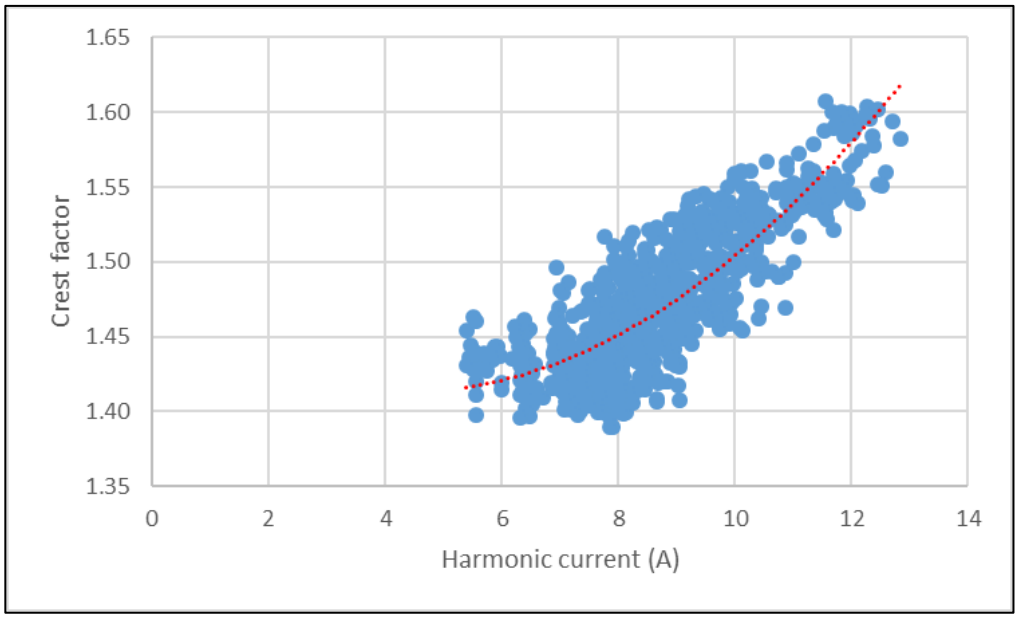

Figure 4-15: Cable 1 – crest factor vs. harmonic current

4.1.2 Cable 2

For cable 2, between the switching and the secondary station, a seven-day dataset containing 1 008 ten-minute samples from 17 February 2015 at 00:00 to 23 February 2015 at 23:50, used for the data analysis on Cable 2. To verify the time settings on both instruments, the Pearson's correlation coefficient was calculated as 1, and the output/input relationship as 98%. This was confirmed when the two load profiles were plotted on the same axis, as depicted in Figure 4-16 below. Therefore, configuration of both instruments on Cable 2 can be accepted as correct.

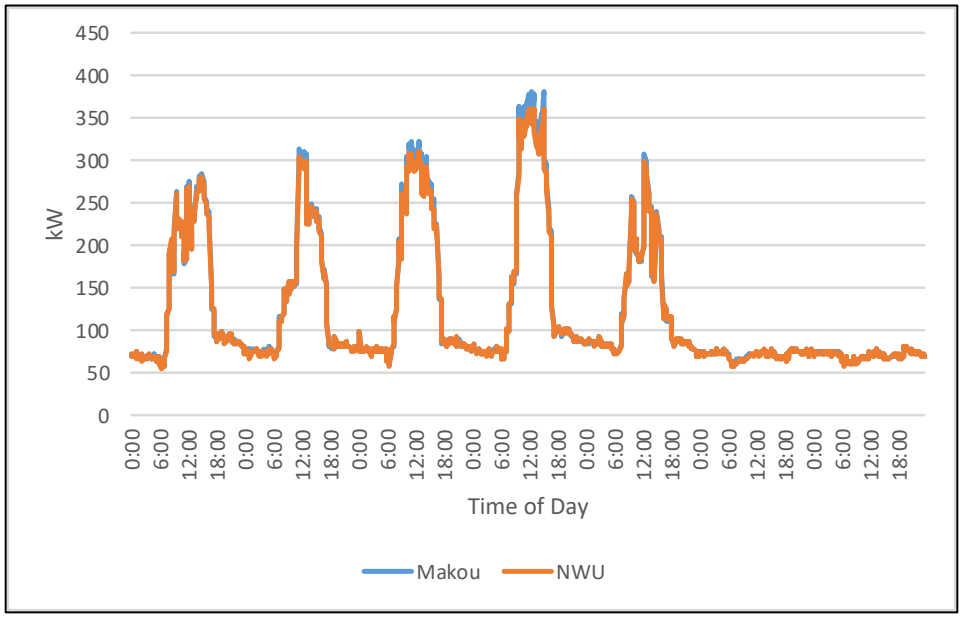

Figure 4-16: Cable 2 – load profile

4.1.2.1 Active power losses in Cable 2

The active power loss in Cable 2 was calculated in two ways:

- ***Method 1:*** using the collected meter data and subtracting the output from the input.
- ***Method 2:*** calculating the fundamental component of equation 3-25 by using a standard resistance of 0.1494 Ω/km, as stated in the Aberdare brochure [78].

The active power losses incurred by Cable 2 is depicted in Figure 4-17 below.

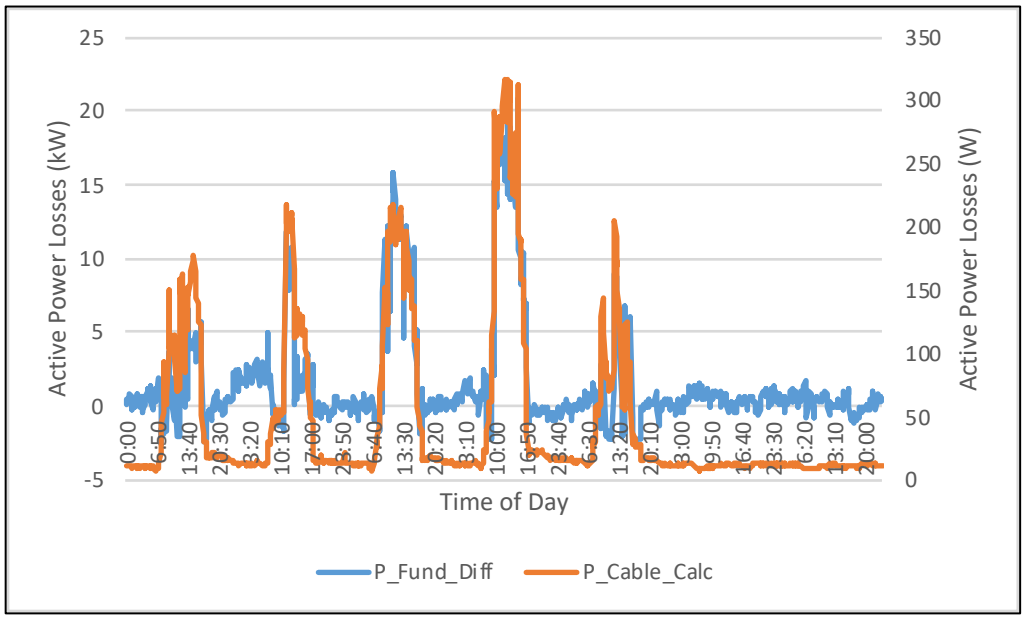

Figure 4-17: Cable 2 – active power losses

Although the two methods of calculation reveal a similar pattern in the losses, the actual values differ significantly. This could be due to inaccuracies in the measurement equipment, or the fact that the simplified *R* model is not effective at determinig the real cable parameters.

The results in Table 4-4 below indicate the same pattern as for Cable 1. This is evident from the difference in reduction towards the maximum loss.

Table 4-4: Cable 2 – Compare methods to calculate active power loss

Calculation	Method 1 result (kW)	Method 2 result (kW)	% Difference
Minimum	0,325	0,00027	120 836
Average	2,936	0,04700	6 205
Maximum	11,005	0,31700	3 373

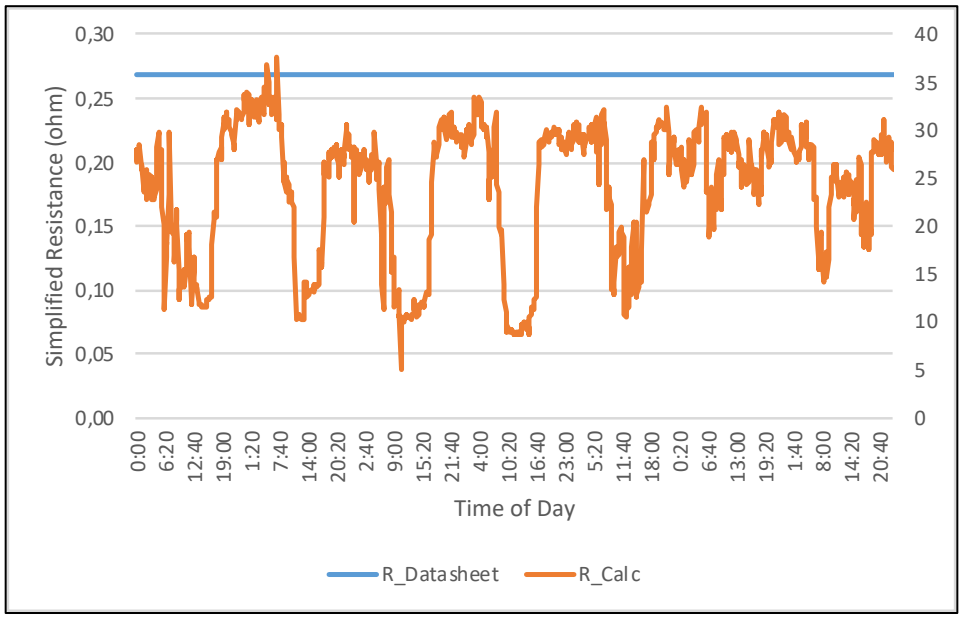

Figure 4-18: Cable 2 – simplified R

The simplified *R* calculation supports the variance in the active power losses of the cable results, as is evident from Figure 4-18 above. It was found that the two methods delivered vastly different simplified *R* values with the actual meter data yielding an *R* value in the order of 100 times larger than the value stated in the brochure.

When comparing the active power loss to the effective current (as depicted in Fig 4-19 below), a clear linear relation becomes visible. This relation is defined by a 4th order polynomial trend line (red-dash curve) with an R^2 value of 0.9989 and defined by the following equation:

$$y = -0.1562x^4 + 9.3504x^3 - 195.03x^2 + 2214.2x - 5067.5 \quad (4\text{-}11)$$

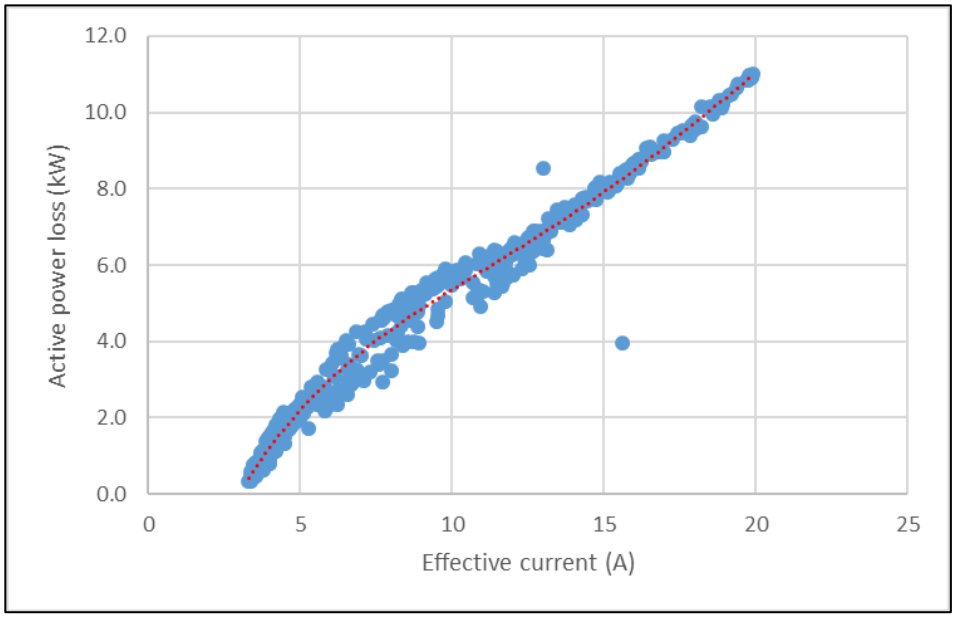

Figure 4-19: Cable 2 – active power loss vs. effective current

The distribution of the data points makes it impossible to determine a relationship between the active power loss and the harmonic current with an acceptable correlation coefficient. It can, therefore, be confirmed that the harmonic current has limited to zero influence on the active power losses in the mentioned cable.

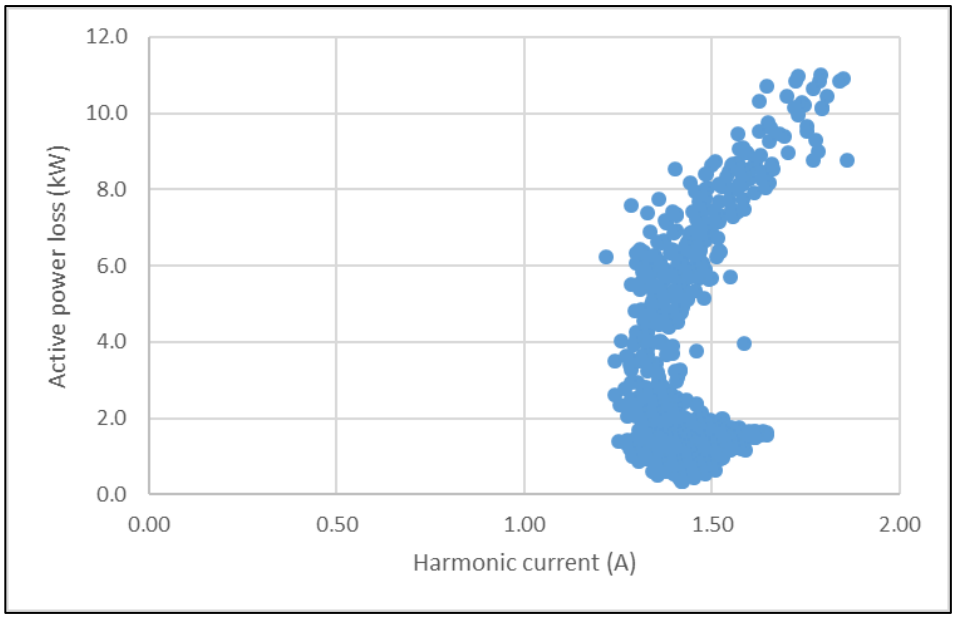

Figure 4-20: Cable 2 – active power loss vs. harmonic current

The active power loss was compared to the current THD, as portrayed in Figure 4-20 above. This comparison indicated is a definite decline in the active power loss as the current THD increases. This finding thus shows that current THD is not a driving factor behind the active power losses in a cable.

The active power loss as a percentage of the input power can be calculated for Cable 2. The results are presented in Table 4-5 below, which reveals that the active power loss percentage is so low that it can be viewed as negligible.

Table 4-5: Cable 2 – active power losses

Calculation	Method 1 (%)	Method 2 (%)
Minimum	0.60	0.00
Average	2.45	0.04
Maximum	3.07	0.09

4.1.2.2 Apparent power losses in Cable 2

For the apparent power losses, a clear relation becomes evident between the apparent capacity loss and the current THD (cf. Fig 4-21 below). The relationship between capacity loss and current THD can be defined by a power trend line (red-dash curve) with an R^2 value of 0.4574 and written in terms of the following equation:

$$y = 0.0429x^{2.2497} \quad (4\text{-}13)$$

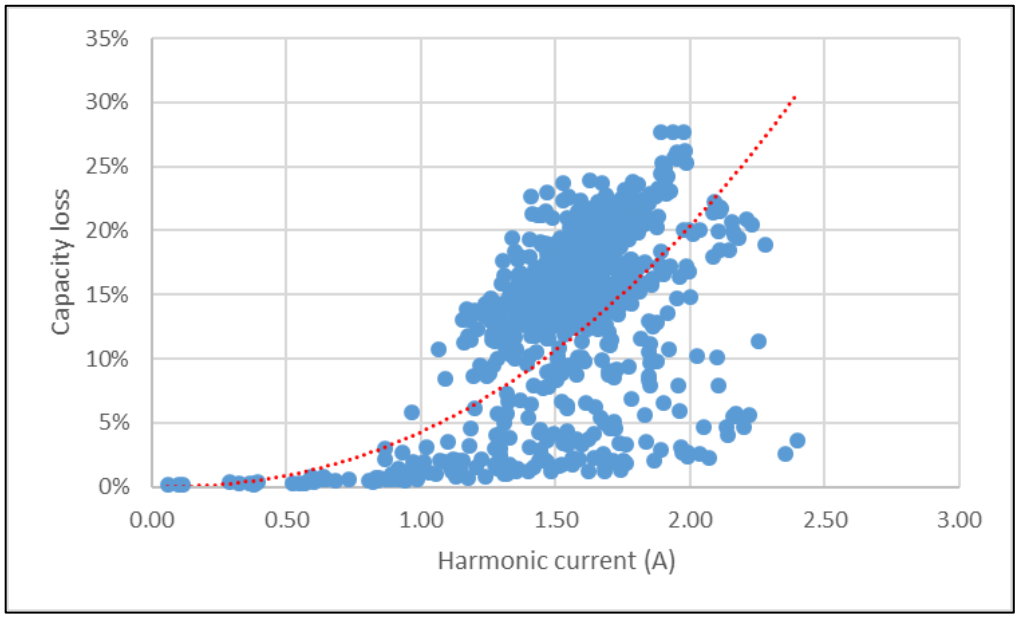

Figure 4-21: Cable 2 – capacity loss vs. harmonic current

To establish whether the capacity loss is driven by the voltage THD or harmonic current, the capacity loss was also plotted against voltage THD, as depicted in Figure 4-21 above. The 4th

order polynomial trend line (red-dash curve) indicates an R^2 value of only 0.3723. This confirms the weak relationship between capacity loss and voltage THD. The mentioned relationship can be defined by the following equation:

$$y = 1 \times 10^6 x^4 - 265370x^3 + 19114x^2 - 593.65x + 67601 \quad (4\text{-}14)$$

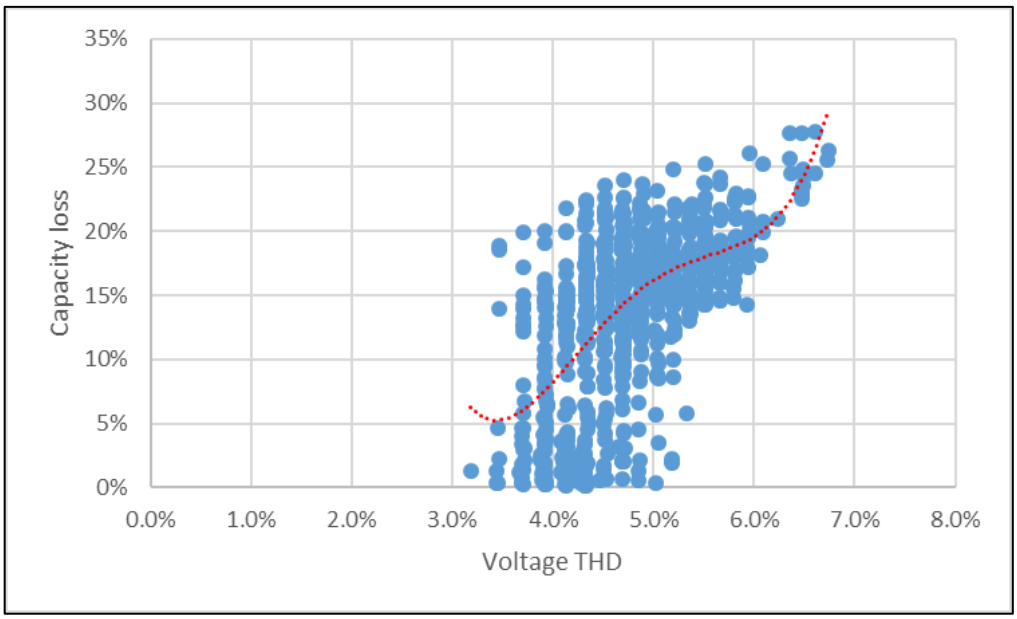

Figure 4-22: Cable 2 – capacity loss vs. voltage THD

The QoS parameters in South Africa are driven from the voltage perspective. Knowledge of the relationship between the harmonic current and voltage distortion should make it possible to determine the capacity loss based on the estimated distortion of the voltage. This is not possible since no definite correlation was found between the harmonic current and voltage THD in this cable, as indicated by Figure 4-23 below. The lack of relation between capacity loss and voltage THD is confirmed by the analysis according to which no type of trendline could achieve an acceptable R^2 value.

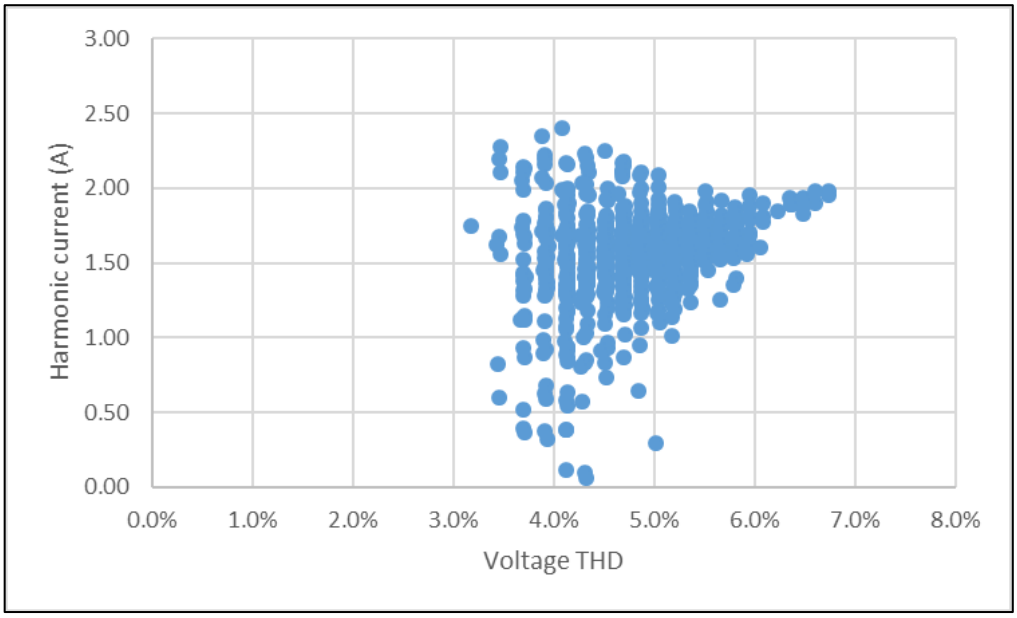

Figure 4-23: Cable 2 – current THD vs. voltage THD

Figure 4-24 below depicts the relationship between capacity loss and effective fundamental apparent power. This relationship can be defined in terms of a power trend line with an R^2 value of 0.8248 and written as:

$$y = 2966.6x^{-2.263} \quad (4\text{-}16)$$

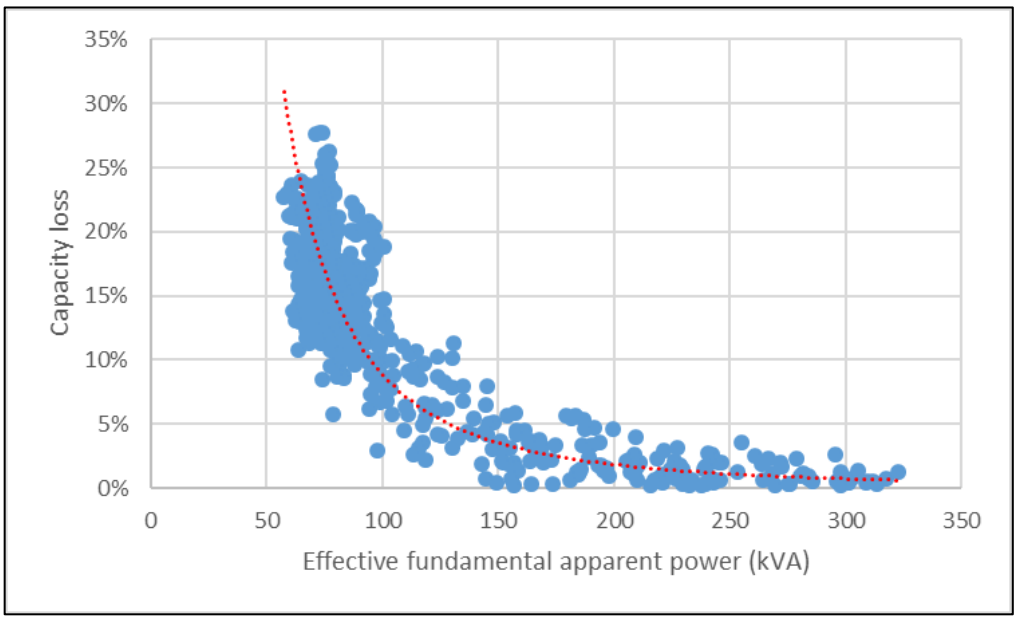

Figure 4-24: Cable 2 – capacity loss vs. effective fundamental apparent power

The reduction in the capacity loss as the effective fundamental apparent power increases suggests that the harmonic current decreases as the effective fundamental apparent power increases. However, as is evident from Figure 4-25 below, there is no relationship between the harmonic current and the effective fundamental apparent power.

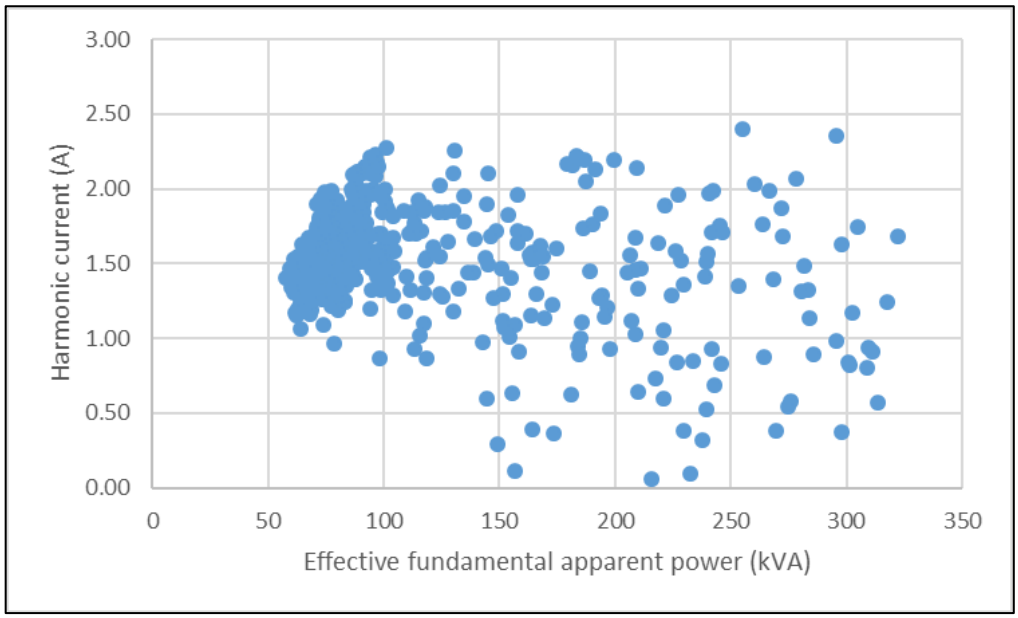

Figure 4-25: Cable 2 – harmonic current vs. effective fundamental apparent power

Figure 4-26 below, depicts the contribution of each non-fundamental apparent power. This indicates that the current distortion power is clearly the largest contributor towards the loss in apparent power capacity.

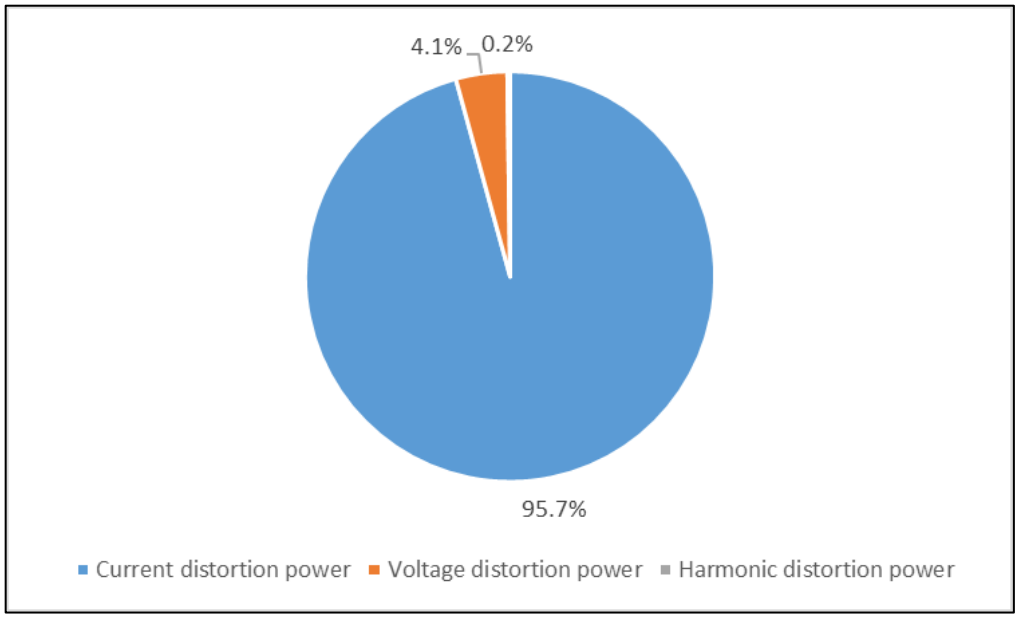

Figure 4-26: Cable 2 – non-fundamental apparent powers

4.1.3 Cable 3

For cable 3, from the secondary distribution substation to the end-user transfromer, a seven-day dataset containing 1 008 ten-minute samples from 15 November 2014 at 00:00 to 21 November 2014 at 23:50, was used for the data analysis on Cable 3. To verify the configuration of both instruments, Pearson's correlation coefficient was calculated as 0.99, and the output/input ratio as 85.32%. This was confirmed when the two load profiles were plotted on the same axis (cf. Fig 4-27 below), and the configuration of both instruments on Cable 3 was, therefore, accepted as correct.

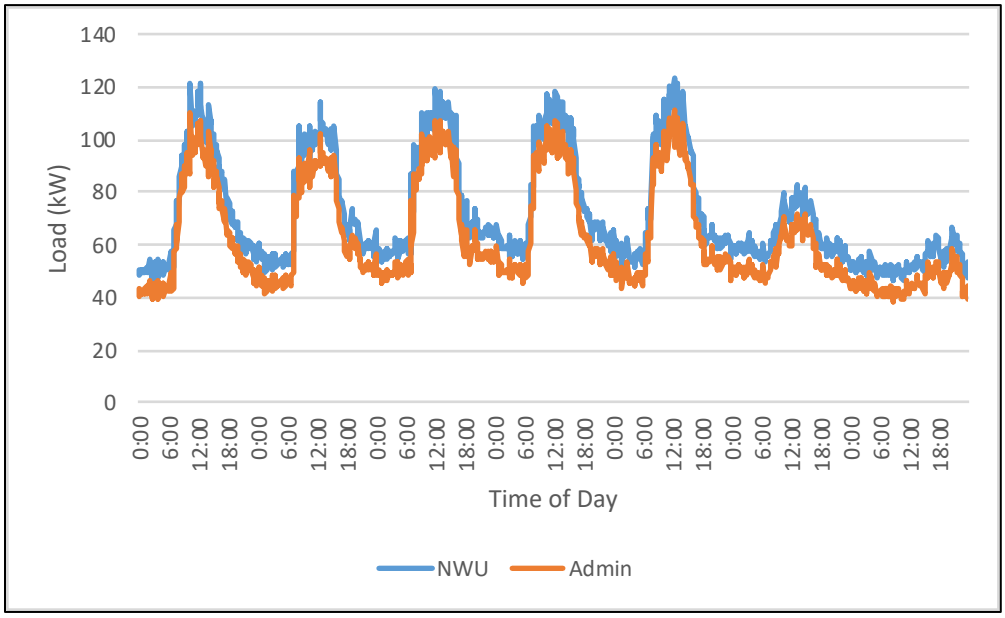

Figure 4-27: Cable 3 – load profile

4.1.3.1 Active power losses in Cable 3

The portion of the network between the monitoring instruments includes both a section of cable and a transformer. Therefore, the standard load loss for a transformer was added to the values at the output instrument to isolate the losses in the cable. The results for active power losses are depicted in Figure 4-28 below. This indicates that the calculated cable losses were found to be extremely limited and barely distinguishable from the base transformer's loss.

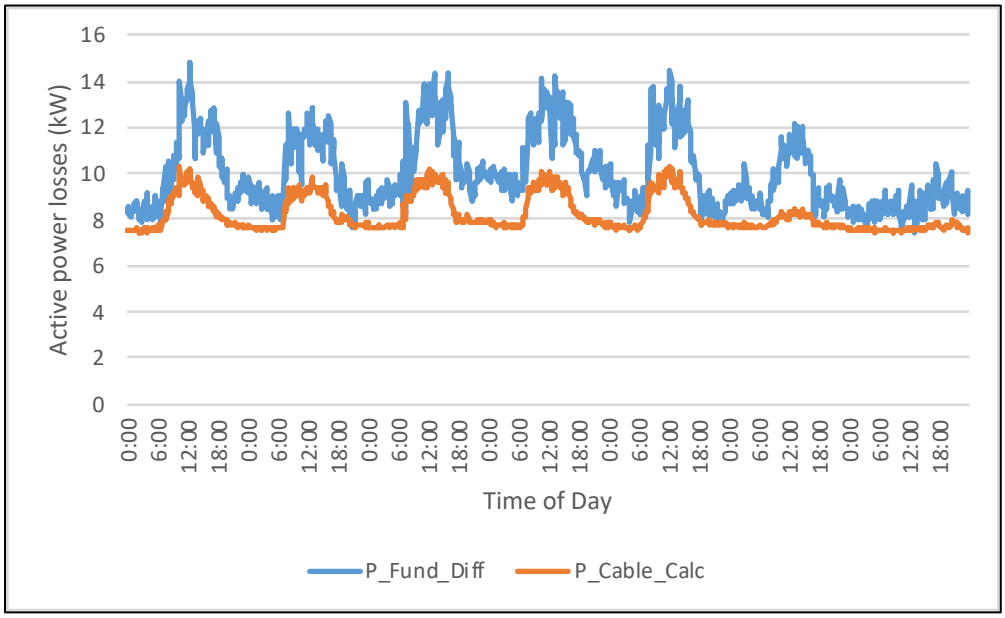

Figure 4-28: Cable 3 – active power losses

The active power losses were calculated in two ways:

- ***Method 1:*** using the collected meter data and subtracting the output plus transformer loss from the input power. Due to a lack of information, the transformer loss of 7 kW, defined in section 3.4.1.2, was used in the calculations.
- ***Method 2:*** calculating the fundamental component of equation 3-25 by using a standard resistance of 0.2316 Ω/km, as stated in the Aberdare brochure [78].

The results of the two calculation methods are presented in Table 4-6 below, indicating the limited contribution of the calculated results. Where the results differ from the results in the other cables, the reason is that the difference increases in correspondence with the increasing losses. This increase may be due to the presence of the transformer and the fact that the load loss is estimated and remains constant throughout the period of assessment.

Table 4-6: Cable 2 – comparing methods to calculate active power loss

Calculation	Method 1 result (kW)	Method 2 result (kW)	% Difference
Minimum	7,443	7,000	6
Average	10,022	7,001	43
Maximum	14,888	7,003	113

Despite removing the transformer's estimated load loss from the equation, the simplified R between the two calculation methods does not correspond, as indicated by Figure 4-29 below.

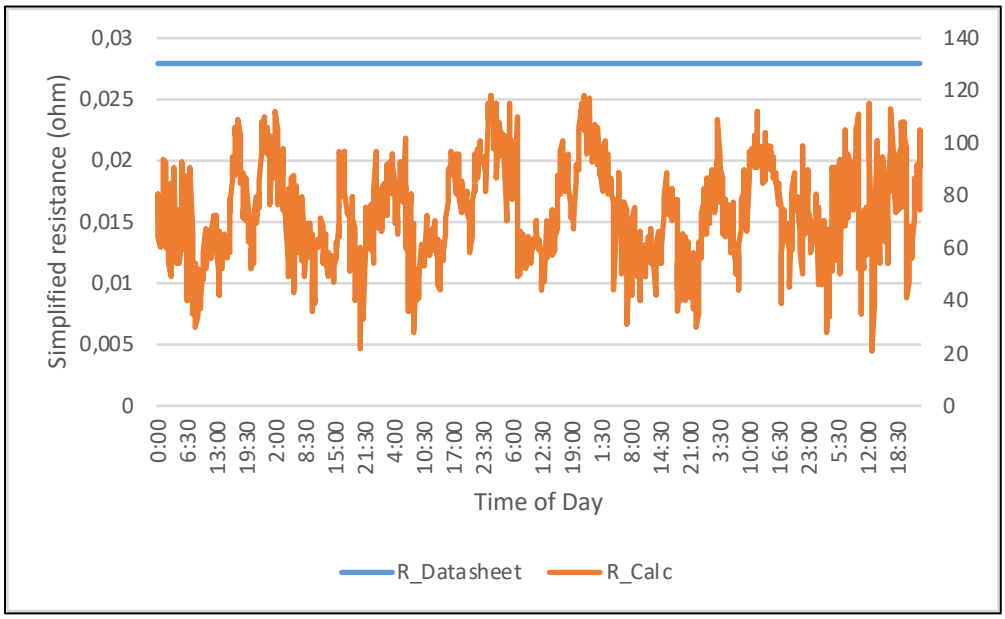

Figure 4-29: Cable 3 – simplified R

For Cable 3, the active power loss increases as the effective current increases, as is depicted clearly in Figure 4-30 below. This relationship can be defined by a 3rd order polynomial trend line (red-dash curve) with an R^2 value of 0.8389 and calculated in terms of the following equation:

$$y = 106.11x^3 - 1423.5x^2 + 7469.6x - 3355.3 \quad (4\text{-}18)$$

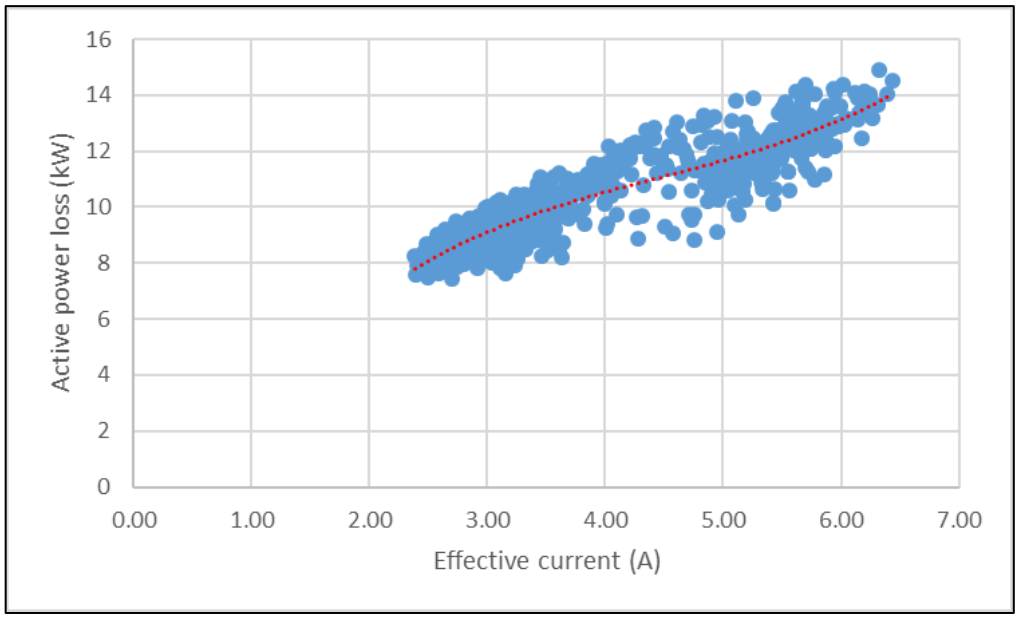

Figure 4-30: Cable 3 – active power loss vs. effective current

In the case of Cable 3, the active power loss remains relatively stable as the harmonic current changes (cf. Fig 4-31 below). The weak relationship between active power loss and harmonic

current is confirmed by the low R^2 value, 0.6963, of the 5th order polynomial trend line (red-dash curve) defined by the following equation:

$$y = 2 \times 10^6 x^5 - 5 \times 10^6 x^4 + 8 \times 10^6 x^3 - 5 \times 10^6 x^2 + 2 \times 10^6 x - 208700 \quad (4\text{-}19)$$

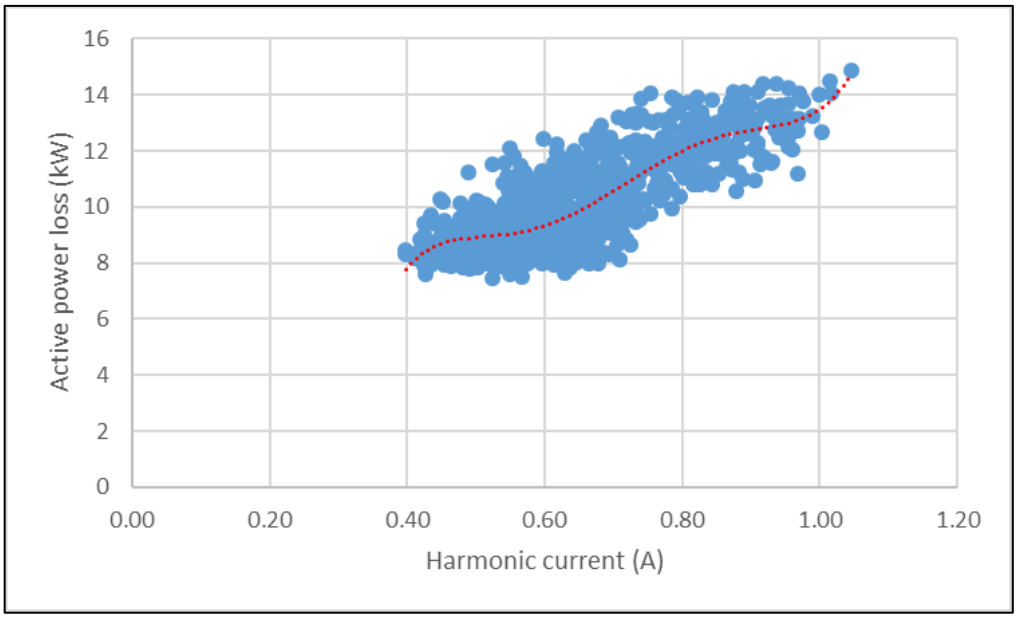

Figure 4-31: Cable 3 – active power loss vs. harmonic current

The results of the two calculation methods are presented in Table 4-7 below. Although, the values differ between the two methods, the loss percentages are closer to each other and follow the same pattern.

Table 4-7: Cable 3 – active power losses

Calculation	Method 1 (%)	Method 2 (%)	% Difference
Minimum	17	16	6
Average	14	10	40
Maximum	12	6	100

4.1.3.2 Active power losses in the transformer for Cable 3

For the MV/LV transformer supplying the end-user. Similar to the active power losses in a cable, a formula calculates the additional active power losses in a transformer due to the presence of harmonics (*see* equation 3-25). By using the methodology described in section 3.4.1.2, the

additional active power losses were calculated for the transformer at the Admin mini-substation. The results are shown in Table 4-8 below.

Table 4-8: Transformer 3 – additional active losses for transformer

Calculation	Result (%)
Minimum	0.25
Average	0.42
Maximum	0.77

These additional losses for the transformer indicate a clear relationship with the total active power flowing through the transformer, as depicted in Figure 4-32 below. This relationship can be defined by the 2nd order polynomial trend line (red-dash curve):

$$y = 5 \times 10^{-8}x^2 + 0.0004x + 13.245 \quad (4\text{-}20)$$

where the trendline has an R^2 value of 0.9609, which indicates a close correlation with the dataset.

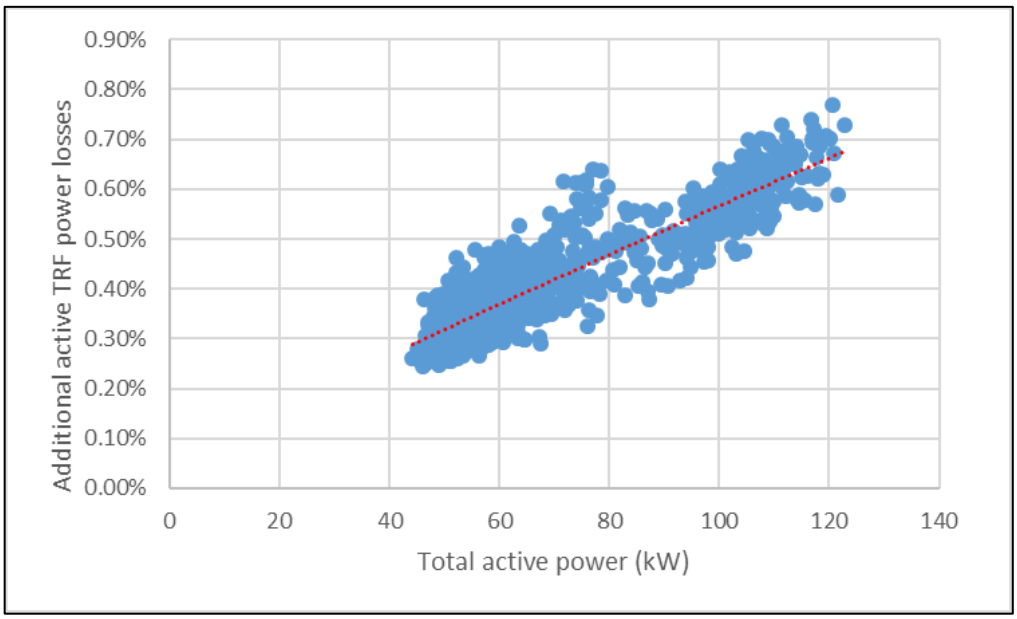

Figure 4-32: Transformer 3 – additional active losses for transformer vs. total active power

The additional transformer losses barely show any relation with the harmonic current, as is evident from Figure 4-33 below. This is supported by the low R^2 value of 0.9307 for the 5th order polynomial trend line (red-dash curve) defined by the following equation:

$$y = 0.5886x^5 - 2.0673x^4 + 2.82x^3 - 1.8621x^2 + 0.6019x - 0.074 \quad (4\text{-}21)$$

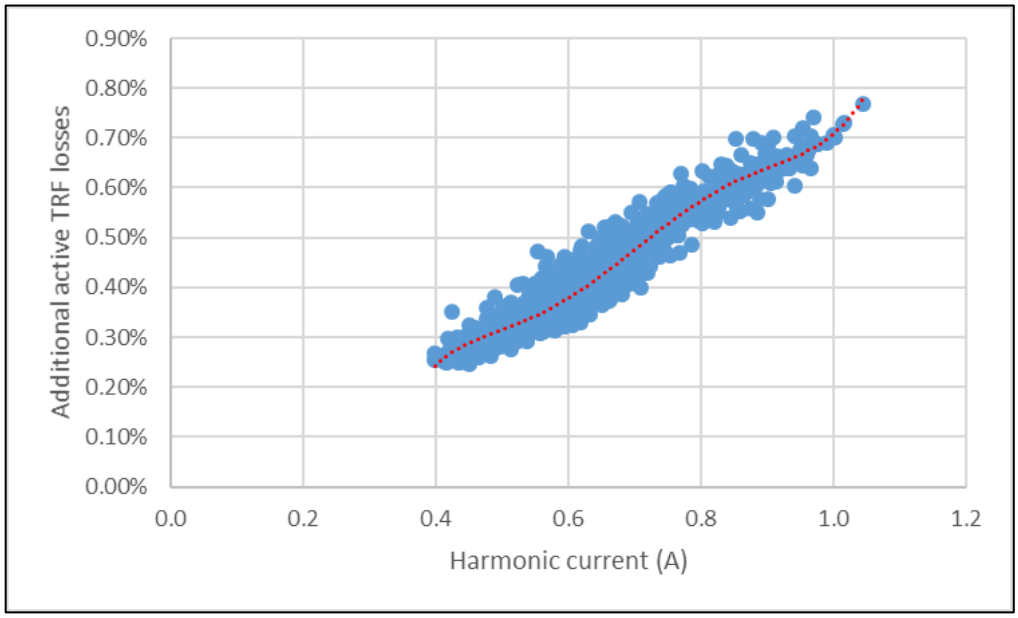

Figure 4-33: Transformer 3 – additional active losses for transformer vs. current THD

4.1.3.3 Apparent power losses in Cable 3

The loss of capacity again shows no relationship to the harmonic current, as depicted in Figure 4-34 below. This is supported by the low R^2 value (0.011) of the 4th order polynomial trend line (red-dash curve).

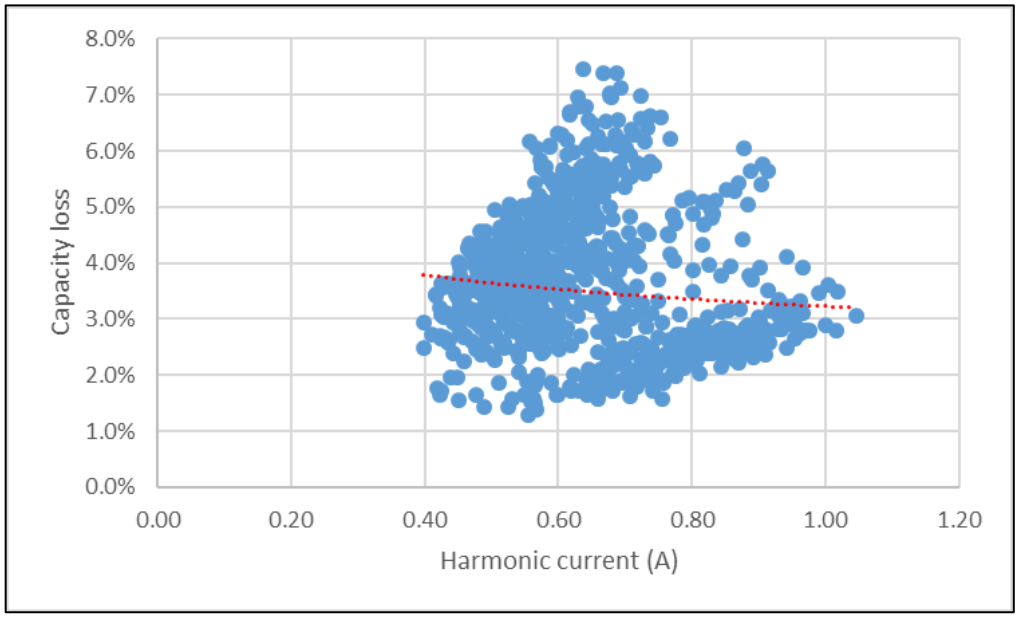

Figure 4-34: Cable 3 – capacity loss vs. harmonic current

To determine the driving factor behind the capacity loss, it was also plotted against the voltage THD. This is depicted by Figure 4-35 below, where a relationship can be seen although not as definitive as the case is with the harmonic current. This relationship is defined by a 2nd order

polynomial trend line (red-dash curve) with an R^2 value of 0.7589 defined by the following equation:

$$y = 7.0546x^2 + 0.2576x - 0.0038 \quad (4\text{-}23)$$

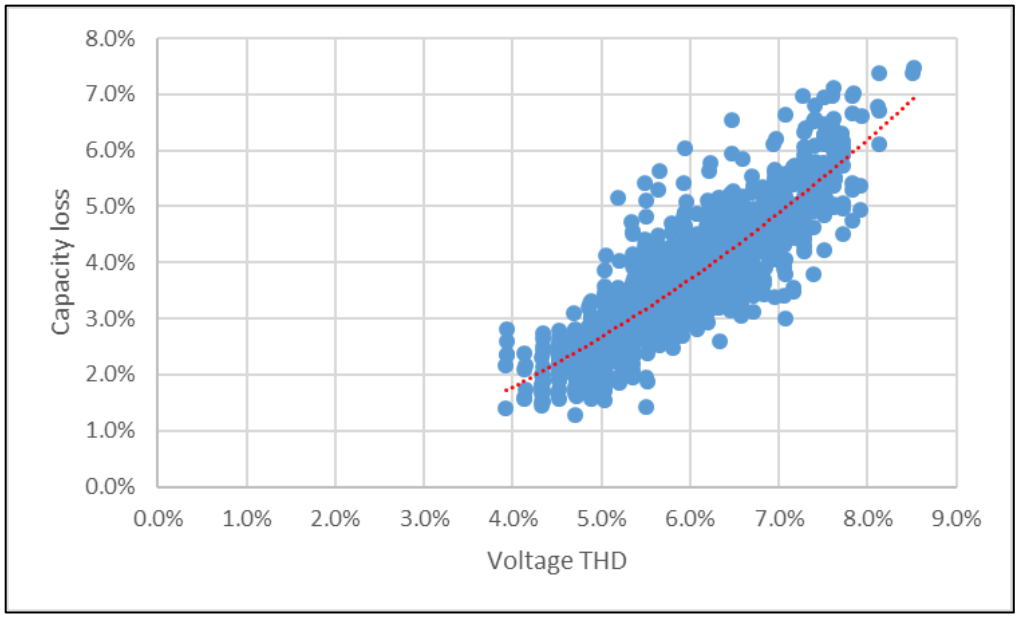

Figure 4-35: Cable 3 – capacity loss vs. voltage THD

As indicated previously, the QoS parameters in South Africa are driven from the voltage perspective. Therefore, knowledge of the relationship between the harmonic current and voltage distortion would make it possible to determine the capacity loss based on an estimated distortion of voltage. In this case is impossible to establish a clear correlation between the harmonic current and the voltage distortion, as is evident from Figure 4-36 below.

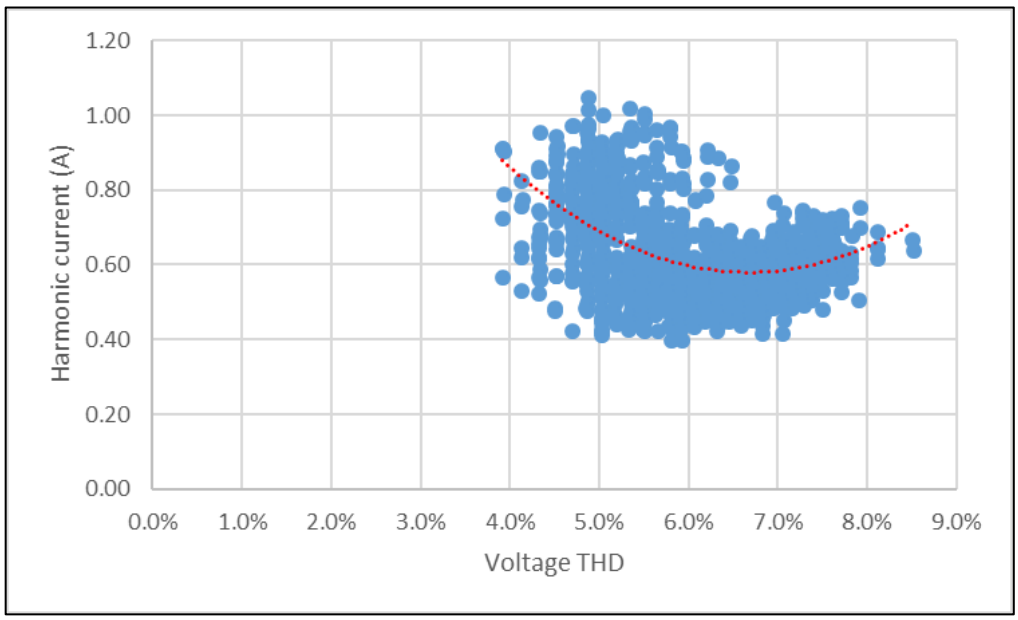

Figure 4-36: Cable 3 – harmonic current vs. voltage THD

When the loss of capacity was plotted against effective fundamental apparent power (cf. Fig 4-36 above), a decrease in the loss of capacity became evident as the effective fundamental apparent power increases. This decrease can be defined by the power trend line (red-dash curve) that has an R^2 value of 0.4755 and calculated in terms of the following equation:

$$y = 551.04x^{-0867} \quad (4\text{-}25)$$

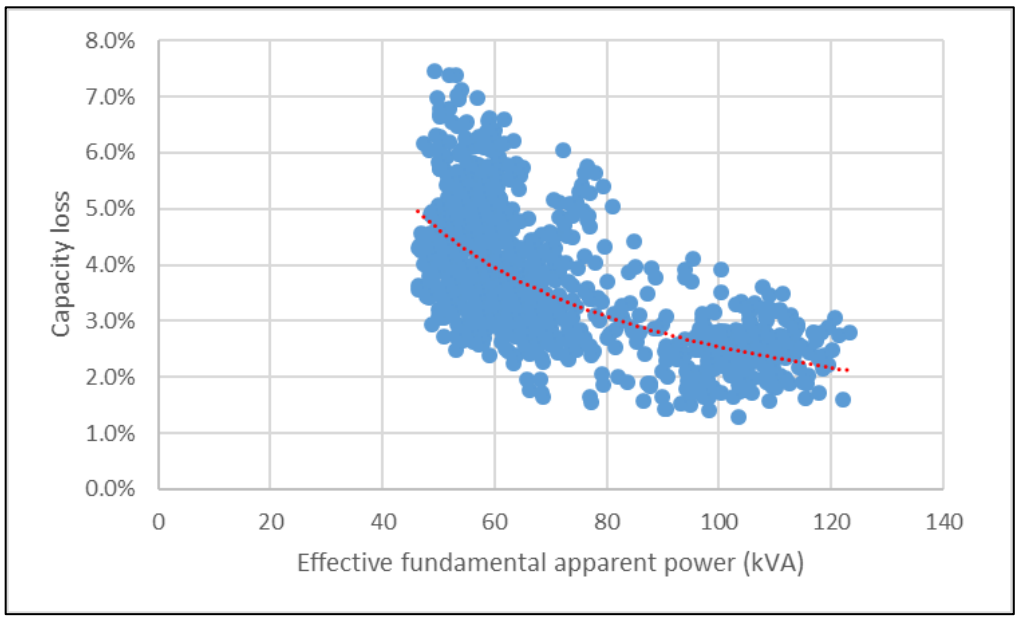

Figure 4-37: Cable 3 – capacity loss vs. effective fundamental apparent power

The result depicted by Figure 4-37 above, suggests that the current THD decreases as the effective fundamental apparent power increases. This is confirmed by Figure 4-38 below. In this depiction, the relationship between the current THD and effective fundamental apparent power is defined by a power trend line with an R^2 value of 0.6261, calculated in terms of the following equation:

$$y = 0.0008x^{0.5982} \quad (4\text{-}26)$$

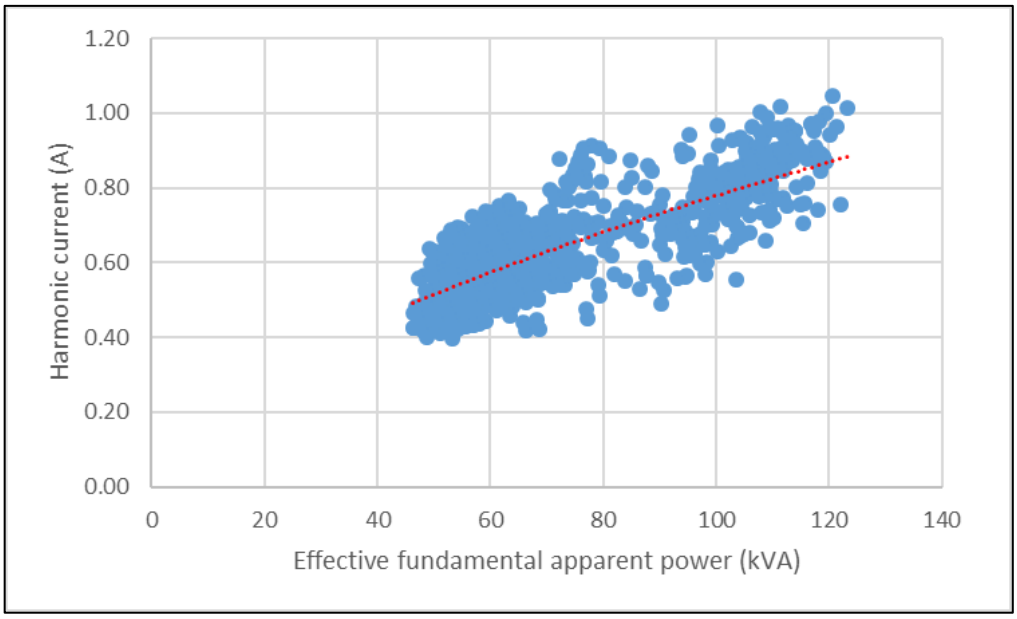

Figure 4-38: Cable 3 – harmonic current vs. effective fundamental apparent power

In combination with Figure 4-38 above, the following Figure 4-39 confirms that the current distortion is the main contributor to the capacity loss in Cable 3.

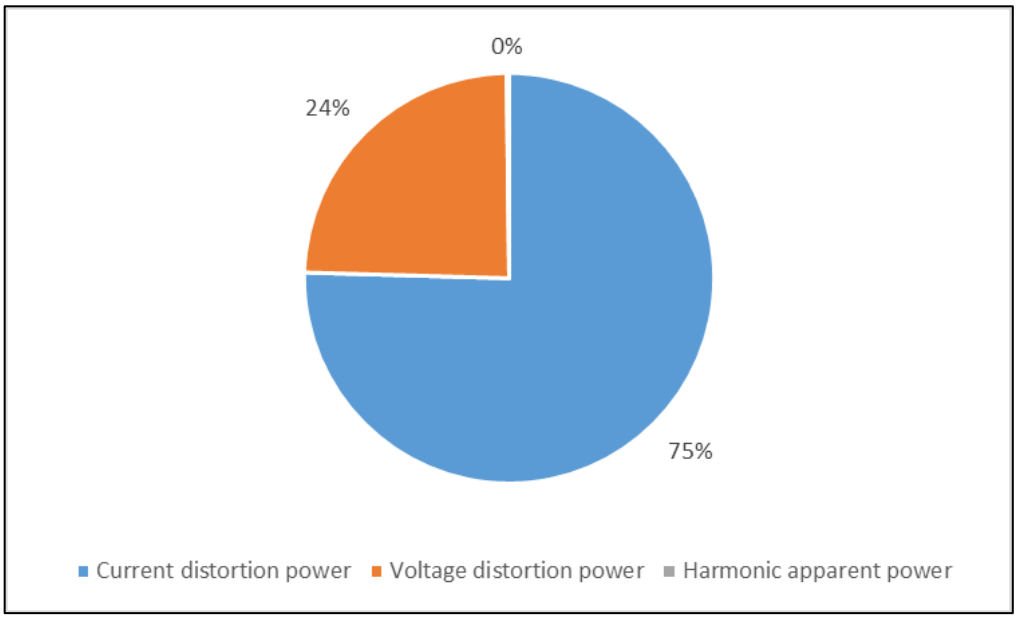

Figure 4-39: Cable 3 – non-fundamental apparent power

4.1.3.4 Transformer's harmonic de-rating

The harmonic de-rating factor for the transformer was calculated by applying equation 3-31. This factor was to be related directly to the crest factor of the current waveform, creating the expectation of a clear relationship between the crest factor and the level of harmonic current

present in the transformer. This expectation was refuted as indicated by the logarithmic trend line (red-dash curve), which indicates an R^2 value of 0.0115, as depicted by Figure 4-40 below.

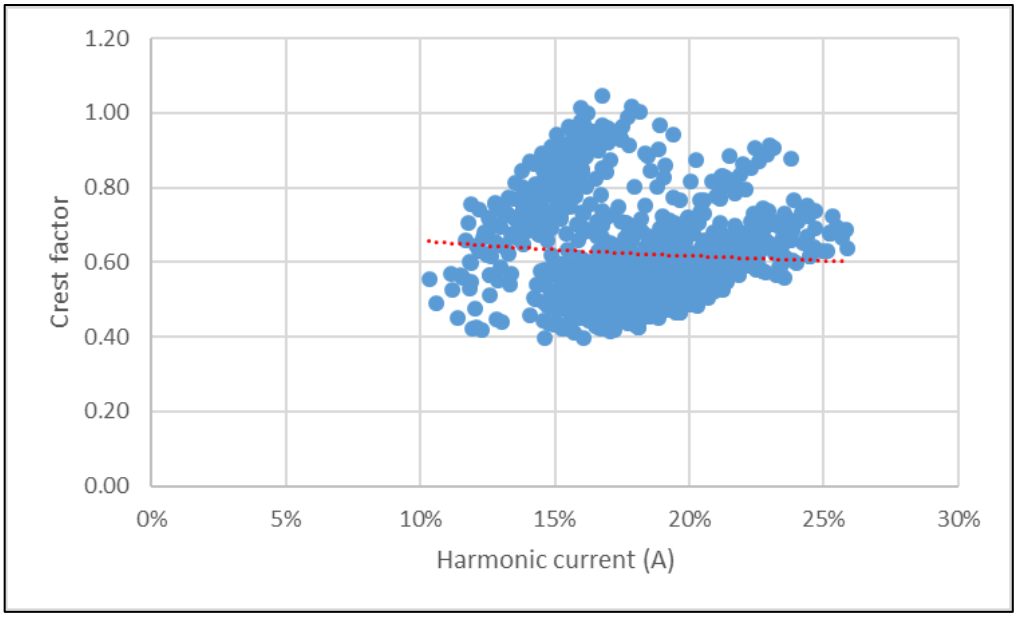

Figure 4-40: Transformer 3 – crest factor vs. current THD

4.2 Summary of work

In summary, useful data were recorded for the network analysis. No problems were experienced during the processing of the data. Both the recorded and calculated data could be verified through comparison.

4.2.1 Network analysis

The network analysis revealed definite relationships between the various PQ parameters and system losses, to such an extent that it would be possible to estimate the system losses for a given level of voltage THD.

It was also concluded that the active power losses were extremely limited and the harmonic levels did not play a major part in influencing the active power losses. Therefore, these losses were not extrapolated into the planning tool.

The following chapter (Chapter 5) provides the results of the phase-angle analysis, after which the network planning tool will be discussed in Chapter 6.

CHAPTER 5: Phase-angle analysis

The phase-angle results recorded at three sites, with various sizes of renewable DG in the form of solar PV installed, are presented and discussed in this section. As indicated previously, the datasets are:

I. NWU Engineering Campus:
    a. NWU solar plant (solar PV only).
II. BDB Auditors, Klerksdorp:
    a. before installation of a solar PV plant;
    b. after installation of a solar PV plant.
III. Silwerjare Old-age Home, Schweizer-Renecke:
    a. before installation of a solar PV plant;
    b. the solar PV plant only;
    c. after the installation of the solar PV plant.

It is an accepted fact that solar PV can only generate during sunlight hours. Therefore, only the sunlight hours were considered in the present investigation. Sunlight hours are defined as starting at 6:00 am and ending at 6:00 pm daily. In addition, the datasets were filtered to eliminate the 10% lowest power and 10% highest power values. This helped eliminate possible false readings or “noise” and provided a clearer answer.

Throughout the discussions, the current values were magnitude only, which should be read in conjunction with the relevant phase angles. In terms of the convention for active power flow, generation is viewed as negative power flow, and consumption as positive power flow.

5.1 NWU Engineering Campus

This site was recorded as a control dataset to compare to the data recorded at the solar PV plants in the field.

5.1.1 NWU solar plant

The first site and dataset that was investigated was the NWU solar PV plant. This plant comprises two 5 kW SMA inverters on the red phase and one 5 kW Danfoss inverter on each of the white and blue phases. The fundamental 10-minute aggregated data of the phase angles are depicted in Figure 5-1 below.

It should be noted that the analysis of the aggregated data from all of the investigated harmonic phase angles for each of the 10 minutes, follows a similar structure, which can be divided into four quadrants summarising the phase angle data for each dataset: polar plot, phase angle values, phase angle relation to current magnitude and active power. This four quadrant presentation method is used to summarize the phase angle data for all the datasets used in the phase-angle analysis.

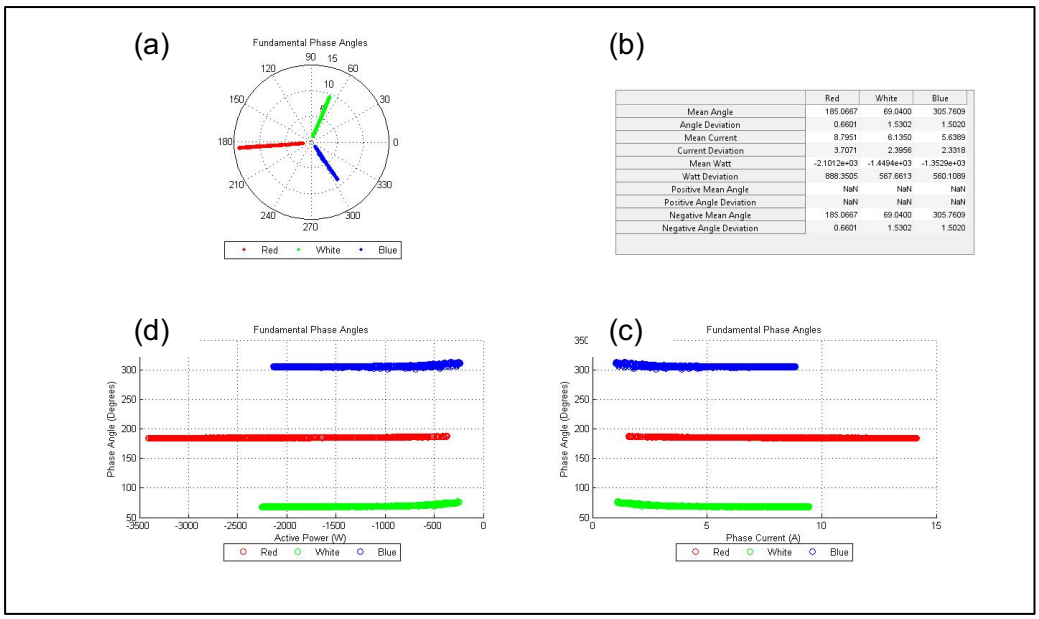

Figure 5-1: NWU solar plant – fundamental phase-angle analysis

As expected, the solar plant demonstrates highly stable phase angles, with each phase showing a clearly distinct angle. This data were used to calculate the PAR values and the prevailing phasors as presented in Table 5-1 below.

Table 5-1: NWU solar plant – calculations of fundamental current phasor

Fundamental	Red	White	Blue
Prevalence	H	H	H
PAR	1.00	1.00	1.00
Magnitude	9.54	6.59	6.1
Angle	-175.19	68.59	-54.63

All three phases returned valid PAR values, which made it possible to use the prevailing phasors in network evaluations. These phasors are depicted in Figure 5-2 below, alongside a polar plot of the aggregate data for verification regarding the phase angles. As expected, the red phasor is significantly larger than the others due to the increases in solar capacity.

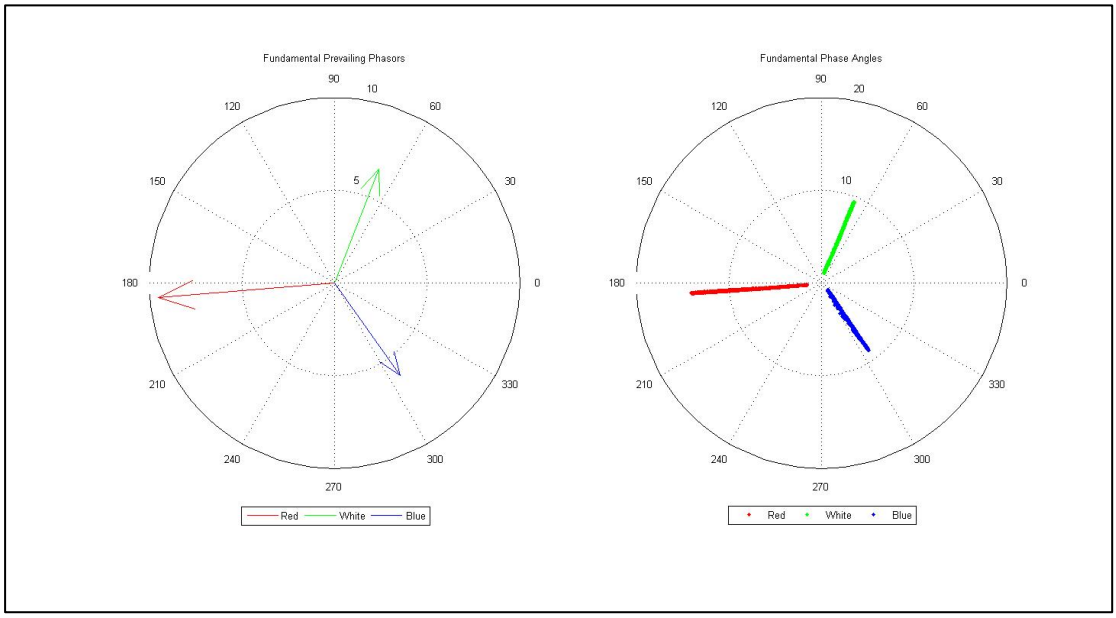

Figure 5-2: NWU solar plant – fundamental prevailing current phasors

The results from the third harmonic phase angle are depicted in Figure 5-3 below, following the described four quadrant presentation method.

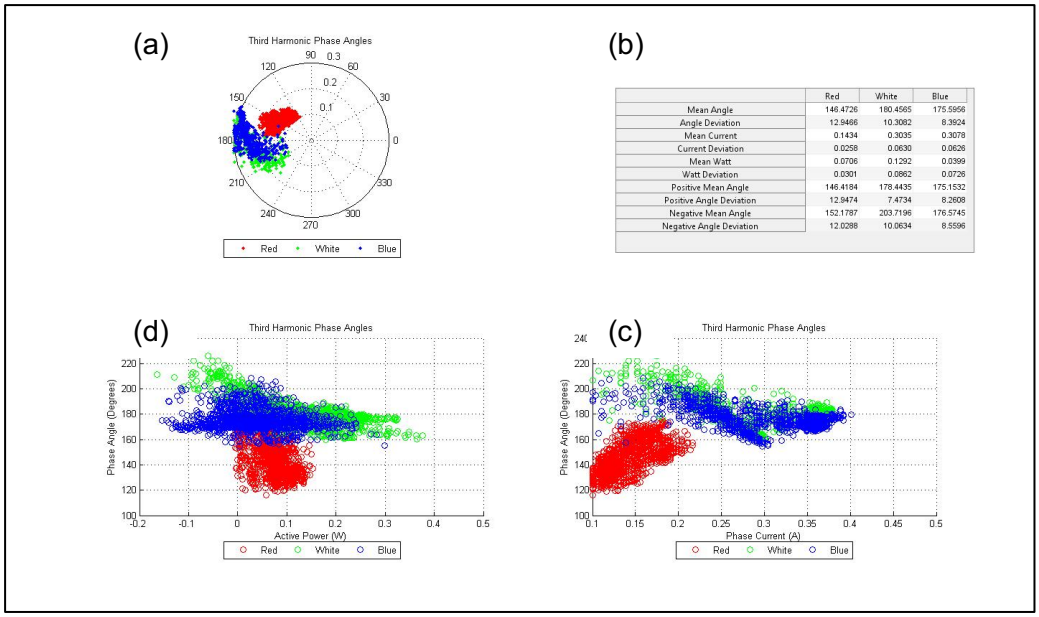

	Red	White	Blue
Mean Angle	146.4726	180.4565	175.5956
Angle Deviation	12.9466	10.3082	8.3924
Mean Current	0.1434	0.3035	0.3078
Current Deviation	0.0258	0.0630	0.0626
Mean Watt	0.0706	0.1292	0.0399
Watt Deviation	0.0301	0.0862	0.0726
Positive Mean Angle	146.4184	178.4435	175.1532
Positive Angle Deviation	12.9474	7.4734	8.2608
Negative Mean Angle	152.1787	203.7196	176.5745
Negative Angle Deviation	12.0288	10.0634	8.5596

Figure 5-3: NWU solar plant – third harmonic phase-angle analysis

The third harmonic analysis indicates bi-directional power flow, even though the phase angles are grouped in the same quadrant. The data were used to calculate the PAR values and prevailing phasors for each phase, as presented in Table 5-2 below.

Table 5-2: NWU solar plant – calculations of third harmonic current phasor

Third	Red	White	Blue
Prevalence	H	H	H
PAR	0.98	0.99	0.99
Magnitude	0.14	0.30	0.31
Angle	147.95	179.4	174.65

All three phases returned high prevalence values, which validates their use to calculate prevailing current phasors. These phasors are depicted in Figure 5-4 alongside a polar plot of the aggregated values for verification regarding the phase angles.

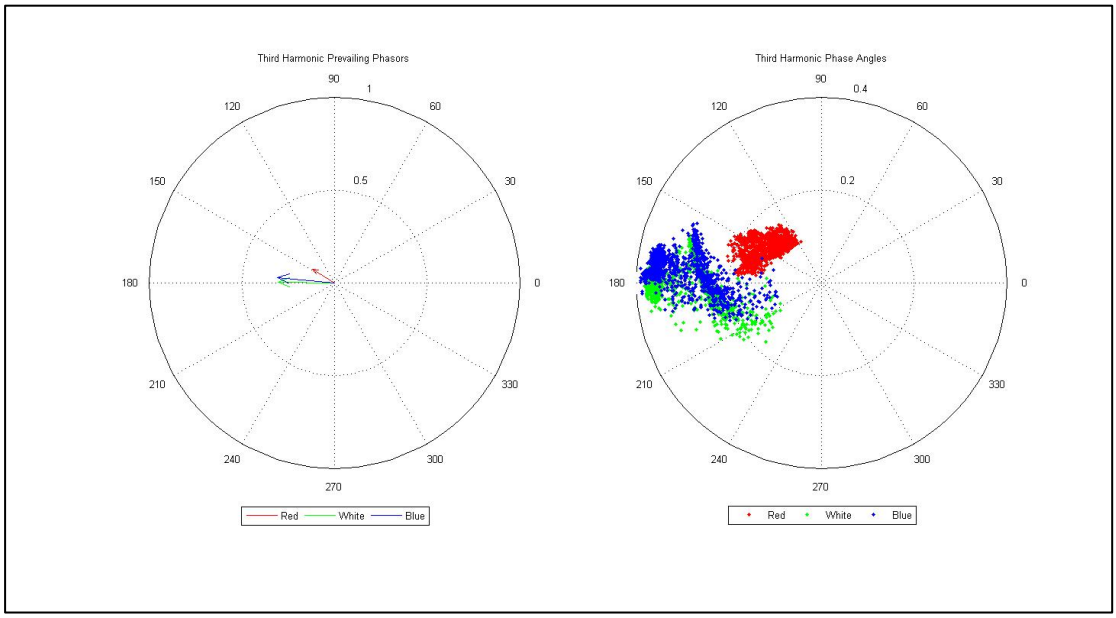

Figure 5-4: NWU solar plant – third harmonic prevailing current phasors

The results from the fifth harmonic phase angle are depicted in Figure 5-5 below, following the described four quadrant presentation method.

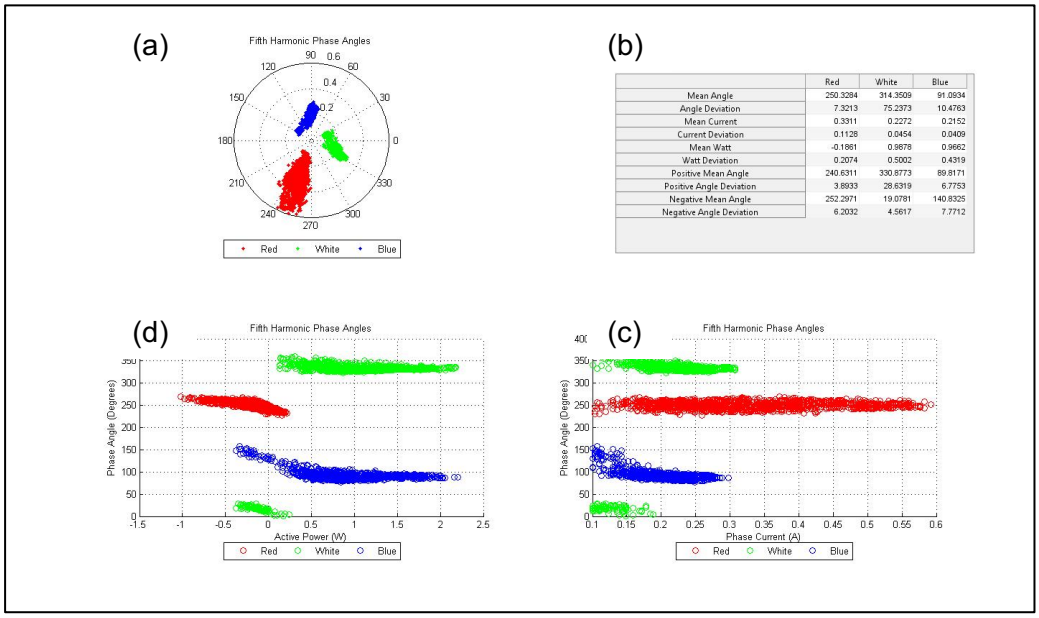

Figure 5-5: NWU solar plant – fifth harmonic phase-angle analysis

From Figure 5-5 above, it is evident that the fifth harmonic characteristics differ between the phases, and thus between inverter types as well. The red phase (SMA) only recorded negative power flow on the fifth harmonic, while the white and blue phases recorded bi-directional power flow along with the expected change in phase angle. This data were used to calculate the PAR values and prevailing phasors as presented in Table 5-3 below.

Table 5-3: NWU solar plant – calculations of fifth harmonic current phasor

Fifth	Red	White	Blue
Prevalence	H	H	H
PAR	0.99	0.99	0.99
Magnitude	0.34	0.23	0.22
Angle	-109.6	-25.79	89.73

As expected, all three phases returned valid PAR results, which made it possible to use their phasors in network evaluations. These phasors are depicted in Figure 5-6 below, alongside a plot of the aggregated phase-angle data for verification.

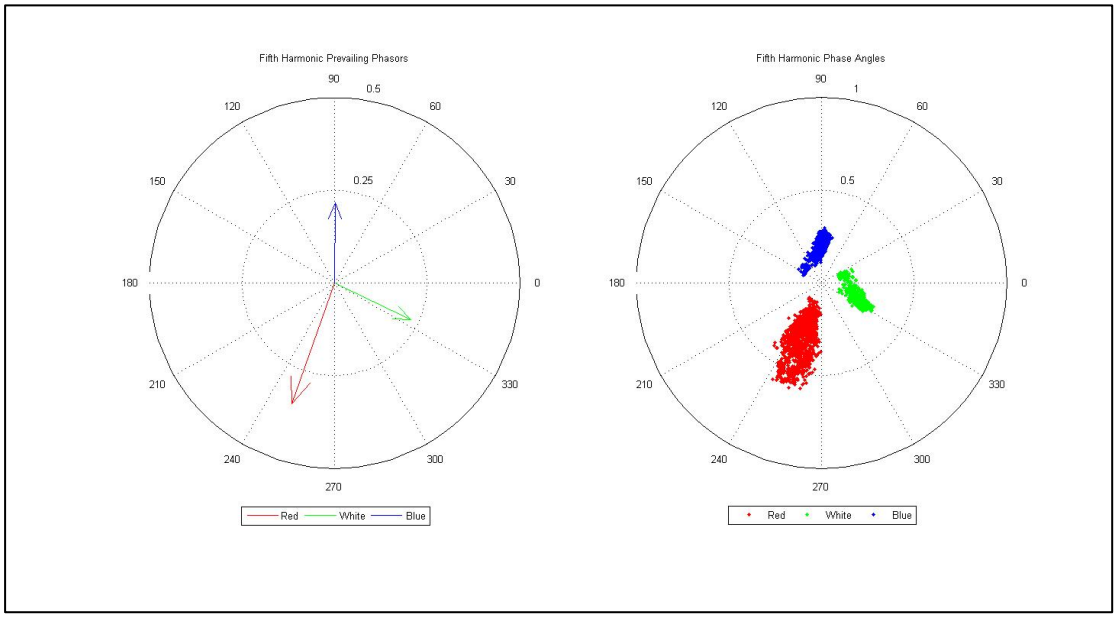

Figure 5-6: NWU solar plant – fifth harmonic prevailing current phasors

The results from the seventh harmonic phase angle are depicted in Figure 5-7 below, following the described four quadrant presentation method.

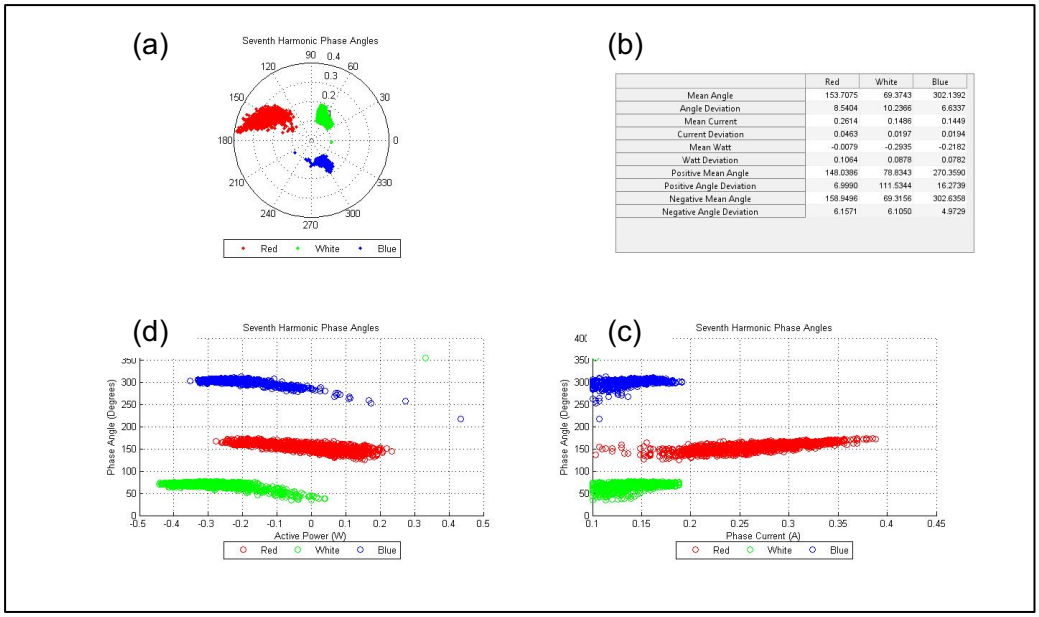

	Red	White	Blue
Mean Angle	153.7075	69.3743	302.1392
Angle Deviation	8.5404	10.2366	6.6337
Mean Current	0.2614	0.1486	0.1449
Current Deviation	0.0463	0.0197	0.0194
Mean Watt	-0.0079	-0.2935	-0.2182
Watt Deviation	0.1064	0.0878	0.0782
Positive Mean Angle	148.0386	78.8343	270.3590
Positive Angle Deviation	6.9990	111.5344	16.2739
Negative Mean Angle	158.9496	69.3156	302.6358
Negative Angle Deviation	8.1571	6.1050	4.9729

Figure 5-7: NWU solar plant – seventh harmonic phase-angle analysis

As was the case previously, differing response were found between the phases (inverter brands) with the red phase (SMA) that recorded bi-directional power flow with a near- constant phase angle. In contrast, the other phases recorded predominantly negative power flow and indicated a definite change in phase angle when the flow nears zero. This data were used to calculate the PAR and prevailing phasors for each phase, as presented in Table 5-4 below.

Table 5-4: NWU solar plant – calculations for seventh harmonic current phasor

Seventh	Red	White	Blue
Prevalence	H	H	H
PAR	0.99	0.99	0.99
Magnitude	0.26	0.15	0.14
Angle	154.84	69.61	-57.34

All three phases yielded excellent PAR values, which validates their prevailing phasors for use in network evaluations. These phasors are depicted in Figure 5-8 below, alongside a plot of the aggregated phase-angle data for verification.

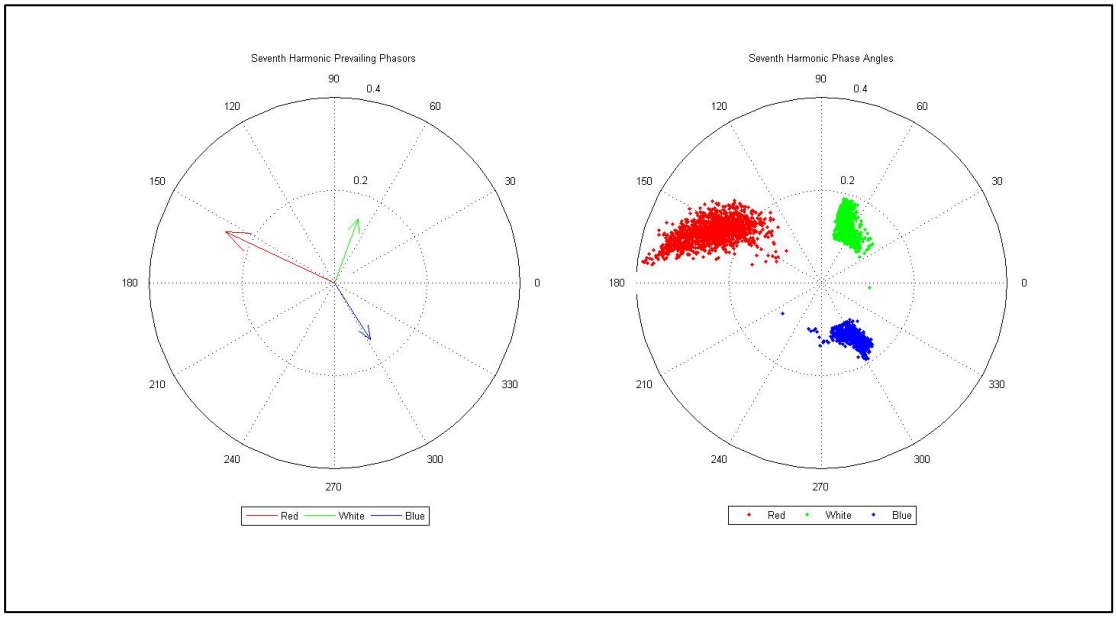

Figure 5-8: NWU solar plant – seventh harmonic prevailing current phasors

5.2 BDB Auditors

Due to the network configuration at this site it was not possible to record data for the PV plant only. The data that was recorded pre- and post-installation is presented in the following sections.

5.2.1 BDB auditors pre-solar

The first dataset of the second site is BDB Auditors before the installation of their solar PV system. The results from the fundamental phase angle are depicted in Figure 5-9 below, following the described four quadrant presentation method.

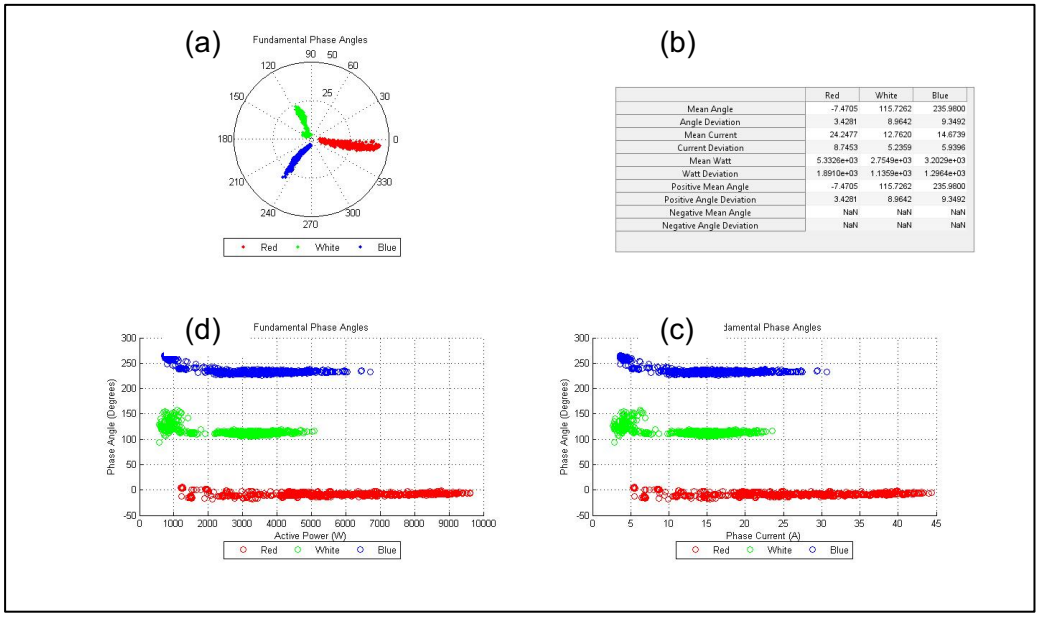

Figure 5-9: BDB Auditors pre-solar – fundamental phase-angle analysis

The aggregated phase-angle data recorded for each phase, constantly differs by approximately 120^0, as read from the results depicted in Figure 5-9 (a) above. This indicates that equipment with differing circuit topologies were installed during each phase.

Based on the collected aggregated phase-angle data depicted in Figure 5-9 above, it is possible to calculate the prevailing angle ratio (PAR) by applying equation 2.29 together with the prevailing phasor. These results are presented in Table 5-5 below.

Table 5-5: BDB Auditors' pre-solar – calculations of fundamental current phasor

Fundamental	Red	White	Blue
Prevalence	H	H	H
PAR	1.00	0.99	1.00
Magnitude	25.73	13.73	15.78
Angle	-7.64	113.36	-126.6

All three phases show high levels of prevalence, which means the calculated phasor can be used in the network evaluation. The phasors for the three phases are compared to the polar plot of the aggregated data for the phase angle (cf. Fig 5-10 below) to verify their relevance.

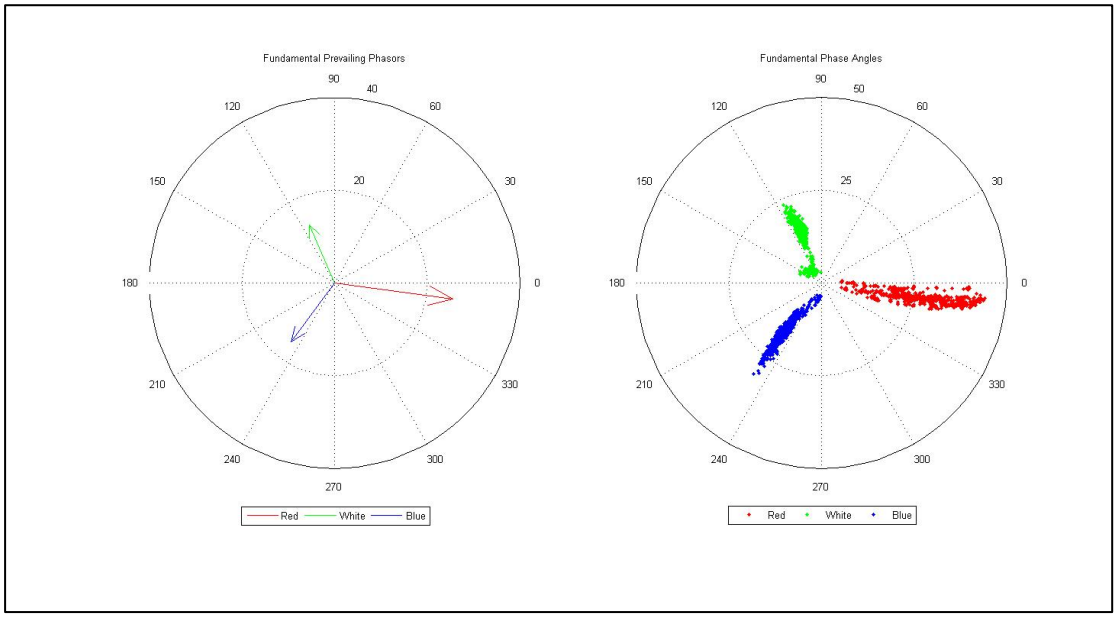

Figure 5-10: BDB Auditors pre-solar – fundamental prevailing current phasors

The results from the third harmonic phase angle are depicted in Figure 5-11 below, following the described four quadrant presentation method.

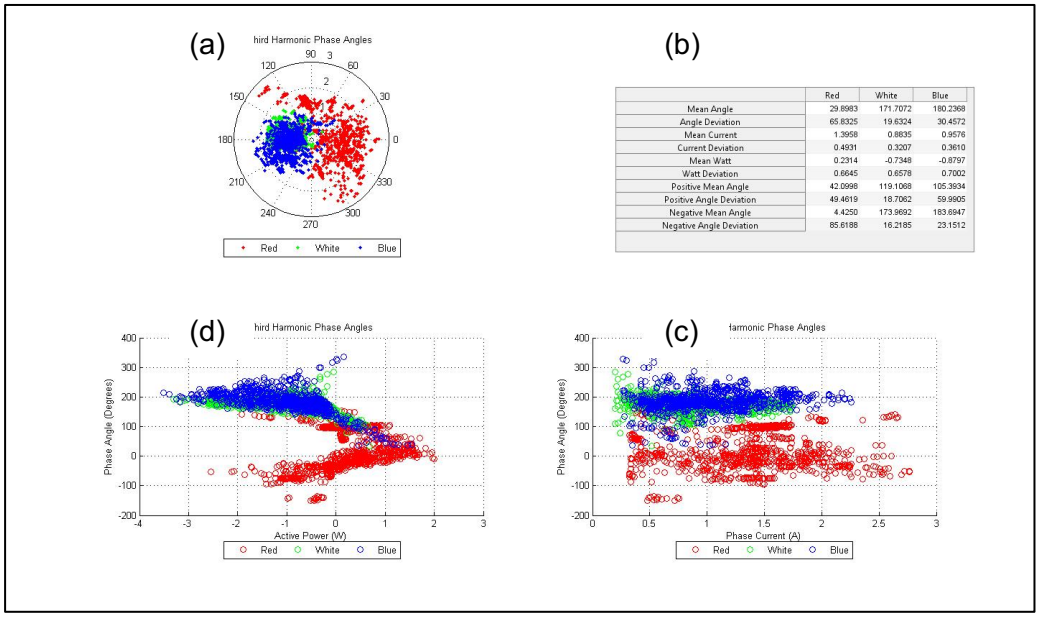

Figure 5-11: BDB Auditors pre-solar – third harmonic phase-angle analysis

In the case of the third harmonic, the aggregated phase angles were calculated to be grossly unstable as indicated by Figure 5-11 (a) above. It is evident that all three phases incurred negative active power flow (d), which indicates the presence of equipment that generate third harmonic power. This explains the randomness of the phase angles in the polar plot since the phase angle becomes unstable near zero.

Based on the collected aggregate data for the phase angle, it is possible to calculate the PAR and, where feasible, the prevailing harmonic phasor. These results are presented in Table 5-6 below.

Table 5-6: BDB Auditors pre-solar – calculations of third harmonic current phasor

Third	Red	White	Blue
Prevalence	N	H	M
PAR	0.47	0.96	0.89
Magnitude	0.82	0.87	0.86
Angle	33.80	170.76	-177.38

The red phase yielded an extremely low PAR value of 0.47. This suggests no prevailing phase angle, which is supported by the polar plot shown in Figure 5-3. The white phase yielded high prevalence, and the blue phase medium prevalence. As a result, the prevailing phasors could be calculated. This is typical of most small-scale electrical installations where electricians tend to favour the red phase when installing equipment. Thus, it can be argued that the red phase has a larger variety of electronic equipment installed. Figure 5-12 below indicates the calculated prevailing phasors and the polar plot of the aggregate phase-angle data to verify their relevance.

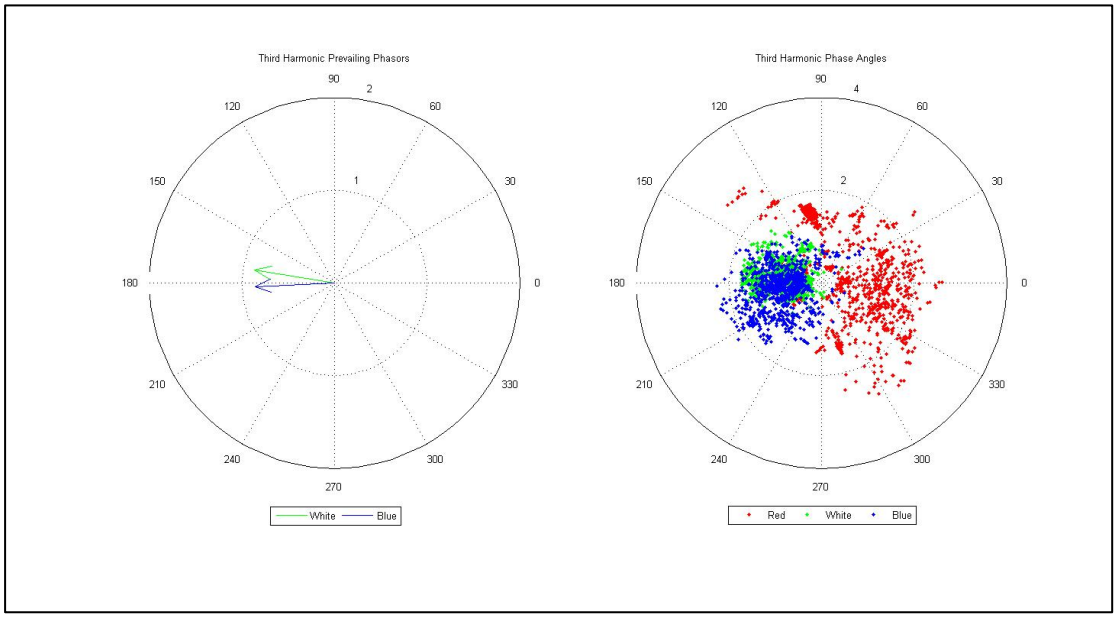

Figure 5-12: BDB Auditors pre-solar – third harmonic prevailing current phasors

The results from the fifth harmonic phase angle are depicted in Figure 5-13 below, following the described four quadrant presentation method.

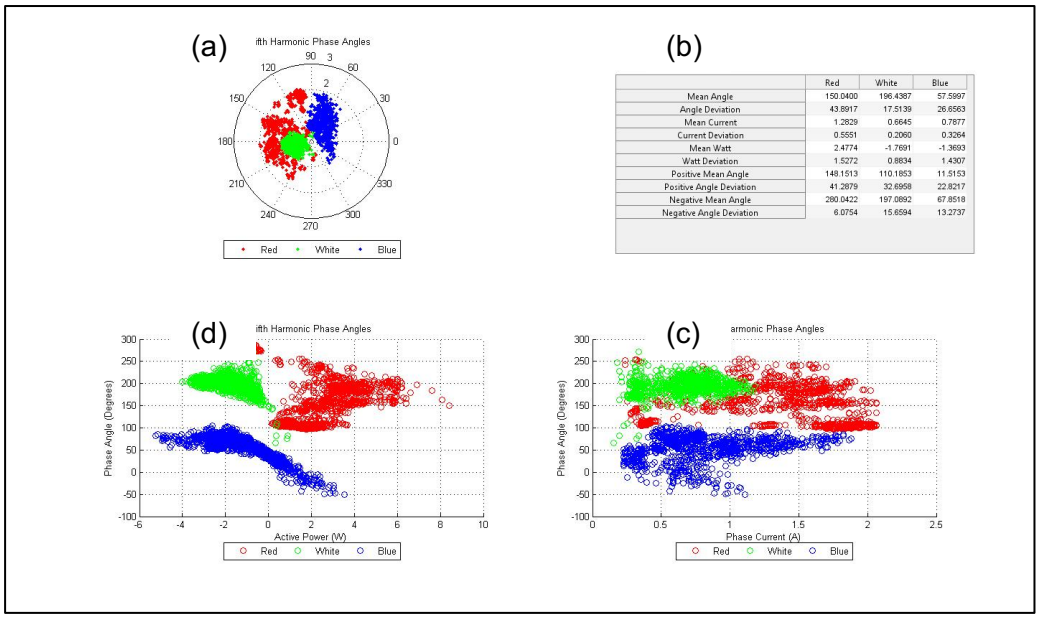

Figure 5-13: BDB Auditors pre-solar – fifth harmonic phase-angle analysis

Significant variations were found in the aggregated phase angles for the fifth harmonic, as seen in the polar plot depicted in Figure 5-13 (a) above. The white phase shows mainly negative power flow, and the red phase mainly positive power flow, while the blue phase incurred bi-directional power flow, which resulted in a 180° phase-angle change. Such a change indicates the presence of equipment with differing circuit topologies to the extent that some generate, and others absorb fifth harmonic powers.

Based on the collected aggregate data for the phase angle, it is possible to calculate the PAR and, where feasible, the prevailing phasors. These results are presented in Table 5-7 below.

Table 5-7: BDB Auditors pre-solar – calculations for fifth harmonic current phasor

Fifth	Red	White	Blue
Prevalence	N	H	M
PAR	0.75	0.97	0.91
Magnitude	0.70	0.66	0.75
Angle	148.22	-162.14	60.66

The phasor calculations confirm that the red phase has too large variations to calculate the prevailing phasor, while the white phasor indicates high prevalence, and the blue phasor medium prevalence. Figure 5-14 below shows the resulting phasors alongside the aggregated phase-angle polar plot to verify the relevance of the harmonic phasors.

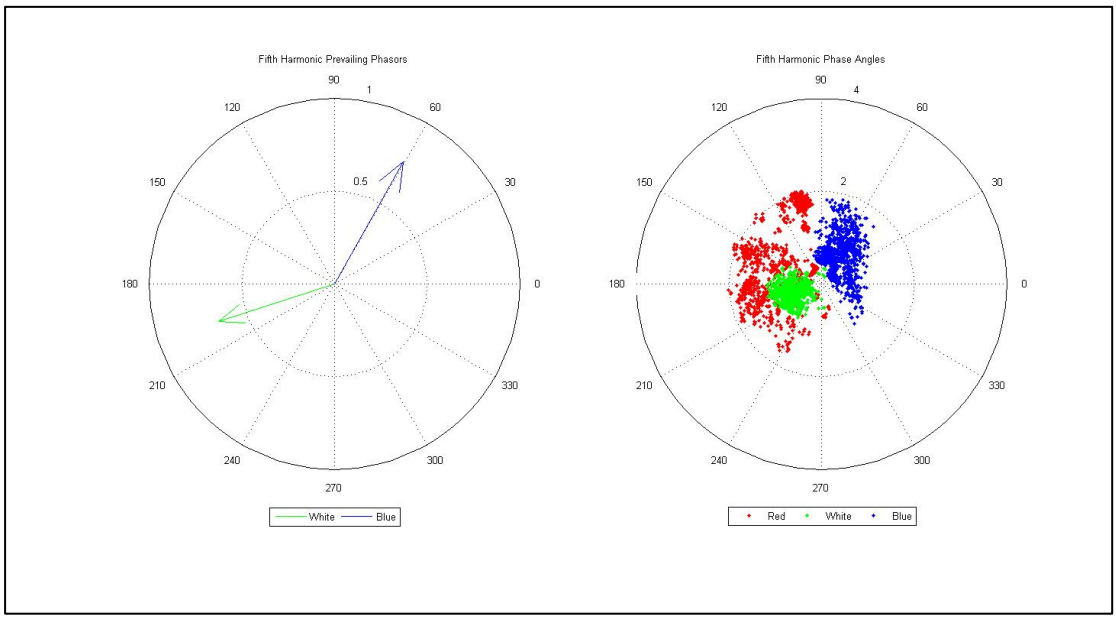

Figure 5-14: BDB Auditors pre-solar – fifth harmonic prevailing current phasors

The results from the seventh harmonic phase angle are depicted in Figure 5-15 below, following the described four quadrant presentation method.

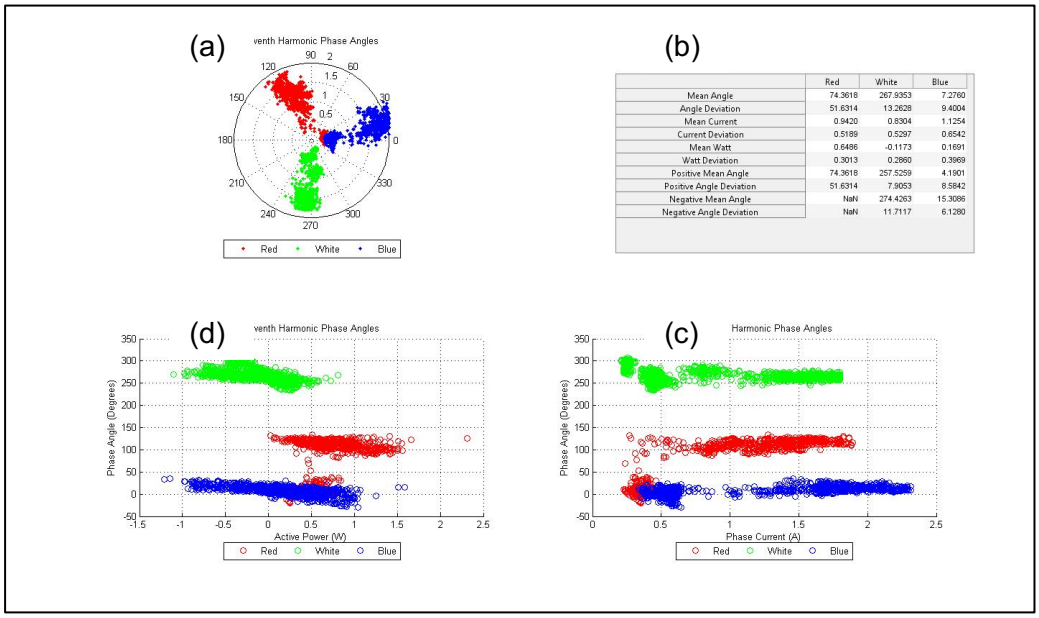

	Red	White	Blue
Mean Angle	74.3618	267.9353	7.2760
Angle Deviation	51.6314	13.2628	9.4004
Mean Current	0.9420	0.8304	1.1254
Current Deviation	0.5189	0.5297	0.6542
Mean Watt	0.6486	-0.1173	0.1691
Watt Deviation	0.3013	0.2860	0.3969
Positive Mean Angle	74.3618	257.5259	4.1901
Positive Angle Deviation	51.6314	7.9053	8.5942
Negative Mean Angle	NaN	274.4263	15.3086
Negative Angle Deviation	NaN	11.7117	6.1280

Figure 5-15: BDB Auditors pre-solar – seventh harmonic phase-angle analysis

The polar plot of the aggregated phase angles indicates closely grouped angles for each phase. Both white and blue phases recorded negative active power flow, while the red phase recorded only positive active power. Again, these results highlight the different responses of the inverter technologies that were installed during each phase.

Based on the collected aggregated data for the phase angle, it was possible to calculate the PAR and, where feasible, the prevailing phasor; these results are presented in Table 5-8 below.

Table 5-8: BDB Auditors pre-solar – calculations of seventh harmonic current phasor

Seventh	Red	White	Blue
Prevalence	L	H	H
PAR	0.83	0.99	0.99
Magnitude	1.01	0.97	1.28
Angle	104.61	-94.30	10.38

From Table 5-8 above, it is evident that both the white and blue phases yielded high PAR values, while the red phase indicated low prevalence. The prevailing phasors are depicted in Figure 5-16 below, plotted next to the aggregated phase-angle polar plot to verify their relevance.

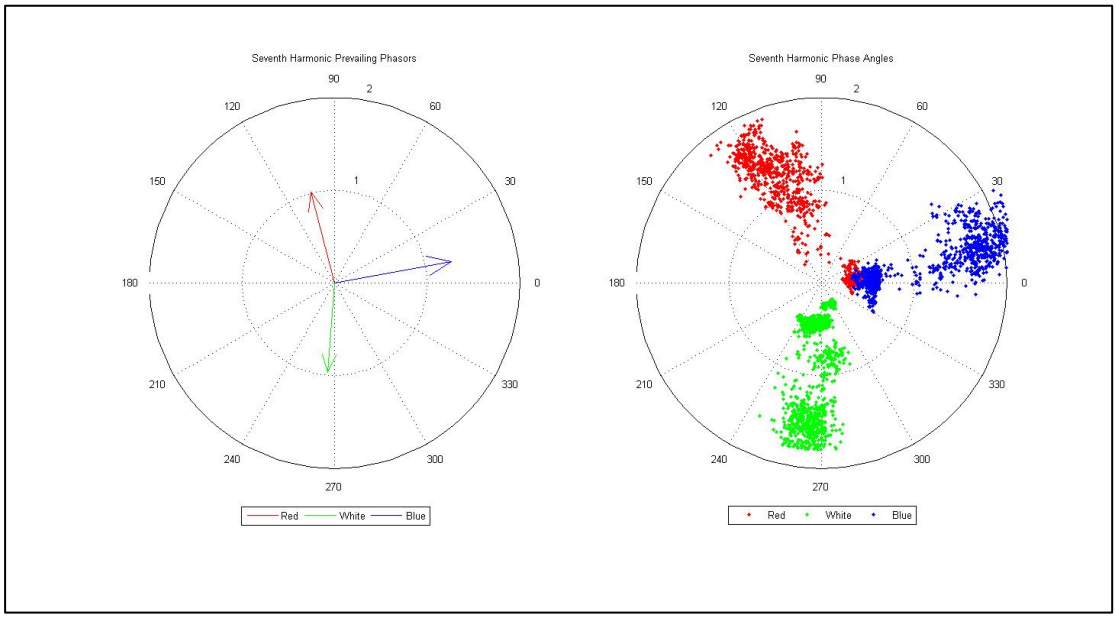

Figure 5-16: BDB Auditor pre-solar – seventh harmonic prevailing phasors

5.2.2 BDB Auditors post-solar

The second dataset of the second site is BDB auditors after the installation of their solar PV system. The results from the fundamental phase angle are depicted in Figure 5-17 below, following the described four quadrant presentation method.

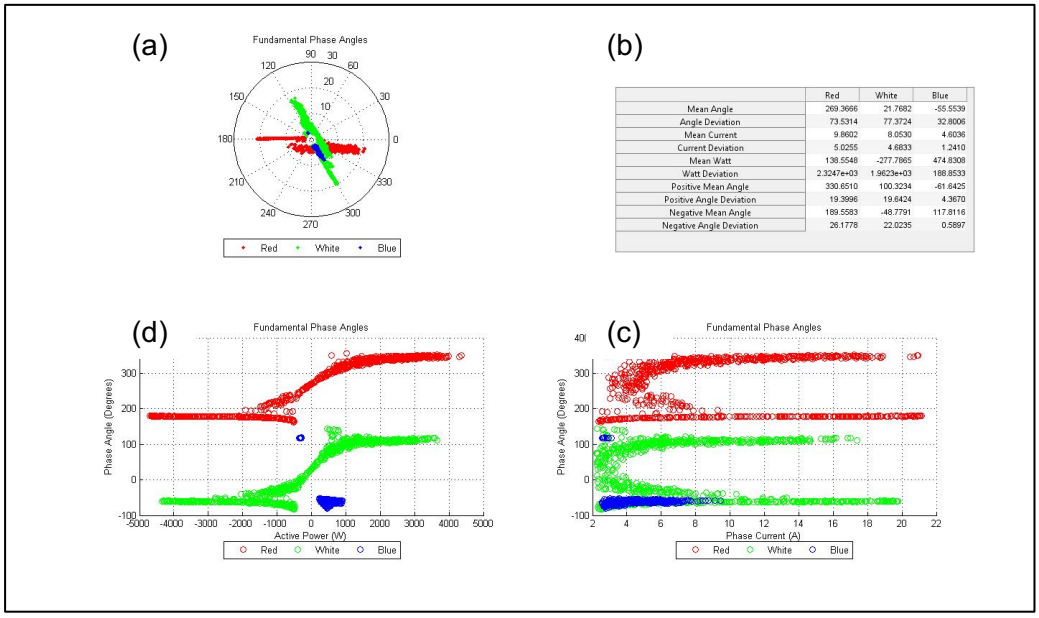

Figure 5-17: BDB Auditors post-solar – fundamental phase-angle analysis

Seeing that the PV system has no form of active power control, bi-directional active power flow was recorded on all three phases, as shown by Figure 5-17 (d) above. During the shift from positive to negative active power flow, the phase angle was found to be extremely unstable around zero, after which it changed by 180° as the direction of the power flow changed.

Based on the data above, the PAR was calculated for each phase as well as the prevailing phasor. The results of these calculations are presented in Table 5-9 below.

Table 5-9: BDB Auditors post-solar – calculations of fundamental current phasor

Fundamental	Red	White	Blue
Prevalence	N	N	H
PAR	0.24	0.21	0.96
Magnitude	10.48	8.99	4.75
Angle	-71.73	-14.27	-61.22

Due to excessive changes in active power flow on the red and white phases, the phase angle showed a large difference. Therefore, both these phases yielded no prevalence and the harmonic phasor for these two phases can be regarded as extremely unreliable. The blue phase was reduced to almost zero throughout the recording period and showed high prevalence during this time. Figure 5-18 below depicts the prevailing phasor for the blue phase alongside the polar plot of the aggregated data for verification regarding the phase angle.

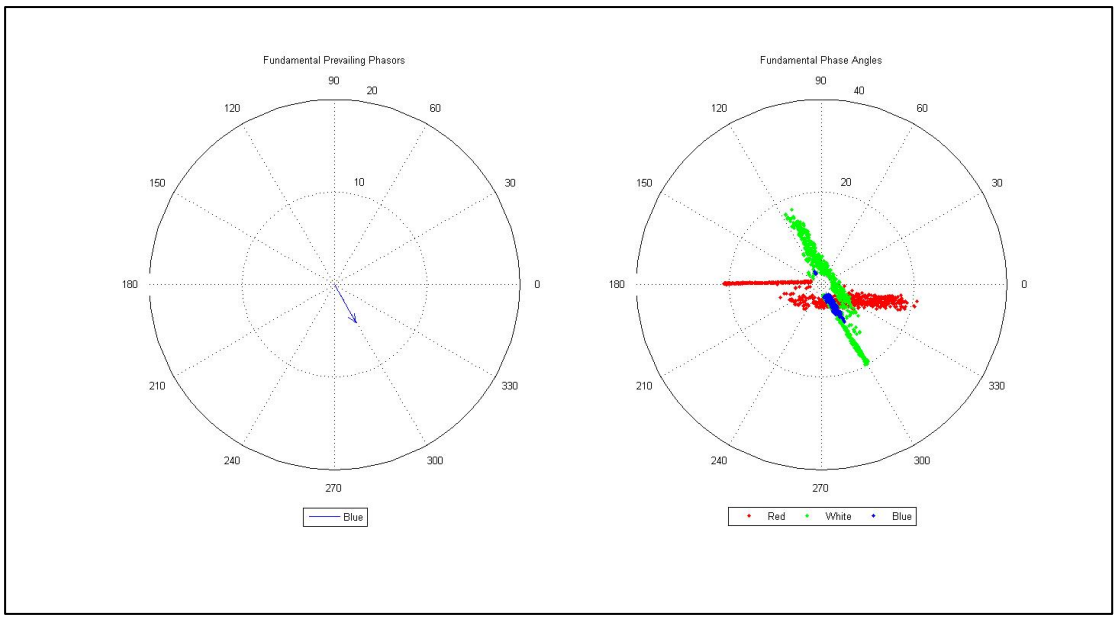

Figure 5-18: BDB Auditors post-solar – prevailing fundamental current phasors

The results from the third harmonic phase angle are depicted in Figure 5-19 below, following the described four quadrant presentation method.

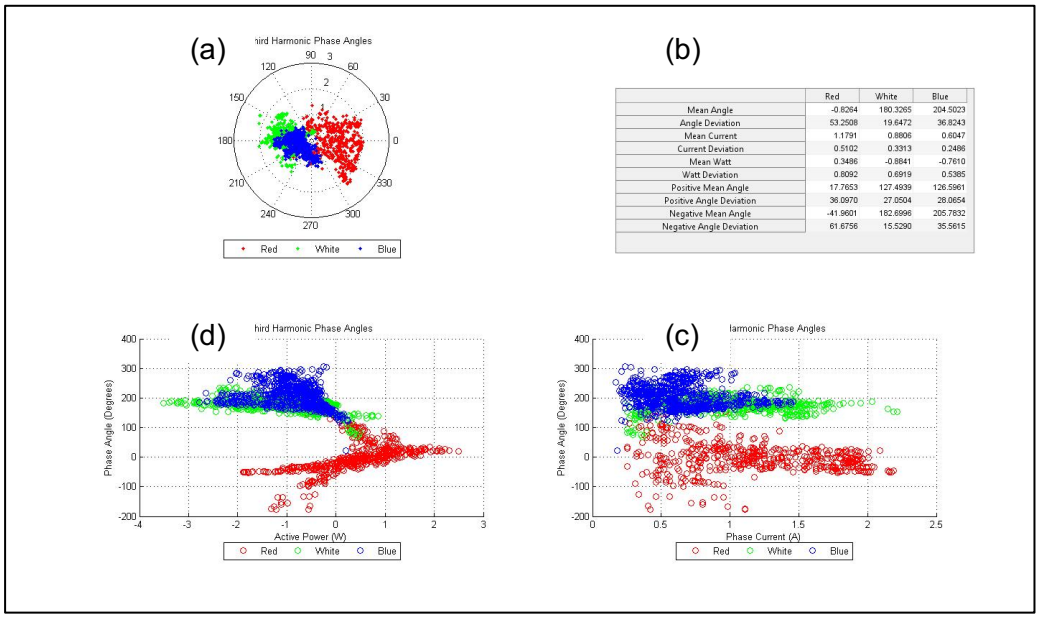

Figure 5-19: BDB Auditors post-solar – third harmonic phase-angle analysis

The data of the third harmonic shows unstable phase angles, and all three phases were found to have incurred bi-directional power flow.

Based on the collected aggregated phase-angle data, the PAR was calculated along with the prevailing phasors, and these results are presented in Table 5-10 below.

Table 5-10: BDB Auditors post-solar – calculations of third harmonic current phasor

Third	Red	White	Blue
Prevalence	N	H	L
PAR	0.78	0.95	0.81
Magnitude	0.98	0.85	0.46
Angle	-7.59	-179.56	-160.49

In accordance with the significant variations shown in Figure 5-19 above, the red phase yielded a low PAR value. This indicated that a prevailing phasor would not provide an accurate representation of the data. Both the white and blue phases yielded acceptable PAR values, and their phasors are depicted in Figure 5-20 below.

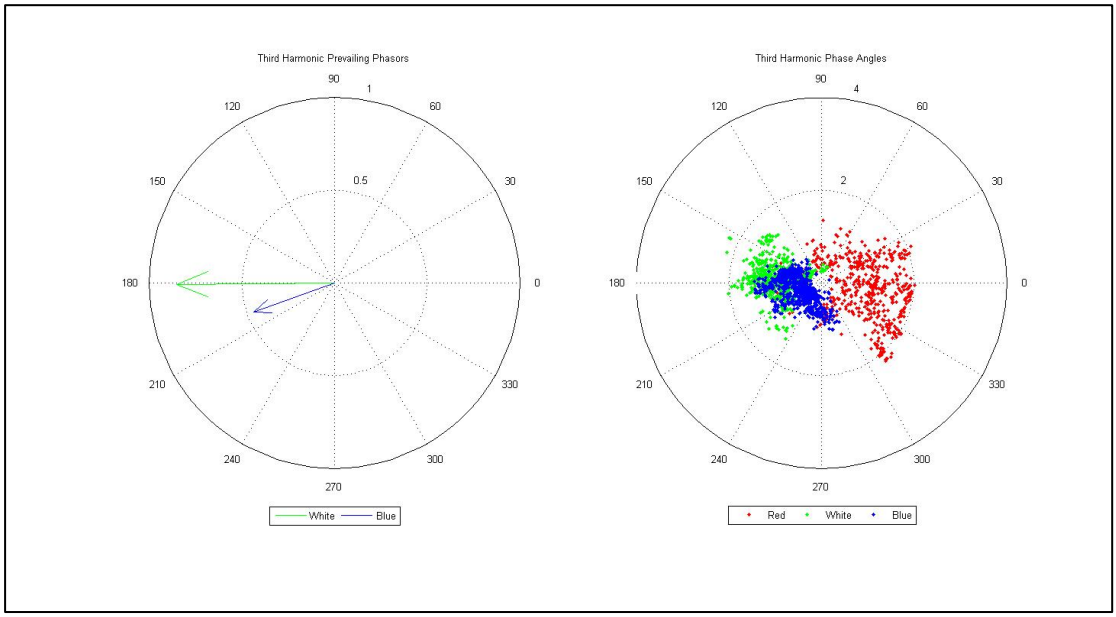

Figure 5-20: BDB Auditors post-solar – third harmonic prevailing current phasors

The results from the fifth harmonic phase angle are depicted in Figure 5-21 below, following the described four quadrant presentation method.

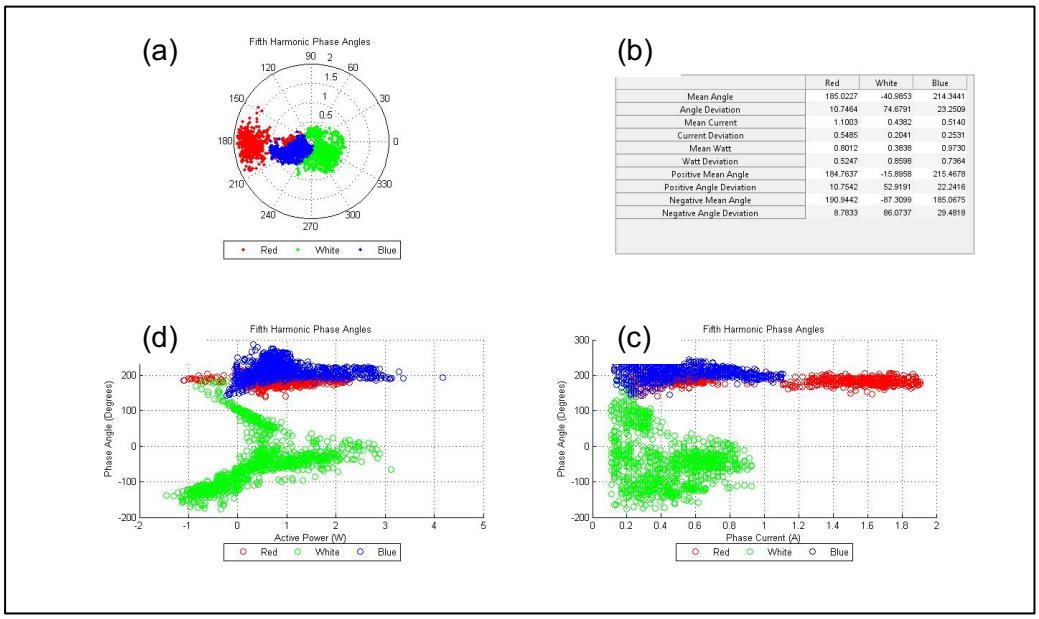

Figure 5-21: BDB Auditors post-solar – fifth harmonic phase-angle results

The red and blue phases recorded predominantly positive power flow, whereas the white phase indicated bi-directional power flow. During negative power flow on the white phase, two distinct phase angles emerge. This can be attributed to equipment with different circuit topologies that do not operate simultaneously, but both causing negative power flow on the fifth harmonic. The phase angles on all three phases show growing stability as the active power flow increases. This data were used to calculate the PAR and prevailing phase angles. The results are presented in Table 5-11 below.

Table 5-11: BDB Auditors post-solar – calculations of fifth harmonic current phasor

Fifth	Red	White	Blue
Prevalence	H	N	H
PAR	0.99	0.60	0.95
Magnitude	1.20	0.27	0.53
Angle	-176.22	-59.9	-149.72

The white phase calculated a low PAR value. This can be attributed to the bi-directional power flow and change in the direction of the phase angle during this process. Both the red and blue phases indicated high prevalence, which can be attributed to the stable phase angles during positive power flow. Therefore, only the red and blue prevailing phasors were calculated, and are

depicted in Figure 5-22 below. The polar plot of the aggregated phase-angle data were used to confirm the relevance of the prevailing phasors.

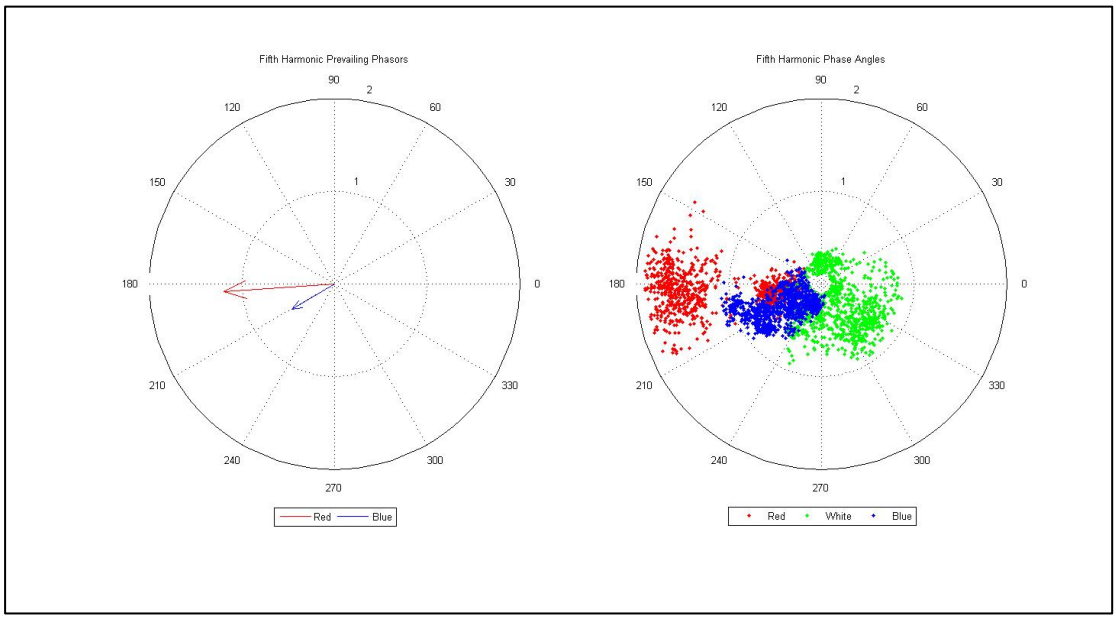

Figure 5-22: BDB Auditors post-solar – fifth harmonic prevailing current phasors

The results from the seventh harmonic phase angle are depicted in Figure 5-23 below, following the described four quadrant presentation mehtod.

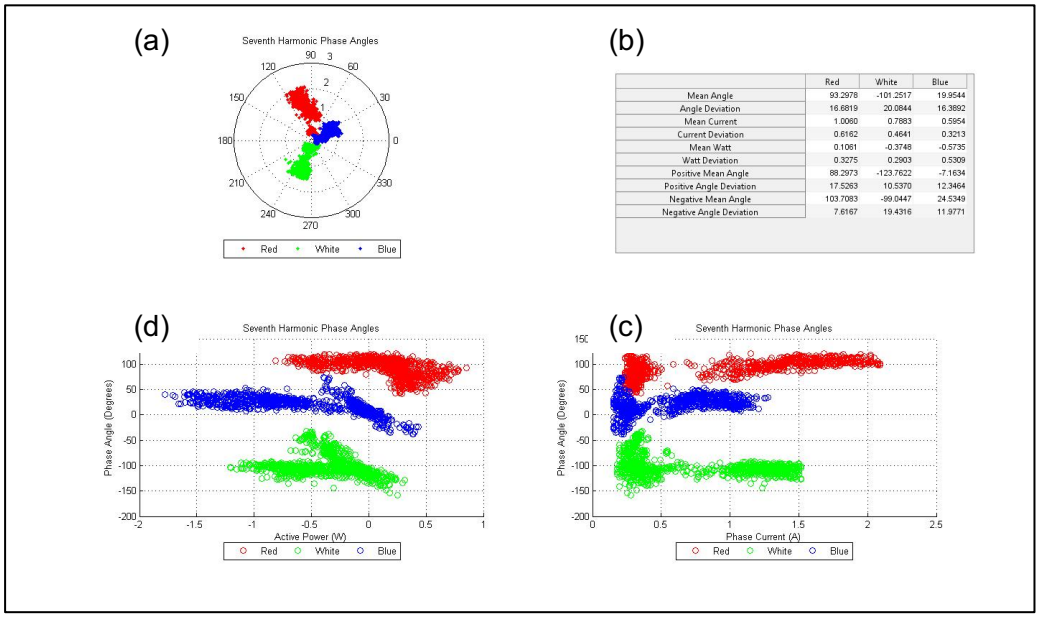

	Red	White	Blue
Mean Angle	93.2978	-101.2517	19.9544
Angle Deviation	16.6819	20.0844	16.3892
Mean Current	1.0060	0.7883	0.5954
Current Deviation	0.6162	0.4641	0.3213
Mean Watt	0.1061	-0.3748	-0.5735
Watt Deviation	0.3275	0.2903	0.5309
Positive Mean Angle	88.2973	-123.7622	-7.1634
Positive Angle Deviation	17.5263	10.5370	12.3464
Negative Mean Angle	103.7083	-99.0447	24.5349
Negative Angle Deviation	7.6167	19.4316	11.9771

Figure 5-23: BDB Auditors post-solar – seventh harmonic phase-angle analysis

All three phases recorded bi-directional power flow during the recording period, but the direction of power flow did not cause significant deviation in the phase angle. The phase angle on all three

phases shows stronger stability as the current increases. This data were used to calculate the PAR and prevailing phasors, as presented in Table 5-12 below.

Table 5-12: BDB Auditors post-solar – calculations of seventh harmonic current phasor

Seventh	Red	White	Blue
Prevalence	H	H	H
PAR	0.98	0.97	0.98
Magnitude	1.15	0.89	0.65
Angle	99.75	-105.55	23.78

As expected, all three phases returned good PAR results, which means the prevailing phasors can be used in the network evaluation. The prevailing phasors can be viewed alongside the polar plot of the aggregated phase-angle data as depicted in Figure 5-24 below.

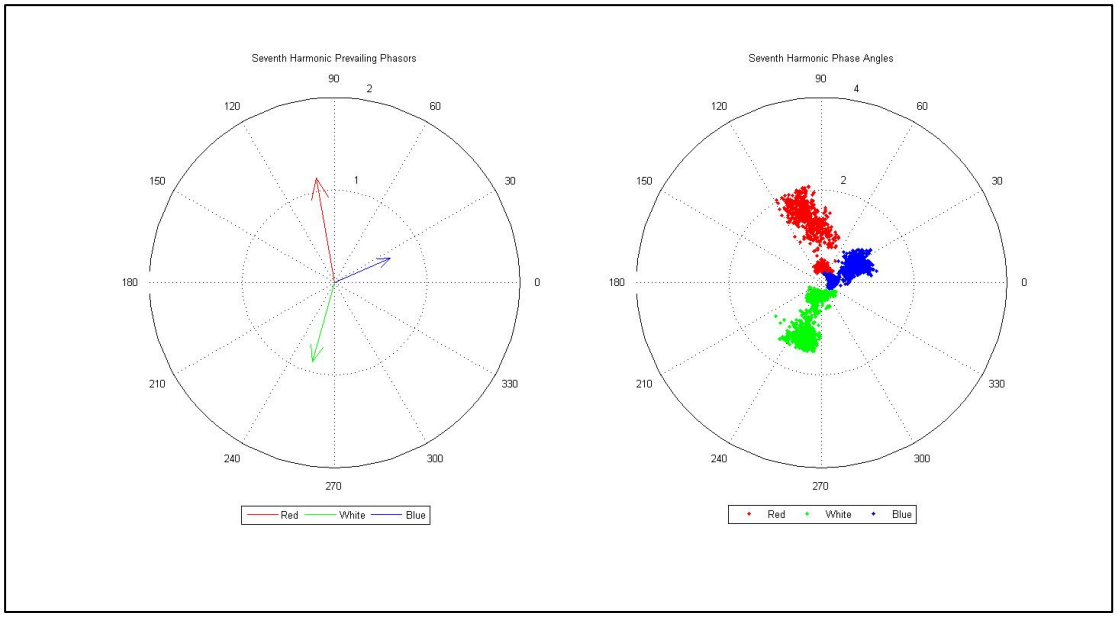

Figure 5-24: BDB Auditors post-solar – seventh harmonic prevailing current phasors

5.3 Silwerjare Old-age Home

The recorded pre- and post-installation as well as PV plant only data will be presented in the following sections.

5.3.1 Silwerjare Old-age Home pre-solar

The first dataset of the third site is Silwerjare Old-age Home before the installation of their solar PV system. The results from the fundamental phase angle are depicted in Figure 5-25 below, following the described four quadrant presentation method.

As expected, the fundamental phase angles without the installation of solar PV recorded near to textbook values, as indicated by Figure 5-25 below. During this time, all the phases only incurred positive power flow.

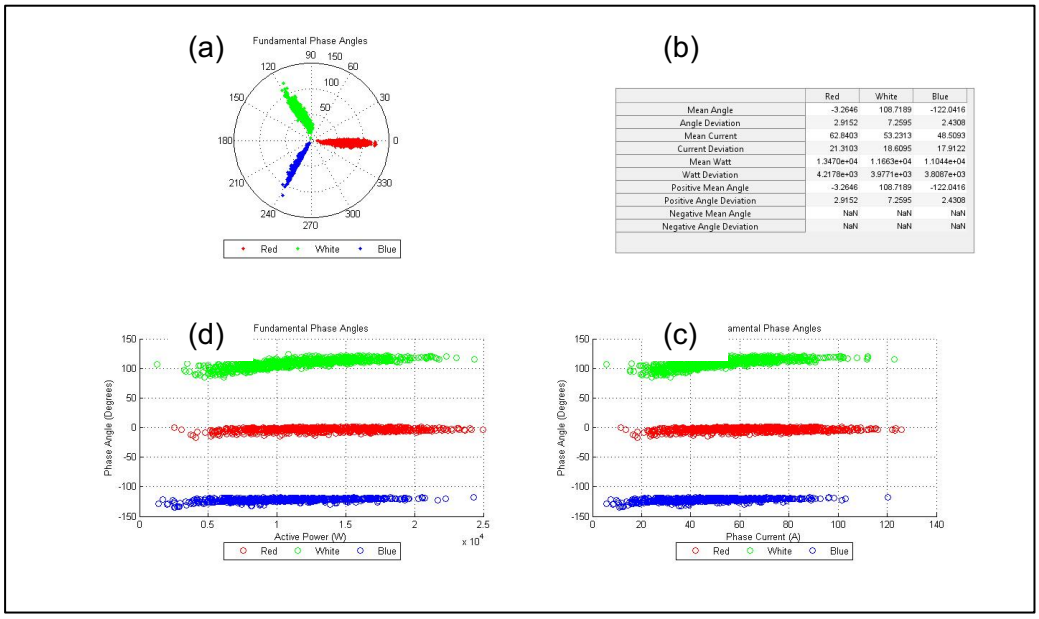

Figure 5-25: Silwerjare Old-age Home pre-solar – fundamental phase-angle analysis

This data from Figure 5-25 above, were used to calculate the PAR and prevailing phasors as presented in Table 5-13 below.

Table 5-13: Silwerjare Old-age Home pre-solar – calculations of fundamental current phasor

Fundamental	Red	White	Blue
Prevalence	H	H	H
PAR	1.00	0.99	1.00
Magnitude	66.21	55.78	51.65
Angle	-3.07	110.65	-121.59

All three phases delivered near-perfect PAR values as expected. Therefore, all three prevailing phasors can be used in the network evaluation. These phasors are depicted in Figure 5-26 below, alongside the polar plot of the aggregated phase-angle data for verification.

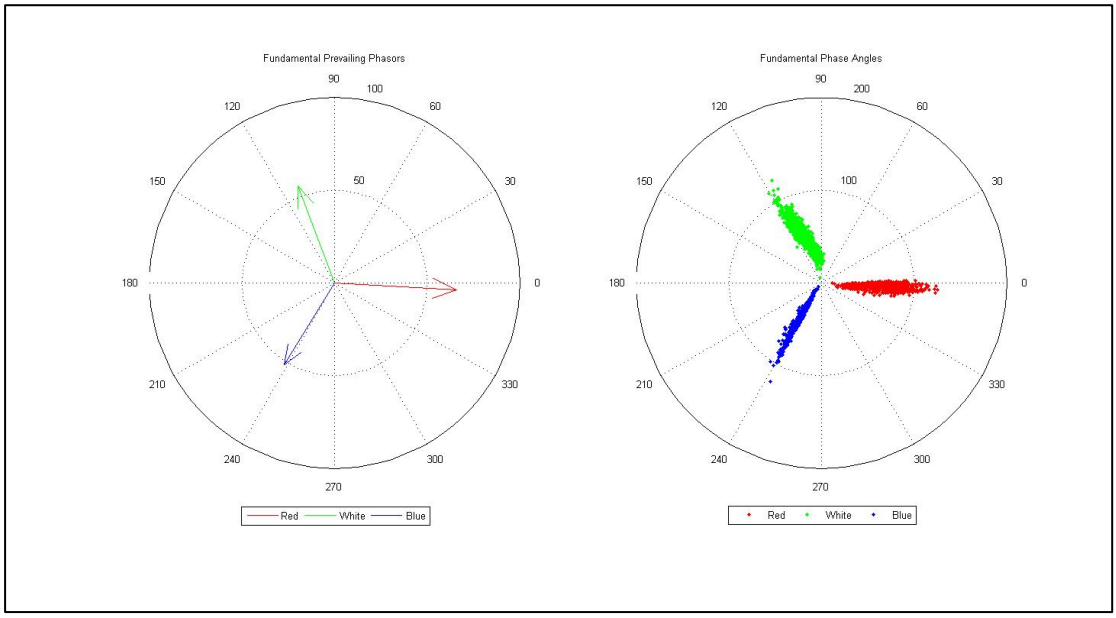

Figure 5-26: Silwerjare Old-age Home pre-solar – fundamental prevailing current phasors

The results from the third harmonic phase angle are depicted in Figure 5-27 below, following the described four quadrant presentation method.

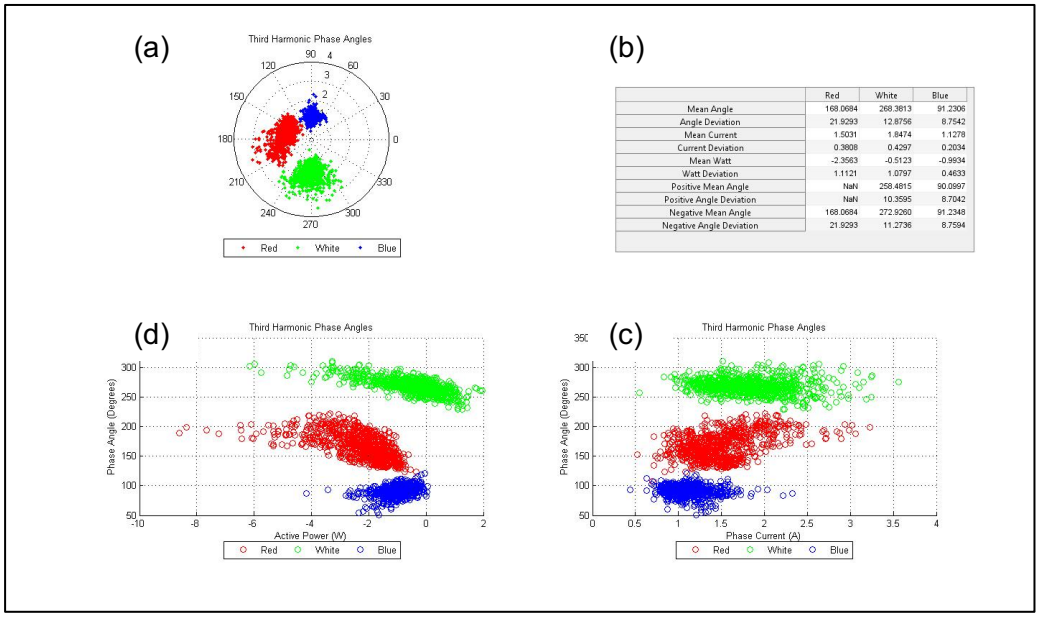

	Red	White	Blue
Mean Angle	168.0684	268.3813	91.2306
Angle Deviation	21.9293	12.8756	8.7542
Mean Current	1.5031	1.8474	1.1278
Current Deviation	0.3808	0.4297	0.2034
Mean Watt	-2.3563	-0.5123	-0.9934
Watt Deviation	1.1121	1.0797	0.4633
Positive Mean Angle	NaN	258.4815	90.0997
Positive Angle Deviation	NaN	10.3595	8.7042
Negative Mean Angle	168.0684	272.9260	91.2348
Negative Angle Deviation	21.9293	11.2736	8.7594

Figure 5-27: Silwerjare Old-age Home pre-solar – third harmonic phase-angle analysis

The data for the third harmonic shows significant variations in the aggregated phase-angle values as is evident from all the plots of Figure 5-27 above. This data were used to calculate the PAR and prevailing phase angles for the third harmonic, of which the results are presented in Table 5-14 below.

Table 5-14: Silwerjare Old-age Home pre-solar – calculations of third harmonic current phasor

Third	Red	White	Blue
Prevalence	M	H	H
PAR	0.92	0.97	0.99
Magnitude	1.31	1.79	1.12
Angle	170.32	-92.03	91.00

Despite the perceived significant variations in aggregated phase angles, all three phases yielded valid PAR results and useful prevailing phasors. These phasors are depicted in Figure 5-28 below, alongside the polar plot of the aggregated phase-angle data for verification.

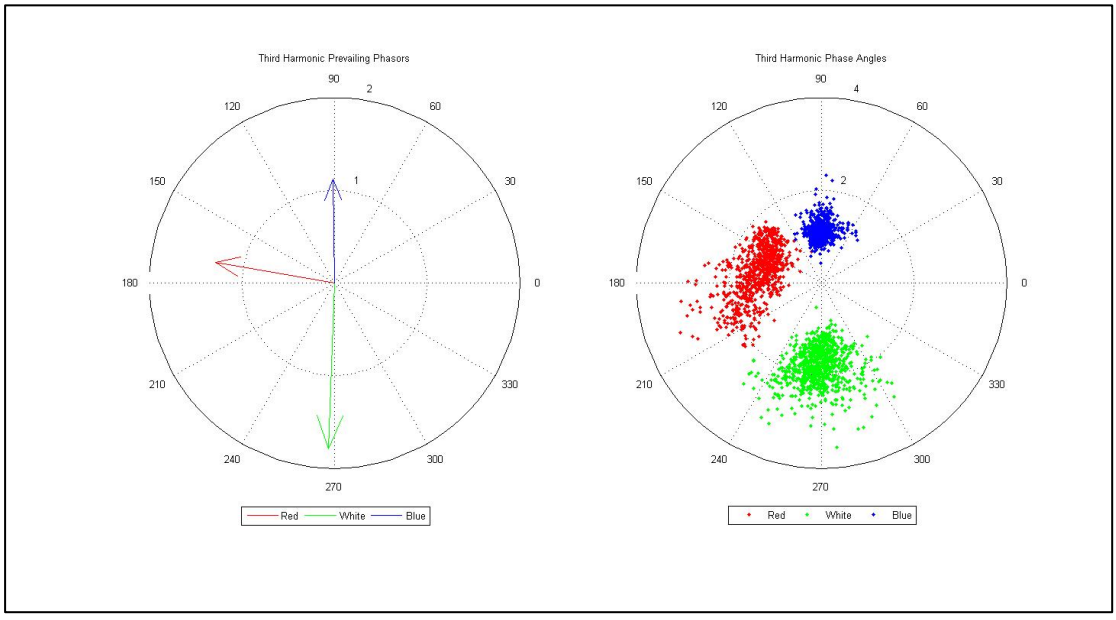

Figure 5-28: Silwerjare Old-age Home pre-solar – third harmonic prevailing current phasors

The results from the fifth harmonic phase angle are depicted in Figure 5-29 below, following the described four quadrant presentation method. The harmonic phase angles for all three phases remained relatively stable irrespective of the power flow's direction, as shown in the figure below.

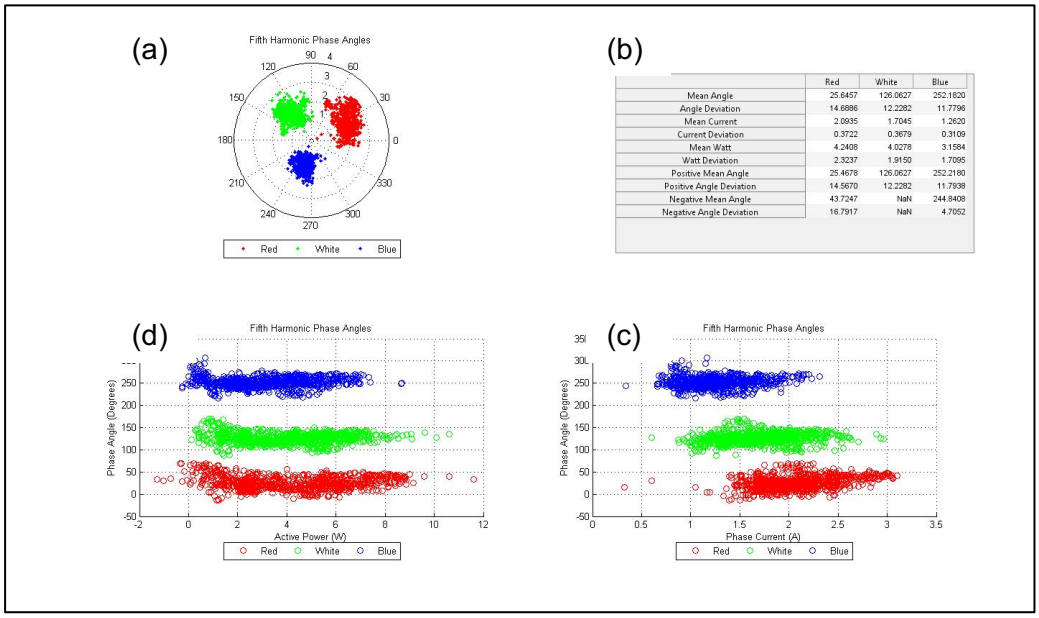

Figure 5-29: Silwerjare Old-age Home pre-solar – fifth harmonic phase-angle analysis

This data were used to calculate the PAR and prevailing phasors as presented in Table 5-15 below.

Table 5-15: Silwerjare Old-age Home pre-solar – calculations of fifth harmonic current phasor

Fifth	Red	White	Blue
Prevalence	H	H	H
PAR	0.97	0.98	0.98
Magnitude	1.99	1.67	1.25
Angle	26.49	126.52	-107.52

All three phases returned high PAR levels of prevalence; thus their prevailing phasors can be used in the network evaluation. These phasors are depicted in Figure 5-30 below, alongside the polar plot of the aggregated phase-angle data for verification.

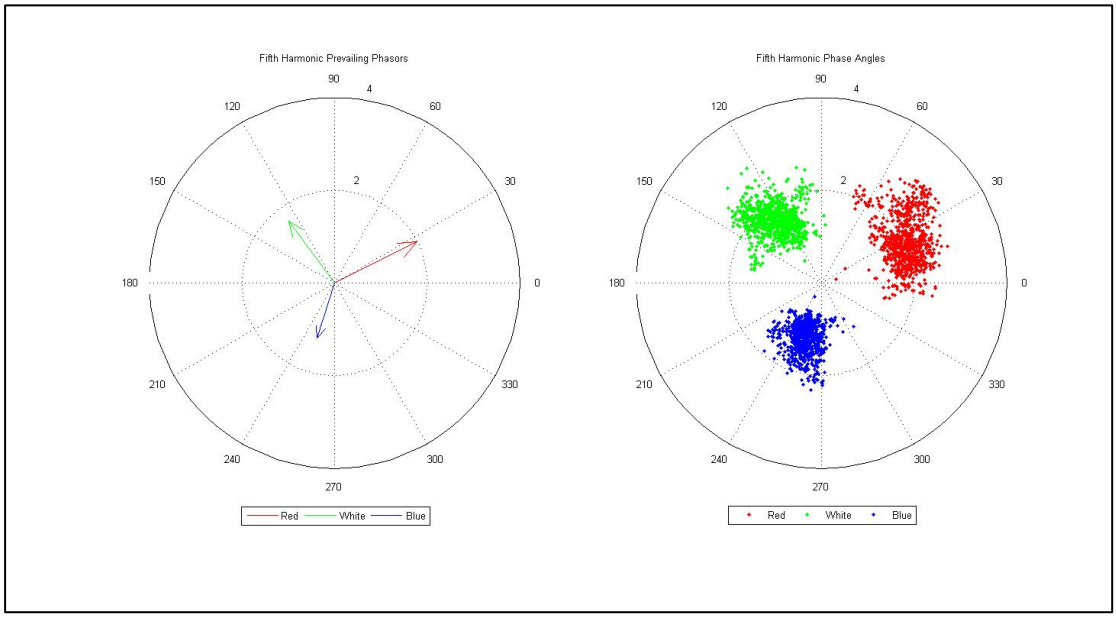

Figure 5-30: Silwerjare Old-age Home pre-solar – fifth harmonic prevailing current phasors

The results from the seventh harmonic phase angle are depicted in Figure 5-30 below, following the described four quadrant presentation method. All three phases recorded bi-directional power flow and a definitive phase angle change through zero.

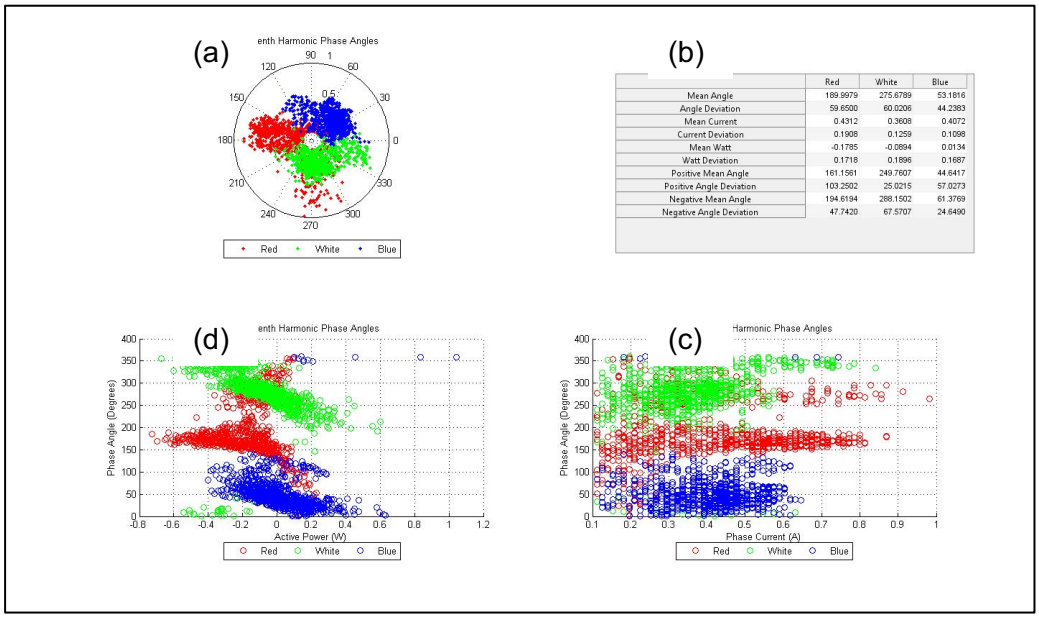

Figure 5-31: Silwerjare Old-age Home pre-solar – seventh harmonic phase-angle analysis

The aggregated phase-angle data from Figure 5-31 above shows the phase angles grouped relatively close to each other on all three phases. Using this data, the PAR and prevailing phasors were calculated and documented in Table 5-16 below.

Table 5-16: Silwerjare Old-age Home pre-solar – calculations of seventh harmonic current phasor

Seventh	Red	White	Blue
Prevalence	N	N	L
PAR	0.67	0.79	0.88
Magnitude	0.34	0.22	0.33
Angle	-174.67	-67.57	47.65

All three phase angles returned insufficient PAR values with only the blue phase meeting the threshold for a valid PAR value. This can be attributed to the change in phase angle when the direction of the active power flow changed. Therefore, only the blue phasor is presented in Figure 5-32 below, alongside the polar plot of the aggregated phase-angle data.

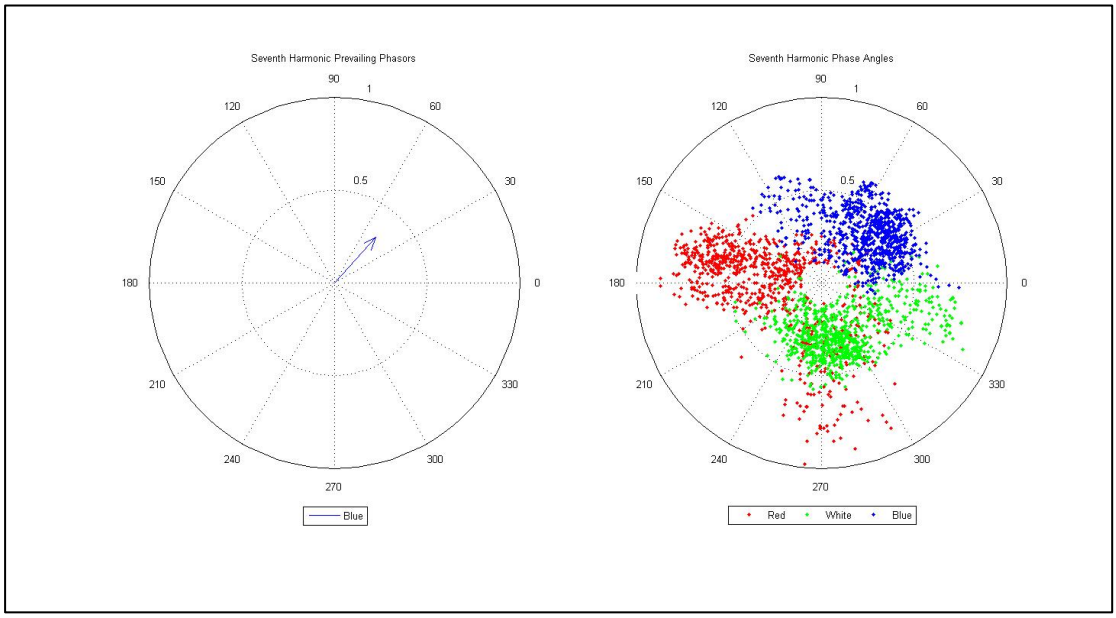

Figure 5-32: Silwerjare Old-age Home pre-solar – seventh harmonic prevailing current phasors

5.3.2 Silwerjare Old-age Home solar plant

The second dataset of the third site is the Silwerjare Old-age Home solar PV plant. This solar PV plant consists of three three-phase 20 kW SMA inverters, producing 60 kW in total. The results from the fundamental phase angle are depicted in Figure 5-33 below, following the described four quadrant presentation method.

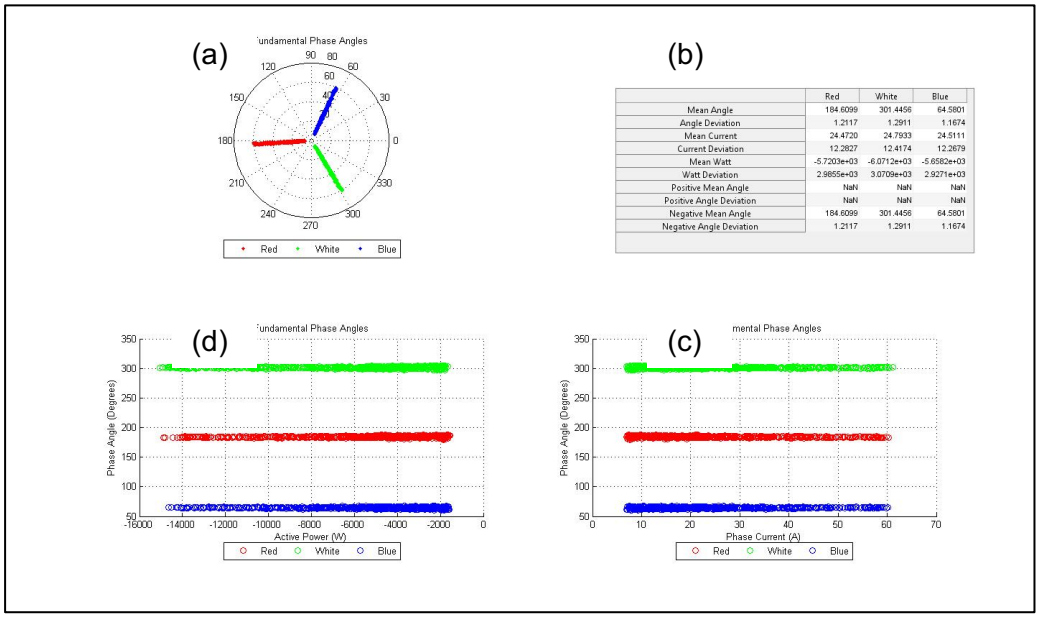

Figure 5-33: Silwerjare Old-age Home solar plant – fundamental phase-angle analysis

As expected, the solar plant demonstrates highly stable phase angles. This data were used to calculate the PAR and prevailing phasors as presented in Table 5-17 below.

Table 5-17: Silwerjare Old-age Home solar plant – calculations of fundamental current phasor

Fundamental	Red	White	Blue
Prevalence	H	H	H
PAR	1.00	1.00	1.00
Magnitude	27.37	27.72	27.4
Angle	-175.57	-58.62	64.62

All three phases returned high PAR values, which validated their prevailing phasors for use in network evaluations. These phasors are shown in Figure 5-34 below, alongside the polar plot of the aggregated phase-angle data for validation.

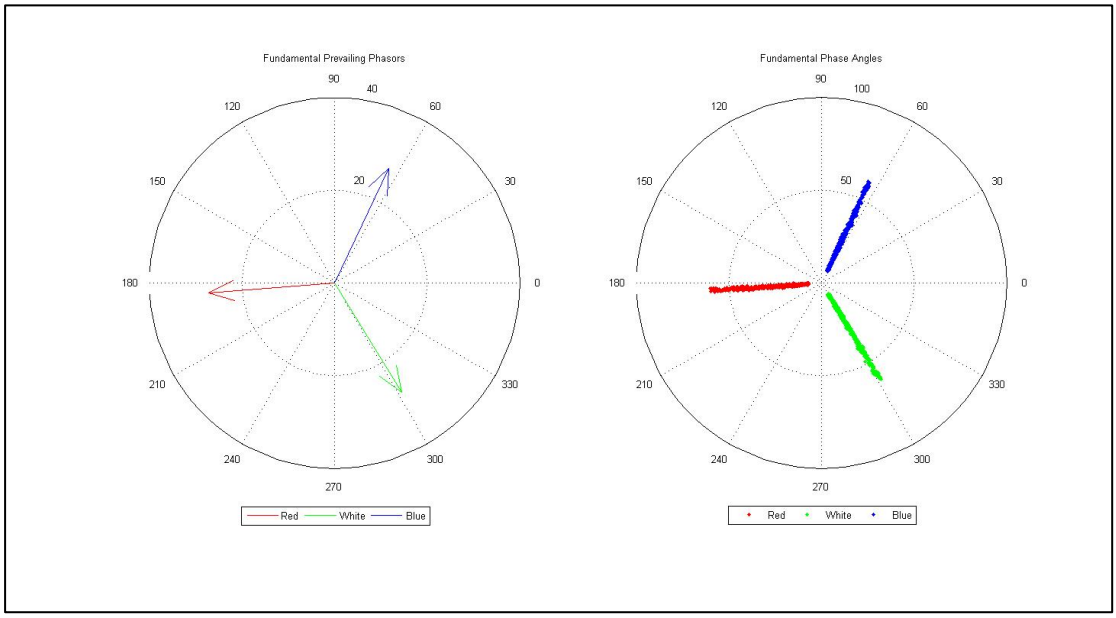

Figure 5-34: Silwerjare Old-age Home solar plant – fundamental prevailing current phasors

The results from the third harmonic phase angle are depicted in Figure 5-35 below, following the described four quadrant presentation method.

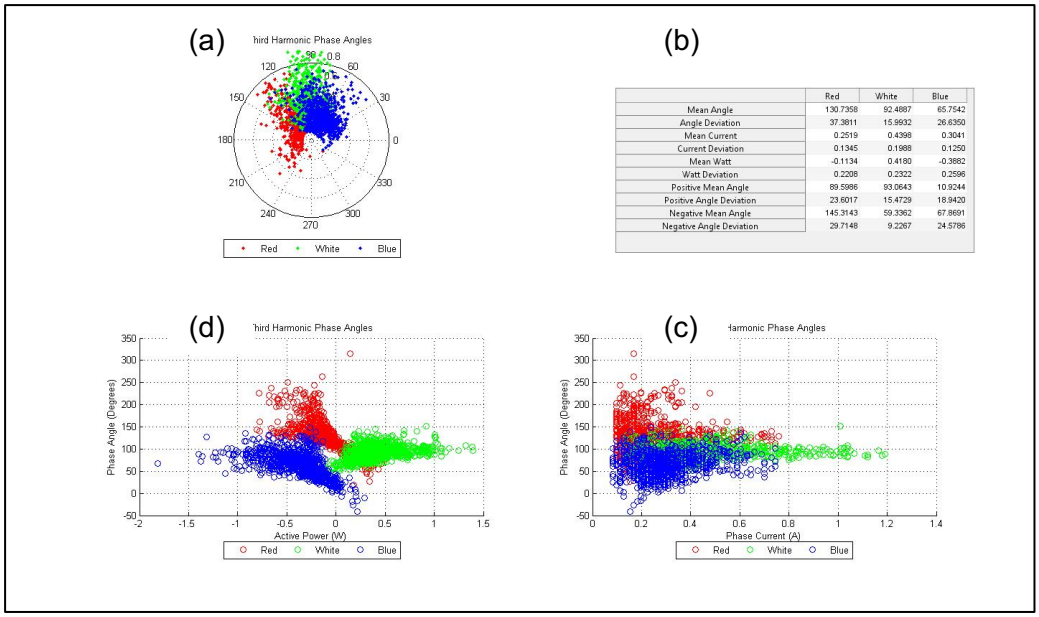

Figure 5-35: Silwerjare Old-age Home solar plant – third harmonic phase-angle analysis

The phases show extremely similar phase-angle values, although the active power values do differ to an extent. In the depiction, the white phase record mainly positive active power flow while the red and blue phase both show mainly negative active power flow at different phase angles. This data were used to calculate the PAR and prevailing phasors, and the results are presented in Table 5-18 below.

Table 5-18: Silwerjare Old-age Home solar plant – calculations of third harmonic current phasor

Third	Red	White	Blue
Prevalence	L	H	M
PAR	0.85	0.97	0.90
Magnitude	0.24	0.46	0.27
Angle	128.59	93.07	67.79

All three phases returned valid PAR values, and their prevailing phasors can, therefore, be used in network evaluations. These phasors are depicted in Figure 5-36 below, alongside the polar plot of the aggregated phase-angle data for verification.

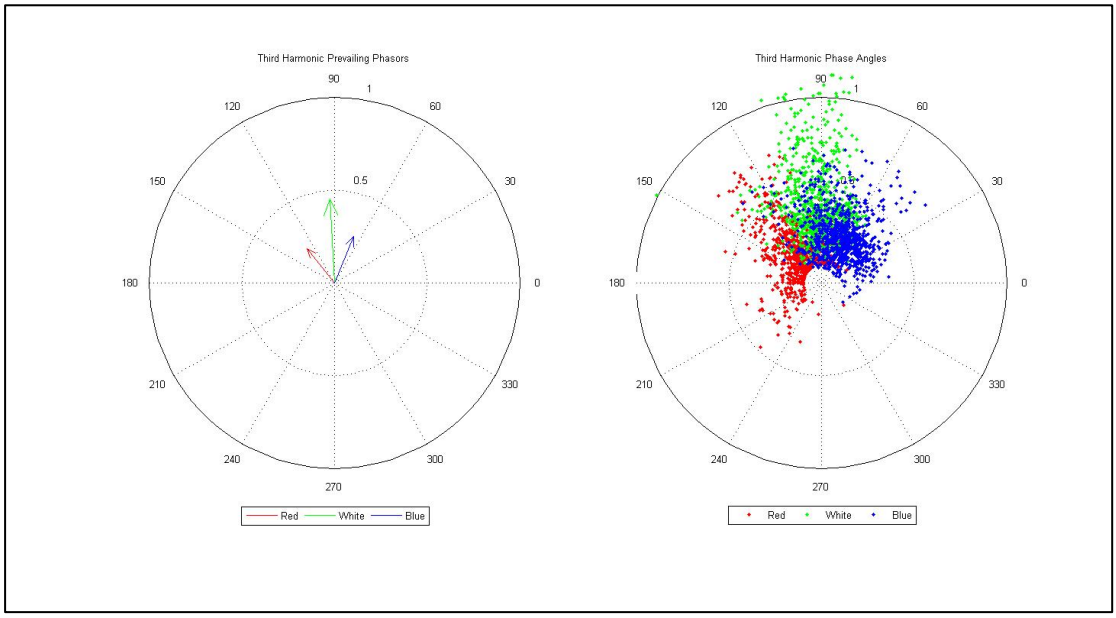

Figure 5-36: Silwerjare Old-age Home solar plant – third harmonic prevailing current phasors

The results from the fifth harmonic phase angle are depicted in Figure 5-37 below, following the described four quadrant presentation method.

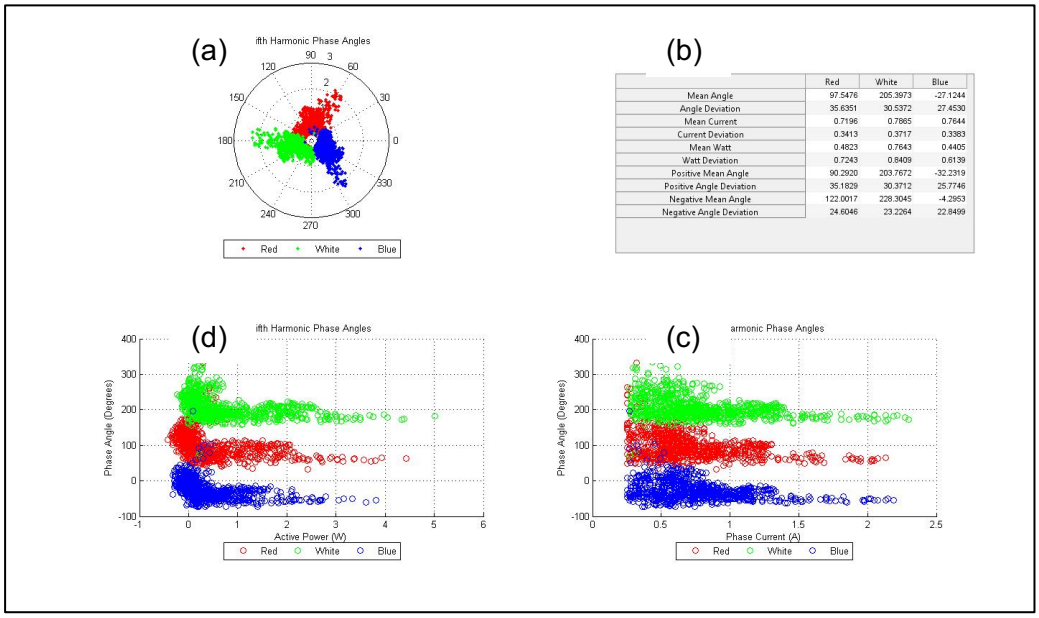

Figure 5-37: Silwerjare Old-age Home solar plant – fifth harmonic phase-angle analysis

The fifth harmonic data recorded mostly positive power flow and several data points around the zero point. This data were used to calculate the PAR and prevailing phasors for all three phases, as documented in Table 5-19 below.

Table 5-19: Silwerjare Old-age Home solar plant – calculations of fifth harmonic current phasor

Fifth	Red	White	Blue
Prevalence	L	M	M
PAR	0.87	0.90	0.92
Magnitude	0.66	0.77	0.74
Angle	89.49	-160.92	-32.00

Despite the variations the data of the phase angle indicated around zero, all three phases returned valid PAR values. Therefore, the prevailing phasors can be used in network evaluations. These phasors are depicted in Figure 5-38 below, alongside the polar plot of the aggregated phase-angle data for verification.

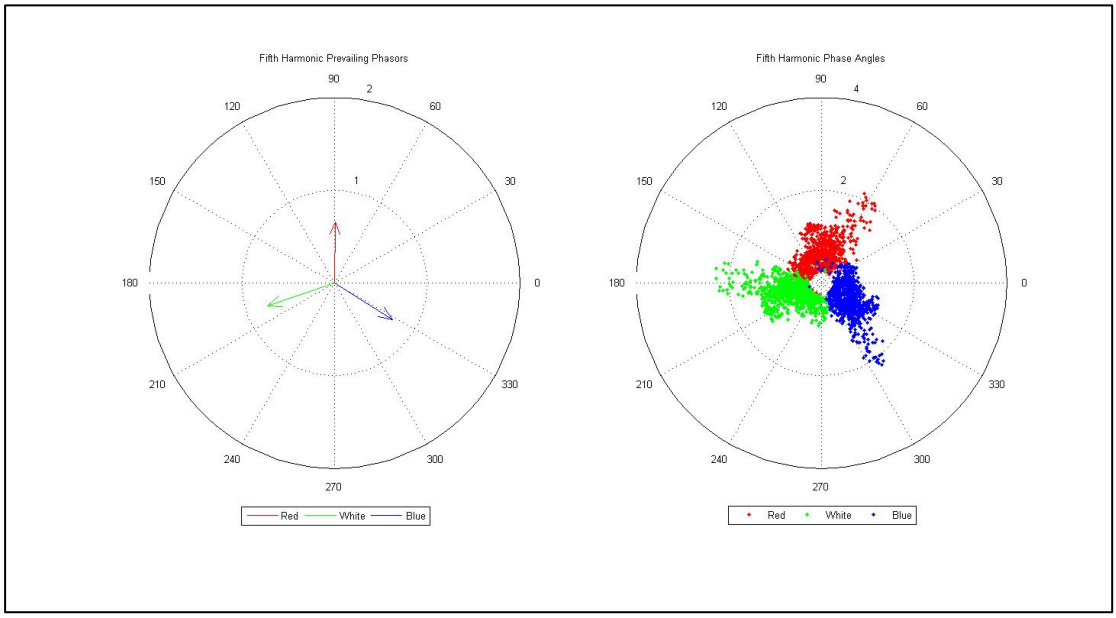

Figure 5-38: Silwerjare Old-age Home solar plant – fifth harmonic prevailing current phasors

The results from the seventh harmonic phase angle are depicted in Figure 5-39 below, following the described four quadrant presentation method.

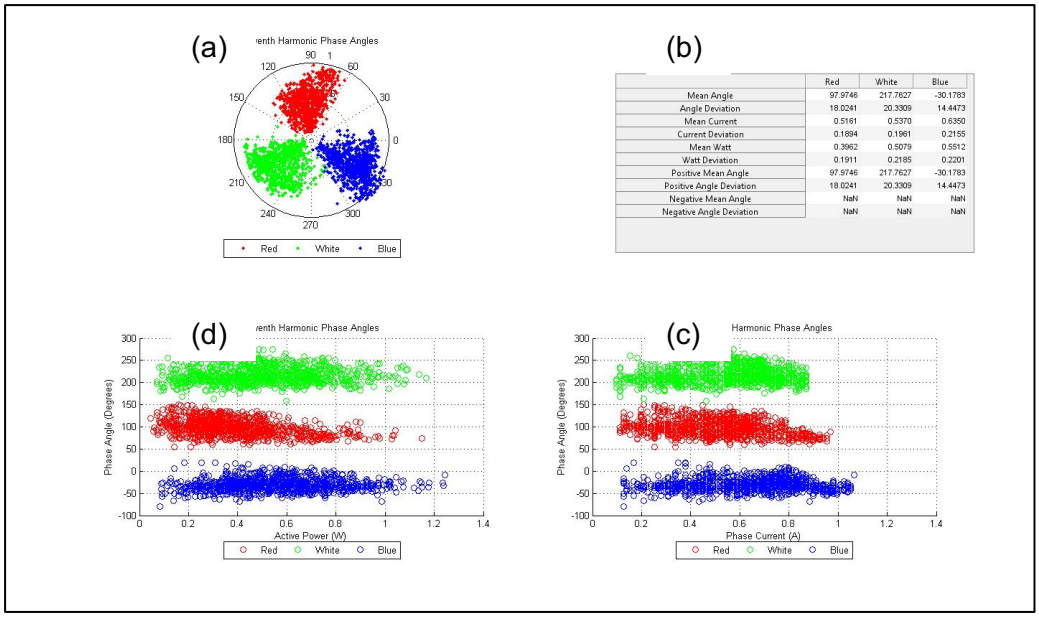

Figure 5-39: Silwerjare Old-age Home solar plant – seventh harmonic phase-angle analysis

The seventh harmonic data also recorded mostly positive active power flow but still demonstrates a clear prevailing angle for each phase. This data were used to calculate the PAR and prevailing phasors for each phase, as presented in Table 5-20 below.

Table 5-20: Silwerjare Old-age Home solar plant – calculations for seventh harmonic current phasor

Seventh	Red	White	Blue
Prevalence	H	M	H
PAR	0.95	0.94	0.97
Magnitude	0.50	0.51	0.63
Angle	95.99	-142.20	-30.73

All three phases returned acceptable PAR values, thus the prevailing phasors are valid for network evaluations. These phasors are depicted in Figure 5-40 below, alongside the polar plot of the aggregated phase-angle data for verification.

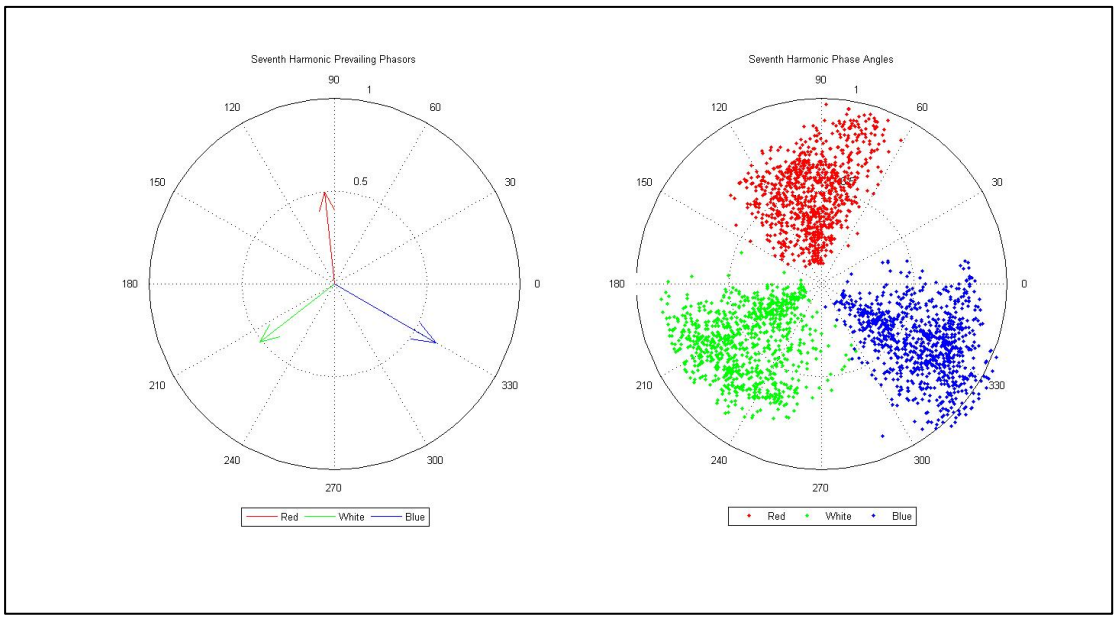

Figure 5-40: Silwerjare Old-age Home solar plant – seventh harmonic prevailing current phasors

5.3.3 Silwerjare Old-age Home post-solar

The third dataset of the third site is Silwerjare Old-age Home after the installation of their solar PV system. The results from the fundamental phase angle are depicted in Figure 5-41 below, following the desribed four quadrant presentation method.

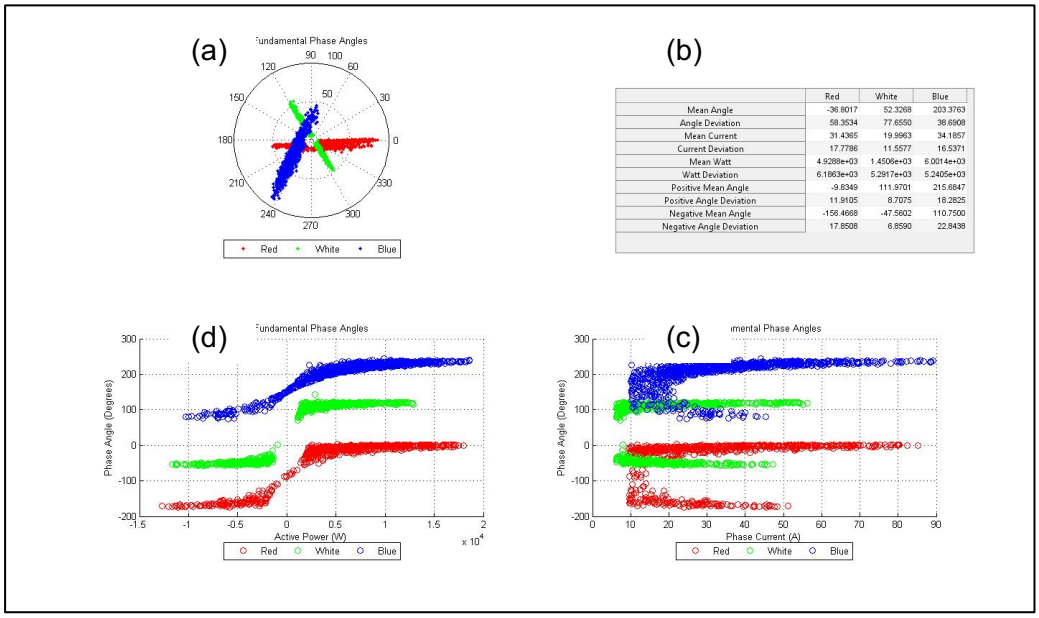

Figure 5-41: Silwerjare Old-age Home post-solar – fundamental phase-angle analysis

Due to the presence of the uncontrolled DG, bi-directional active power flow was recorded. Subsequently, the 180° change in the phase angle are shown in plot (d) of Figure 5-41 above. This data were used to calculate the PAR and prevailing phasors as presented in Table 5-21 below.

Table 5-21: Silwerjare Old-age Home post-solar – calculations of fundamental current phasor

Fundamental	Red	White	Blue
Prevalence	N	N	L
PAR	0.74	0.35	0.86
Magnitude	35.35	22.75	35.65
Angle	-10.32	100.25	-141.94

All three phases recorded valid PAR values that correspond to the approximate angles of the positive power-flow. Thus, it can be concluded that positive power flow occurred during most of the recording period. The prevailing phasors are indicated in Figure 5-42 below, alongside the polar plot of the aggregated data for the phase angle.

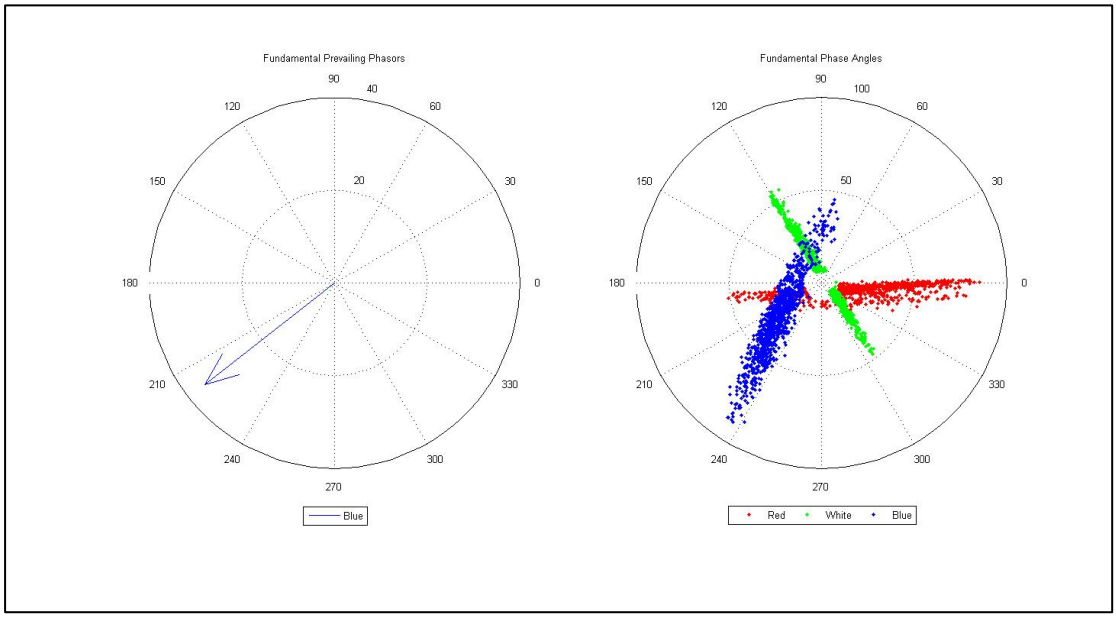

Figure 5-42: Silwerjare Old-age Home post-solar – fundamental prevailing current phasors

The results from the third harmonic phase angle are depicted in Figure 5-43 below, following the described four quadrant presentation method.

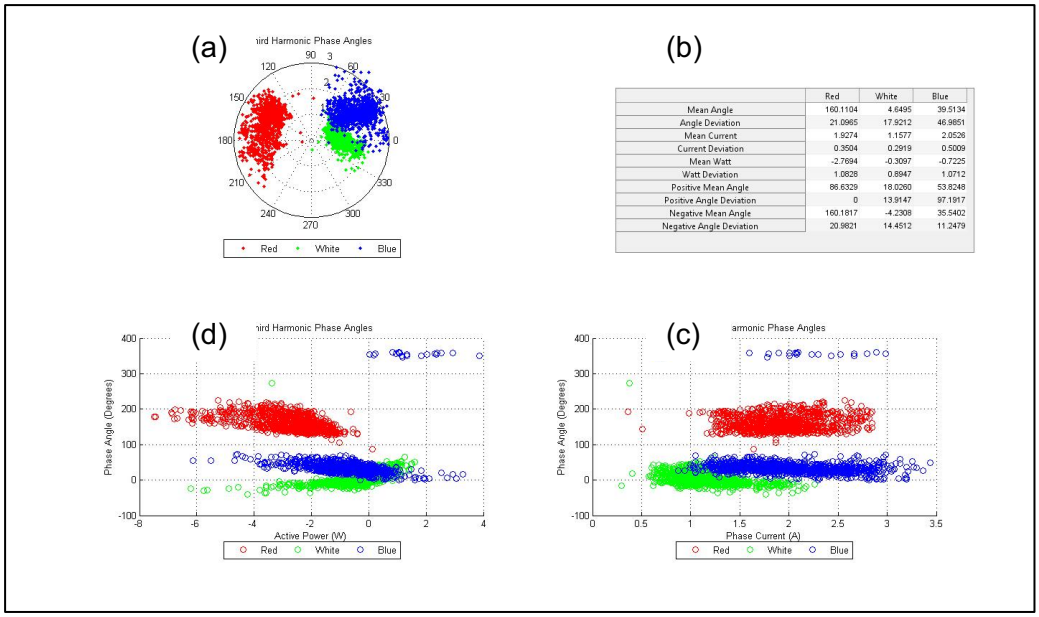

Figure 5-43: Silwerjare Old-age Home post-solar – third harmonic phase-angle analysis

Mostly negative power flow was recorded for the third harmonic, although the phase angles were found to be stable for changes in the magnitude of the phase current. This data were used to calculate the PAR and prevailing phasors for all three phases, and the results are presented in Table 5-22 below.

Table 5-22: Silwerjare Old-age Home post-solar – calculations of third harmonic current phase angle

Third	Red	White	Blue
Prevalence	M	H	H
PAR	0.93	0.96	0.97
Magnitude	1.70	1.11	2.00
Angle	160.17	2.73	31.32

The valid PAR values confirm the angle's stability for all three phases. Thus, the prevailing phasors can be used in network evaluations. These phasors are indicated in Figure 5-44 below, alongside the polar plot of the aggregated phase-angle data for verification.

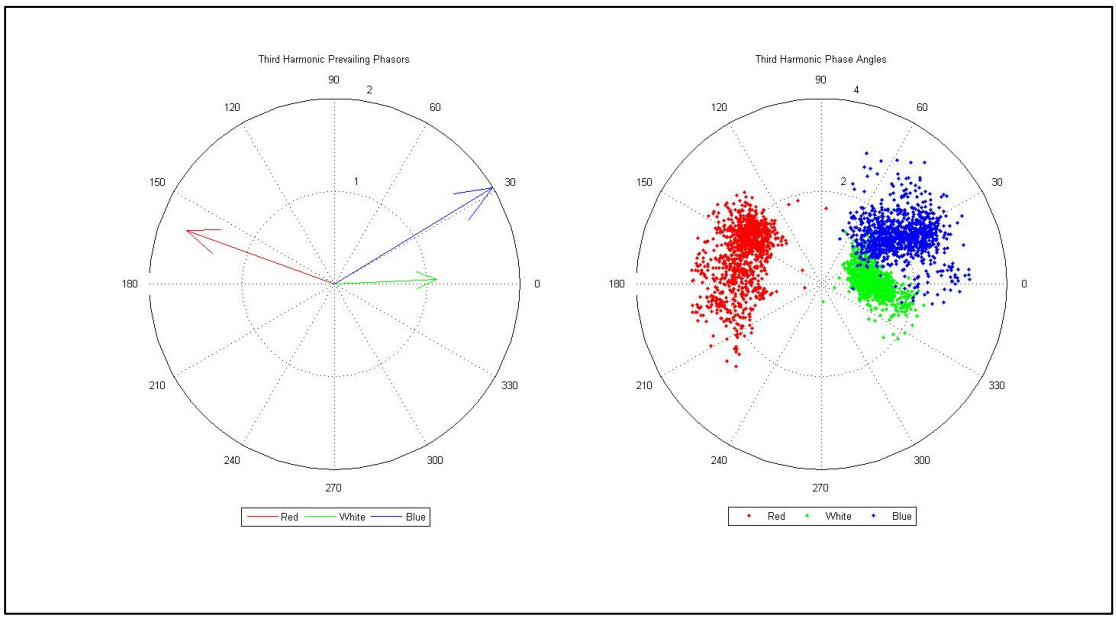

Figure 5-44: Silwerjare Old-age Home post-solar – third harmonic current phasors

The results from the fifth harmonic phase angle are depicted in Figure 5-45 below, following the described four quadrant presentation method.

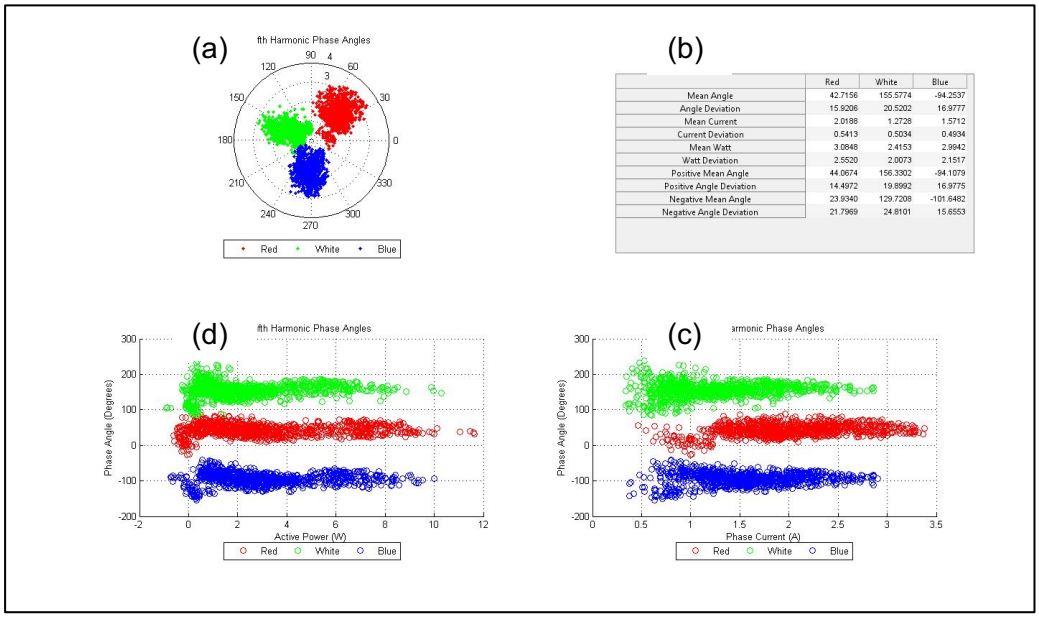

Figure 5-45: Silwerjare Old-age Home post-solar – fifth harmonic phase-angle analysis

This data were used to calculate the PAR and prevailing phasors for all three phases, of which the results are presented in Table 5-23 below.

Table 5-23: Silwerjare Old-age Home post-solar – calculations of fifth harmonic current phasor

Fifth	Red	White	Blue
Prevalence	H	H	H
PAR	0.97	0.95	0.97
Magnitude	1.97	1.28	1.56
Angle	43.94	156.9	-93.92

All three phases returned high PAR values, which means the prevailing phasors are valid for network evaluation. These phasors are shown in Figure 5-46 below, alongside the polar plot of the aggregated phase-angle data for verification.

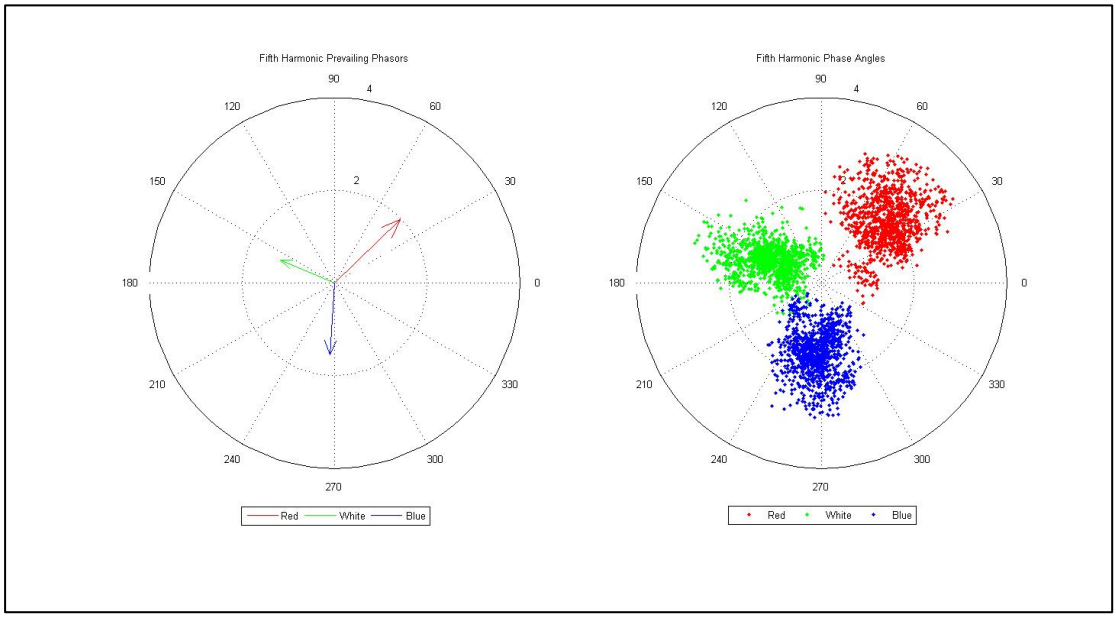

Figure 5-46: Silwerjare Old-age Home post-solar – fifth harmonic current phasors

The results from the seventh harmonic phase angle are depicted in Figure 5-47 below, following the described four quadrant presentation method.

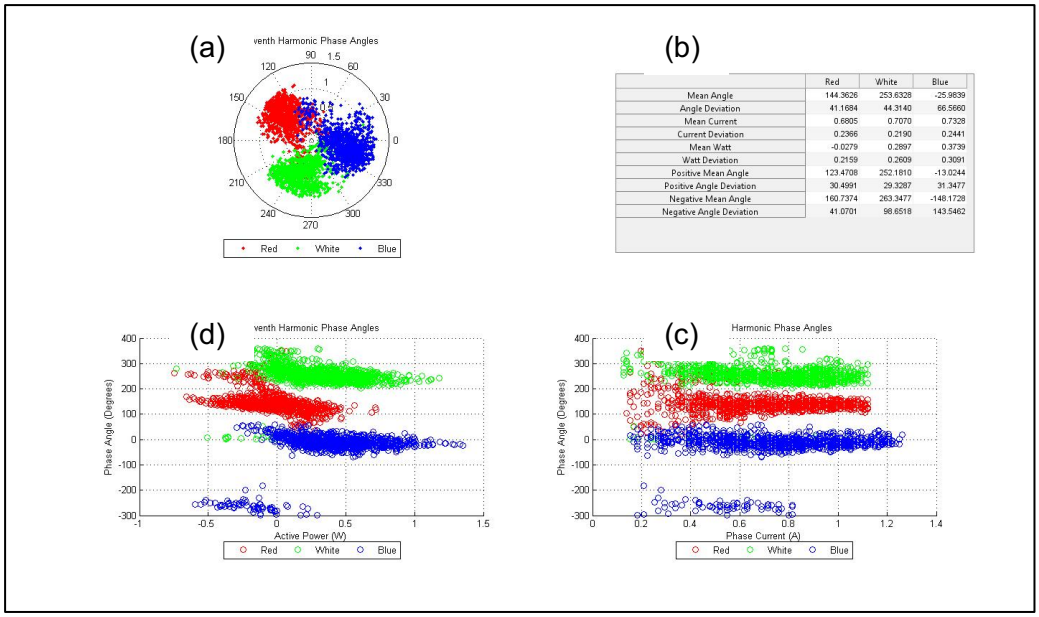

Figure 5-47: Silwerjare Old-age Home post-solar – seventh harmonic phase-angle analysis

The seventh harmonic experienced bi-directional active power flow, although the phase angle remains stable, irrespective of the power flow's direction. Using this data, the PAR and prevailing phasors were calculated and the results are presented in Table 5-24 below.

Table 5-24: Silwerjare Old-age Home post-solar – calculations seventh harmonic prevailing current phasor

Seventh	Red	White	Blue
Prevalence	L	L	L
PAR	0.86	0.88	0.89
Magnitude	0.63	0.62	0.67
Angle	138.86	-105.33	-7.31

All three phases returned relatively good PAR values and can, therefore, be used to calculate prevailing current phasors, as indicated in Figure 5-48 below.

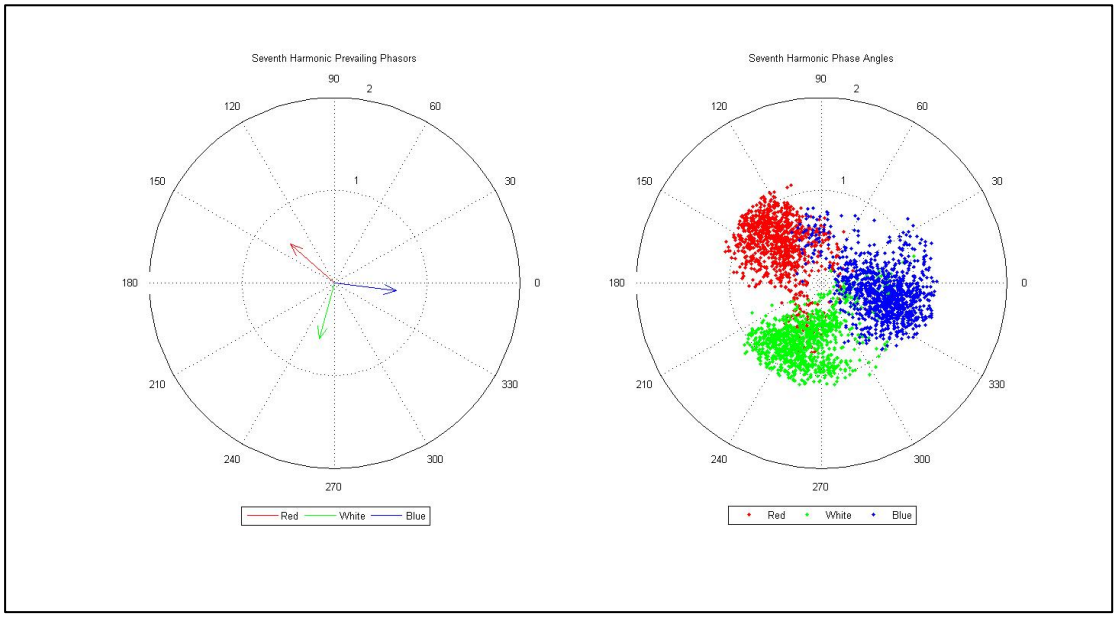

Figure 5-48: Silwerjare Old-age Home – seventh harmonic prevailing current phasors

5.4 Summary of work

To summarise, extensive and useful data were recorded for the analysis of both the network and phase angle. No difficulties were encountered while processing the data. Both the recorded and calculated data could be verified through comparison.

5.4.1 Phase-angle analysis

The results documented in this chapter indicate that the phase-angle method may not be accurate for the fundamental frequency. This applies particularly where DG are present with no form of active power control. The result is negative active power flow during the sunlight hours, which leads to confusing phase-angle data. This is due to the change in phase angle that accompanies an altered direction of the power flow. In contrast, the harmonic phase angles are generally stable, irrespective of the active power flow's direction. It can, therefore, be inferred that harmonic phase angles may prove to be a successful tool to estimate the impact of DG on the distribution network.

A detailed description of the estimation process is provided in the following chapter (Chapter 6).

CHAPTER 6: Planning tools

By using the data collected and calculated in Chapter 4, a network planning tool was developed. This tool uses the relationships between harmonic current, voltage THD, and capacity loss to estimate the expected capacity loss based on estimated harmonic levels within the network.

For the phase angles (Chapter 5), the expected result when introducing renewable DG into a network are compared with the recorded results. This information will be used to comment on the potential influence and predictability that renewable DG have on the harmonic levels in a distribution network.

6.1 Network efficiency

Currently, during the planning of a new electricity distribution network in South Africa, there is no guideline for the integration of expected PQ parameters into the planning process for the network. Such planning is guided mostly by the rule of thumb from the experienced engineers, for example, avoid loading a transformer above 80% without scientific reason, other than that such action would not be conducive for the transformer. Therefore, this section will aim to justify the latter statement, as well as confirm the correct de-rating values and provide a quick-reference tool for future network planning.

6.1.1 Cable 1

By using the relationships established in section 4.1.1 between voltage THD, harmonic current and capacity loss, it is possible to estimate the expected capacity loss for a given voltage THD. This is achieved by the following method:

- Estimate an equivalent harmonic current value for the voltage THD based on equation 4-7, which defines the relationship between harmonic current and voltage THD.
- Apply the estimated harmonic current to equation 4-5, according to which the relationship between capacity loss and harmonic current results in an estimated capacity loss percentage for the given voltage THD.

The THDF, presented in section 4.1.1.4, can be determined in a similar manner:

- Estimate an equivalent harmonic-current value for the voltage THD based on equation 4-7, which defines the relationship between harmonic current and voltage THD.

- Use the estimated harmonic current in equation 4-10 that calculates the relationship between crest factor and harmonic current, to find the equivalent crest factor.
- Apply the value of the equivalent crest factor to equation 3-31, which yields an expected THDF.

The present study determined the voltage level that should be applied to the planning tool in order to demonstrate the impact for Cable 1. For this purpose, a histogram was plotted that indicate the number of data points for a given voltage THD range, as depicted in Figure 6-1 below.

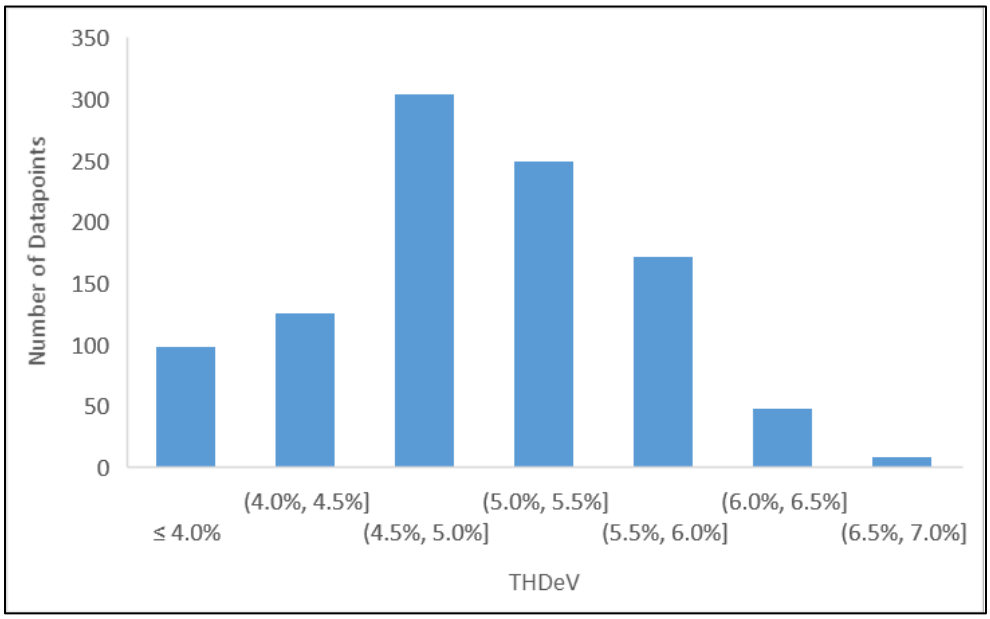

Figure 6-1: Cable 1 – typical voltage THD levels

From Figure 6-1 above, it is evident that the highest number of data points were recorded between 4.5% and 5.5%. Based on these findings, a voltage THD of 5% was selected for further use in the example of the planning impact (*see* section 6.1.4).

Running a range of voltage THD values from 0.5% to 10% through the described network planning tool produced the results recorded in Table 6-1 below. The results for voltage THD of 5% are highlighted in green.

Table 6-1: Cable 1 planning tool

Voltage THD	Harmonic current	Capacity loss	Crest factor	Transformer harmonic de-rating factor
0.50%	6.48	0.51%	1.43	99.02%
1.00%	5.97	0.44%	1.42	99.43%
1.50%	5.63	0.42%	1.42	99.64%
2.00%	5.46	0.42%	1.42	99.72%
2.50%	5.47	0.42%	1.42	99.72%
3.00%	5.65	0.42%	1.42	99.63%
3.50%	6.00	0.44%	1.42	99.40%
4.00%	6.52	0.52%	1.43	98.99%
4.50%	7.22	0.71%	1.44	98.27%
5.00%	8.09	1.08%	1.46	97.12%
5.50%	9.13	1.73%	1.48	95.40%
6.00%	10.34	2.76%	1.52	92.99%
6.50%	11.73	4.29%	1.58	89.78%
7.00%	13.29	6.48%	1.65	85.73%
7.50%	15.02	9.48%	1.75	80.87%
8.00%	16.92	13.46%	1.88	75.31%

6.1.2 Cable 2

It was not possible to estimate the expected capacity loss based on the voltage THD for Cable 2. This is due to the poor correlation between the harmonic current and voltage THD. Thus, no planning tool could be developed for Cable 2.

Despite the poor correlation between the various parameters it is noticeable that the voltage THD level in Cable 2, as depicted in Figure 6-2 below, remain highly similar to the voltage level recorded at Cable 1 shown in Figure 6-1 above.

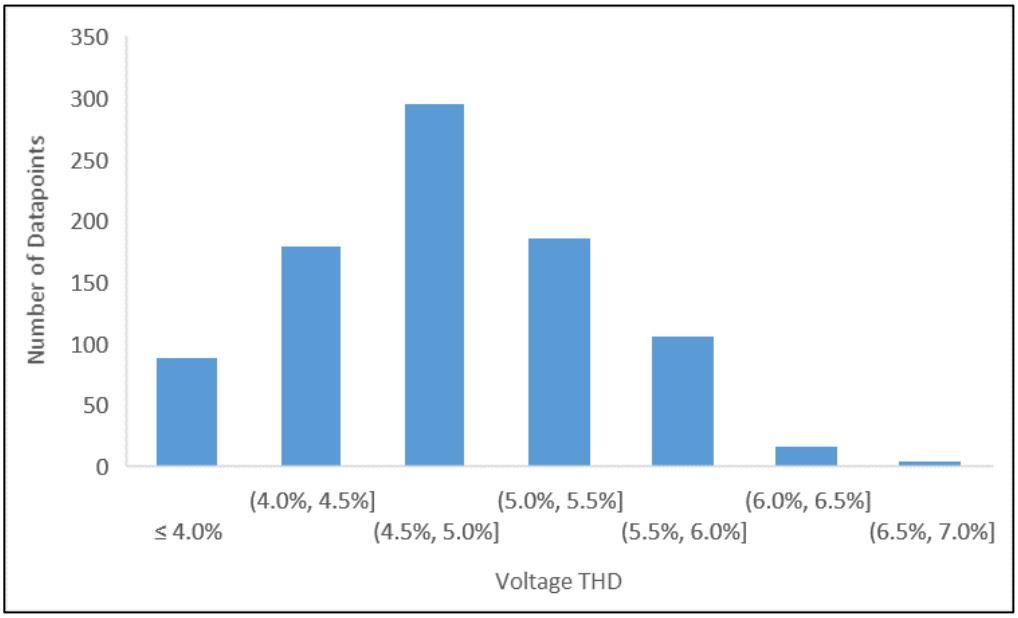

Figure 6-2: Cable 2 – typical voltage THD levels

6.1.3 Cable 3

It was not possible to estimate the expected capacity loss based on the voltage THD for Cable 3. This is due to the poor correlation between the harmonic current and voltage THD, and the capacity loss of the harmonic current.

It is also not possible to estimate the THDF, due to the poor relationship between the crest factor and harmonic current. Thus, no planning tool could be developed for Cable 3.

The voltage THD profile for Cable 3 (cf. Fig 6-3 below), shows a more improved distribution between various voltage THD values than was the case with Cable 1 and 2.

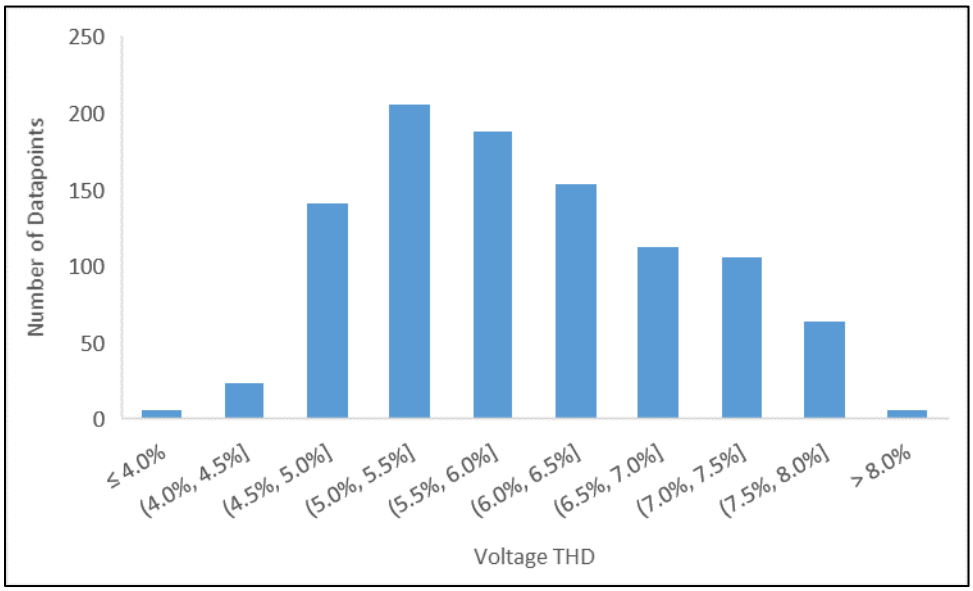

Figure 6-3: Cable 3 – typical voltage THD levels

6.1.4 Planning impact

To summarise, it is possible to estimate the expected capacity losses for a given cable section. However, it is not feasible to apply this method as a generic solution to all medium voltage cable sections. The success of this technique depends mostly on the type of loads and their combined harmonic levels within the distribution system, especially harmonic currents.

The results for the cable section where the proposed technique was successfully applied are presented in Table 6-2 below.

Table 6-2: Planning summary

Cable	Voltage THD	Current THD	Capacity loss	Crest factor	Transformer harmonic de-rating factor
1	5.00%	8.09	1.08%	1.46	97.12%
2	No result				
3	No result				

The predicted losses for the cable still remain extremely low and well within acceptable levels. Since no positive result were found for Cables 2 and 3, it was impossible to evaluate the potential total losses throughout the entire distribution system.

6.2 Phase angle

During the data analysis of the phase angle, the recordings at the various sites were analysed, and the individual prevailing phasors calculated. This section of the report discusses the comparison between the phasors at the same location before and after the installation of renewable DG as well as its potential impact on the greater distribution network.

6.2.1 Overview

The first step would be to ascertain how useful the data regarding the prevailing phasor is. This is then used to assess the impact of renewable DG on the harmonics within the distribution system. This impact depends on the prevalence of the aggregated phase-angle data for each site, phase and harmonic. Table 6-3 below provides an overview of the valid prevailing phasors – of which the absence would make it impossible to comment on the impact renewable DG has on the network. “Y” indicates a valid prevailing phasor and “N” indicates an invalid prevailing phasor.

Table 6-3: Phase angle PAR summary

	Fundamental			Third harmonic			Fifth harmonic			Seventh harmonic		
	R	W	B	R	W	B	R	W	B	R	W	B
NWU solar plant	Y	Y	Y	Y	Y	Y	Y	Y	Y	Y	Y	Y
BDB pre-solar	Y	Y	Y	N	Y	Y	N	Y	Y	Y	Y	Y
BDB post-solar	N	N	Y	N	Y	Y	Y	N	Y	Y	Y	Y
Silwerjare pre-solar	Y	Y	Y	Y	Y	Y	Y	Y	Y	N	N	Y
Silwerjare solar plant	Y	Y	Y	Y	Y	Y	Y	Y	Y	Y	Y	Y
Silwerjare post-solar	N	N	Y	Y	Y	Y	Y	Y	Y	Y	Y	Y

Based on the information in Table 6-3 above, the sites and phases where the effect of renewable DG was evaluated and are presented in Table 6-4 below. The requirement for evaluation was that the dataset for the pre-installation and solar system had to have usable prevalence value. In table 6-4 “R”, “W” and “B” indicate the availability of the red, white and blue phasors for this evaluation.

Table 6-4: Sites for phasor analysis

	Fundamental	Third harmonic	Fifth harmonic	Seventh harmonic
BDB	B	W B	B	R W B
Silwerjare	R W B	R W B	R W B	B

6.2.2 BDB Auditors

Due to the lack of valid prevailing phasors post-solar for the red and white phase, only the blue phase fundamental phasor could be analysed. Although measurements for the solar system are not available, it was possible to estimate the solar phasor. The estimated solar current phasor assumes that the sum of the solar phasor and the pre-solar phasor is the post-solar phasor. This is confirmed by the following equation:

$$Phasor_{solar} = Phasor_{post} - Phasor_{pre} \quad (6\text{-}1)$$

The pre-, post- and estimate phasors are documented in Table 6-5 below.

Table 6-5: BDB fundamental phasor comparison

Phase	Pre-solar	Post-solar	Estimated solar
Blue	15.78∠-126.6°	4.75∠-61.22°	14.46∠36.03°

The post-solar phasor depicted in Figure 6-4 below, indicates a significant reduction in the magnitude as well as a phase shift with the introduction of the solar plant. The post-solar phasor was expected to have a reduced magnitude, and angled approximately halfway between the pre-solar and solar phasors, which is confirmed by the figure below.

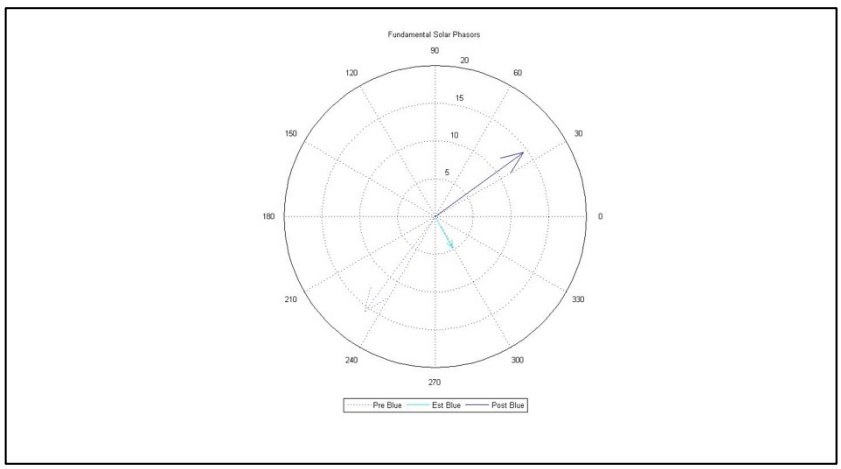

Figure 6-4: BDB Auditors – fundamental phasor comparison

For the third harmonic, the red phasor did not yield a valid PAR result on either the pre-solar or post-solar datasets. Therefore, only the white and blue phasors were analysed as shown in Table 6-6 below. Again, the estimated solar phasor was calculated according to equation 6.1.

Table 6-6: BDB third harmonic phasor comparison

Phase	Pre-solar	Post-solar	Estimated solar
White	0.87∠170.76°	0.85∠-179.56°	0.15∠-86.58°
Blue	0.86∠-177.38°	0.46∠-160.49°	0.44∠-15.03°

Both analysed phasors show only a slight change in phase angle and low reduction in magnitude, as is evident from the phasors depicted in Figure 6-5 below. This points to the fact that the inverter does absorb a measure of third harmonic energy.

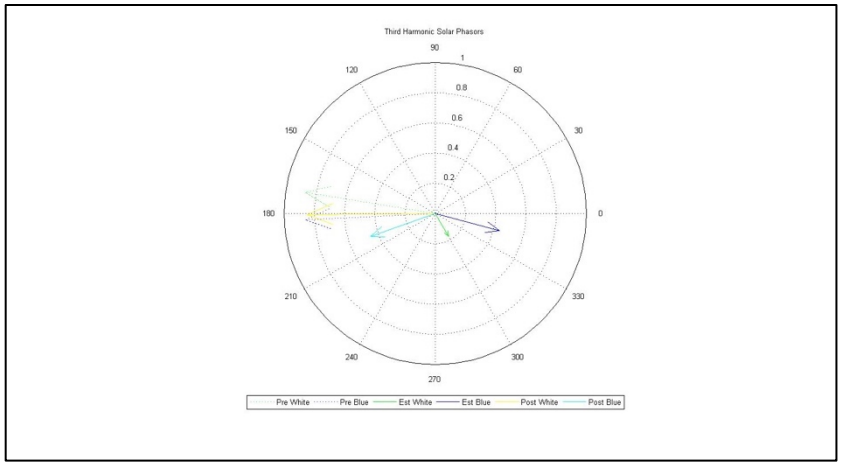

Figure 6-5: BDB Auditors – third harmonic phasor comparison

From Figure 6.5 above, it is evident that the red and white phases did not show valid PAR values pre- and post-solar for the fifth harmonic. Therefore, only the blue phasor was analysed. The estimated solar phasor was calculated by applying equation 6.1. The results are presented in Table 6-7 below.

Table 6-7: BDB fifth harmonic phasor analysis

Phase	Pre-solar	Post-solar	Estimated solar
Blue	0.75∠60.66°	0.53∠-149.72°	1.24∠-131.86°

The phasors, illustrated in Figure 6-6 below, show a significant change to the fifth harmonic's blue phasor. This indicates the inverter's impact in reducing the magnitude and characteristic of this mentioned blue phasor.

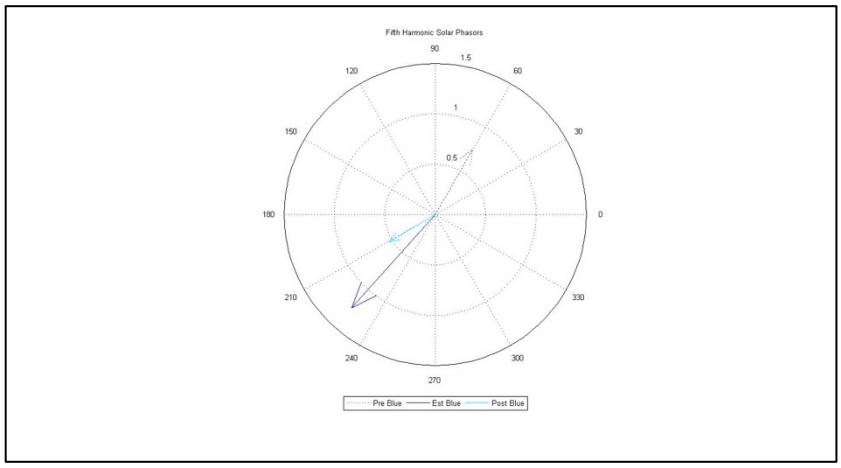

Figure 6-6: BDB fifth harmonic phasor comparison

All three phases indicate high levels of prevalence and, therefore, were used in the analysis. The pre-, post- and estimate solar phasors are presented in Table 6-8 below.

Table 6-8: BDB seventh harmonic phasor analysis

Phase	Pre-solar	Post-solar	Estimated solar
Red	1.01∠104.61°	1.15∠99.75°	0.17∠68.97°
White	0.97∠-94.30°	0.89∠-105.55°	0.19∠146.48°
Blue	1.28∠10.38°	0.65∠23.78°	0.67∠177.29°

All the phasors show a measure of change in magnitude and angle although this alteration is not consistent across the phases. These phasors are represented graphically in Figure 6-7 below.

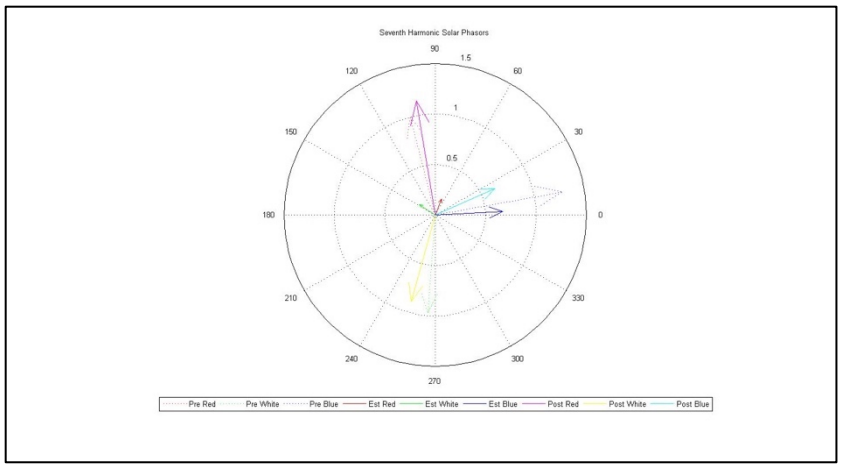

Figure 6-7: BDB seventh harmonic phasor comparison

6.2.3 Silwerjare Old-age Home

The red and white phases did not return valid PAR values on the actual dataset of the results. However, it was still possible to estimate the result phasor by applying the following equation:

$$Phasorl_{pre} + Phasor_{post} = Phasor_{solar} \quad (6\text{-}2)$$

The calculated fundamental phasors for each scenario at Silwerjare Old-age Home can be seen in table 6-9 below.

Table 6-9: Silwerjare fundamental phasor analysis

Phase	Pre-solar	Solar	Estimated result	Actual result
Red	66.21∠-3.07°	27.37∠-175.57°	39.24∠-8.29°	No Prevalence
White	55.78∠110.65°	27.72∠-58.62°	29.00∠100.40°	No Prevalence°
Blue	51.65∠-121.59°	27.40∠64.62°	24.60∠-128.51°	35.65∠-141.94°

The estimated result does differ from the actual result. This can be attributed to the fact that a live network is an uncontrolled environment. Thus, the harmonic content of the load may have changed during this period. The phasors are depicted in Figure 6-8 below.

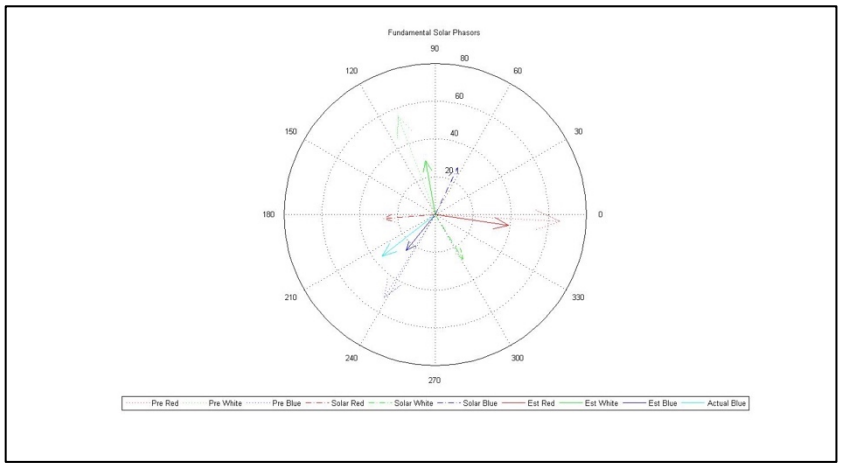

Figure 6-8: Silwerjare fundamental phasor comparison

All three phases returned valid PAR values for the third harmonic analysis. The prevailing phasors are presented in Table 6-10 below.

Table 6-10: Silwerjare third harmonic analysis

Phase	Pre-solar	Solar	Estimated result	Actual result
Red	1.31∠170.32°	0.24∠128.59°	1.50∠164.20°	1.70∠160.17°
White	1.79∠-92.03°	0.46∠93.07°	1.33∠-93.79°	1.11∠2.73°
Blue	1.12∠91.00°	0.27∠67.79°	1.37∠86.55°	2.00∠31.32°

The white phasor shows a reduced magnitude, whereas the other phasors indicate an increased magnitude. All phasors experienced an angle change after the installation of the PV. The phasors are depicted in Figure 6-9 below.

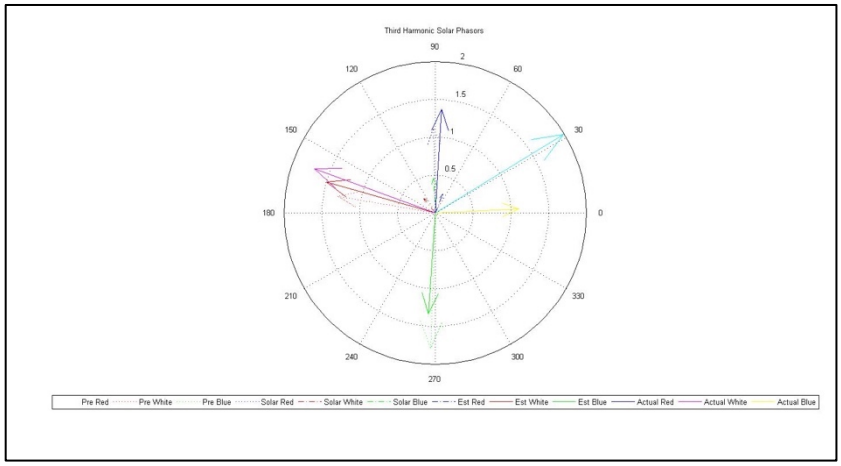

Figure 6-9: Silwerjare third harmonic comparison

For the fifth harmonic, all three phases returned valid PAR values. The prevailing phasors are documented in Table 6-11 below.

Table 6-11: Silwerjare fifth harmonic analysis

Phase	Pre-solar	Solar	Estimated result	Actual result
Red	1.99∠26.49°	0.66∠89.49°	2.36∠40.89°	1.97∠43.94°
White	1.67∠126.52°	0.77∠-160.92°	2.04∠147.65°	1.28∠156.9°
Blue	1.25∠-107.52°	0.74∠-32°	1.60∠-80.99°	1.56∠-93.92°

All three phases indicated a reduced magnitude and change in angle. The recorded phasors are depicted in Figure 6-10 below.

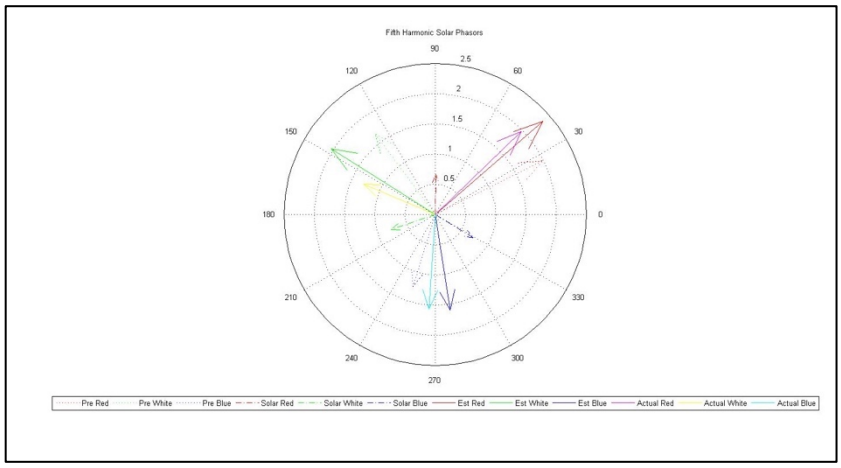

Figure 6-10: Silwerjare fifth harmonic comparison

The seventh harmonic blue phasor yielded positive PAR results, of which the phasors are presented in Table 6-12 below.

Table 6-12: Silwerjare seventh harmonic analysis

Phase	Pre-solar	Solar	Estimated result	Actual result
Blue	0.33∠47.65°	0.63∠-30.73°	0.77∠-5.83°	0.67∠-7.31°

As depicted in Figure 6-11 below, the estimated solar phasor is extremely close to the actual result that was achieved.

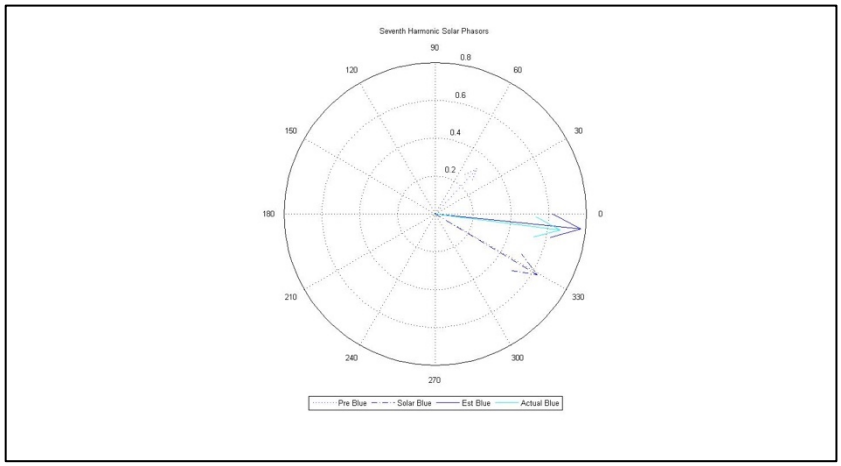

Figure 6-11: Silwerjare seventh harmonic comparison

CHAPTER 7: Conclusions and recommendations

The goal of the present study was to provide insight into the methods employed to answer the initial problem statement: How much do harmonics influence the losses in an MV distribution system?

In addition to the primary problem statement, two secondary statements also had to be answered during the study:

- What is the potential impact of these losses on planning a distribution network?
- Can the introduction of renewable DG influence the harmonic levels in a distribution network, and could this impact be estimated?

After careful analysis and review of the documented results, this section answers the questions and make appropriate recommendations for future studies and improvements on the present research.

7.1 Network efficiency

To evaluate the influence of harmonics on a distribution network, a detailed analysis was done on active power losses, capacity losses and transformer de-rating.

From this analysis, it was found that the active power loss in cables is independent of the level of harmonic current present in the cable. The active power losses are influenced primarily by the heat in the cable and thus by the amount of power flowing through the cable. The same applies to the additional active power losses incurred in a transformer under non-sinusoidal conditions.

It was found that under certain circumstances, the apparent power capacity of transformers and cables is influenced by the level of harmonic current present in the network, up to 13.5%. This implies that apparent harmonic power does limit the amount of fundamental apparent power that can flow through a transformer or cable.

By applying scatter plots and trend lines to the data of Cable 1, it was possible to establish relationships between the voltage and harmonic current as well as between the harmonic current and capacity loss. These relationships were used successfully to project expected capacity losses in the system for various levels of voltage THD and the associated harmonic current. The same method was used to estimate the THDF for different levels of voltage THD. The success of this

technique was limited to Cable 1, and mainly influenced by a successful relationship established between the parameters.

Despite the shortcomings of the current planning tool, it is possible to develop such a tool for engineers, which could add significant value to the body of knowledge in this field.

7.2 Phase angle

In the phase-angle analysis, two sites were evaluated before and after the installation of solar PV systems, and two control solar PV systems were also monitored. The findings show that due to significant variations in the aggregate phase angle, it is not always possible to obtain valid PAR and prevailing phasors for each phase before and after the installation of solar PV. This is true even though the control PV site delivers near perfect PAR values and valid prevailing phasors for all the phases.

The main reason for this unreliability in the PAR after the solar PV was installed, is the influence it exerts on the direction of the active power flow. During peak production times of the solar PV, power is often fed back into the distribution network, which leads to a 180° change in the phase angle. This effectively creates two prevailing phasors: one for power absorption and one for power generation. In these instances, it is impossible to calculate a valid PAR and prevailing phasor for the entire period.

Despite these inconsistencies, it was found that the arithmetic sum of the pre- and solar phasor provides a reasonably accurate portrayal regarding the eventual state of the actual post-solar phasor. This technique is only applicable if the results indicate usable PAR values.

7.3 Improvements on the study

It is recommended that both the primary and secondary study concentrations should be replicated in a controlled environment. This would make it possible to identify of specific load types or a network configuration that may cause capacity losses within the system. A detailed study is also recommended on the lifespan of equipment used for distribution systems in high-distortion networks. Such a study will support the network planning tool that was developed.

The phase-angle analysis was done on actual sites in an open environment connected to a live distribution network. These external factors could influence the aggregated phase angles and thus the validity of the PAR and values of the prevailing phase angle. It is recommended that the present study should be recreated in a controlled environment for various sources of renewable

DG. The method involving prevailing phasors should be expanded to accommodate the variations in DG production and particularly, network feed-in conditions. This should be considered, especially when significant changes become apparent in the aggregated data for the phase angle.

7.4 Final remarks

In closing, the development of a network plannning tool based on predicted voltage THD was only partially successful. The results of this study indicate definite potential for such a tool “higher-up” in the distribution network. Due to the loss of diversity closer to the loads development of such a toll becomes near impossible.

It has been found that DG could have a potentially significant impact on the harmonic levels in distribution networks. The prevailing phasor method proved to be a useful tool in estimating the impact of DG in the distribution network. With more research and refinement of the calculation methods it will be possible to develop a planning tool in the near future.

These tools will greatly assist planning engineers to successfully design future distribution networks and might even contirbute to technical standards and regulations with regards to DG.

List of references

[1] E. du Preez. (2015, August 2). *Load shedding hits home on SA economy* (Fin24). [Online]. Available: *http://www.fin24.com/Economy/Load-shedding-hits-home-on-SA-economy-20150826*

[2] *Standard voltages, currents and insulation levels for electricity supply*, SABS 1019 Ed. 2.4, 2001

[3] Magnet Communications. (2011). *Magnet professional survey 2011 – engineering/technology vs. total all professionals* (South African edition) [Online]. Available: https://www.ecsa.co.za/news/Surveys%20PDFs/310812_PartnerPres_ECSA.pdf

[4] R. G. Koch and E. Tshwele. *(Mar. 20, 2002). NER directive on power quality: a regulatory framework for the management of power quality in South Africa* (Revision 1.5), NERSA, South Africa. [Online]. Available: http://www.nersa.org.za/Admin/Document/Editor/file/Electricity/Compliance%20Monitoring/PQDirective20March02.pdf .

[5] Department of Minerals and Energy*. (2005). Energy efficiency strategy of the Republic of South Africa.* [Online]. Available: http://www.energy.gov.za/files/esources/electricity/ee_strategy_05.pdf

[6] Eskom. (2016, June 8). *South Africa's new build programme ensuring energy security.* [Online]. Available: http://www.eskom.co.za/news/Pages/Jun8.aspx

[7] T. Bantras, V. Cuk, J. F. G Cobben, W. L. Kling, "Estimation and classification of power losses due to reduced power quality," in *Proc. 2012 IEEE Power Energy Society General Meeting*, San Diego, CA, 2012, pp. 1-6. doi: [10.1109/PESGM.2012.6344944].

[8] F. L. Tofoli, A. S. Morais, C. A. Gallo, S. M. R. Sanhueza, A. de Oliveira, "Analysis of losses in cables and transformers under power quality related issues," in *Applied Power Electronics Conf. Expo. APEC'04*, 2004, pp. 1521-1526. doi: [10.1109/APEC.2004.1296066].

[9] F. G. Cobben, V. Cuk, W. L. Kling, "Increasing energy efficiency by improving power quality," in *Proc. 15th WSEAS Int. Conf. Syst.*, Corfu, Greece, 2011, pp. 298-301.

[10] T. Vinnal, K. Janson, H. Kalda, “Analysis of power consumption and losses in relation to supply voltage quality,” in *Proc. 13th European Conf. Power Electronics Applications*, Barcelona, Spain, 2009, pp. 1-9.

[11] F. C. Pereira, J. C. de Oliveira, P. F. Ribeiro, O. C. N. Souto, A. L. A. Vilaca, “An analysis of costs related to the loss of power quality,” in *Proc. 8th Int. Conf. Harmonics Quality Power*, Athens, Greece, 1998, pp. 777-782 vol. 2. doi: [10.1109/ICHQP.1998.760141]

[12] M. Bollen, S. Ronnberg, J. Meyer, “Emmission of modern sources – tutorial 1 – harmonics in distribution networks”, presented at 23rd Int. Conf. Expo. Electricity Distribution, Lyon, France, 2015. [Online]. Available: www.cired2015.org/files/download/106

[13] *IEEE Standard Definitions for the Measurement of Electric Power Quantities under Sinusoidal, Nonsinusoidal, Balanced, or Unbalanced Conditions,* IEEE Std 1459-2010 (Revision of IEEE Std 1459-2000), 2010.

[14] S. Santoso, M. F. McGranaghan, R. C. Dugan, “Power quality and reliability,” in *Standard Handbook for Electrical Engineers,* 16th ed., New York: McGraw-Hill Professional, 2013.

[15] A. J. Dold *et al. (2003). Electricity supply – quality of supply Part 2: Voltage characteristics, compatibility levels, limits and assessment methods,* NRS 048-2:2003, [Online]. Available: http://www.nersa.org.za/Admin/Document/Editor/file/Electricity/IndustryStandards/NRS048%20part%202.pdf

[16] S. Santoso, M. F. McGranaghan, R. C. Dugan, H. W. Beaty, “Introduction” in *Electrical Power Syst. Quality*. 3rd ed. New York: McGraw Hill, 2012.

[17] M. Yazdani-Asrami, S. M. B. Sadati, E. Samadaei, “Harmonic study for MDF industries,” in *2011 IEEE Applied Power Electronics Colloq*. *(IAPEC)*, Johor Bahru, 2011, pp. 149-154.

[18] Department of Energy. *(2015).* “State of renewable energy in South Africa”, SA Dept. of Energy, Pretoria, State Rep. [Online]. Available: http://www.gov.za/sites/www.gov.za/files/State%20of%20Renewable%20Energy%20in%20South%20Africa_s.pdf

[19] C. Ballack. (2017, March). “PQRS – Power quality and renewable services. Solar PV – October 2016 PQRS.” *Ind. Rep*. [Online]. Available: http://pqrs.co.za/s-a-solar-pv-list-2/

[20] South Africa. 2008. *Consumer Protection Act 68 of 2008.* Pretoria, South Africa. Government printers.

[21] South Africa. 2006. *Electricity Regulation Act 4 of 2006.* Pretoria, South Africa. Government printers.

[22] SABS. (2016). *SABS Webstore.* [Online]. Available: http://store.sabs.co.za/catalog/product/view/_ignore_category/1/id/233928/s/nrs-048-2-2007-ed-3-00/

[23] *Unknown. Electricity supply – quality of supply: Power quality monitoring instruments specification,* SANS 1816, 2013.

[24] *Unknown. Electromagnetic compatibility (EMC), Part 4-30: Testing and measurement techniques – Power quality measurement methods,* SANS 61000-4-30, 2009.

[25] CIGRE TB 261. [Online]. Available: http://www.cigre.org/

[26] *Unknown. Electricity supply – quality of supply: Application guidelines for utilities,* NRS 048-4:, 2009.

[27] *Unknown. Electricity supply – quality of supply Part 2: Voltage characteristics, compatibility levels, limits and assessment methods,* NRS 048-2:2014, unpublished.

[28] *Unknown. Electromagnetic compatibility (EMC) – Part 4-30: Testing and measurement techniques – power quality measurement methods,* IEC 61000-4-30:2015, 2015.

[29] H. Albert et al., “Frequency variations,” in *Handbook of Power Quality*, Chichester, UK: Wiley & Sons, 2008.

[30] I. Wasiak, “Voltage and current unbalance,” in *Handbook of Power Quality*, Chichester, UK: Wiley & Sons, 2008.

[31] B. W. Kennedy *(2000).* “Power quality characteristics,” in *Power Quality Primer*. New York: McGraw-Hill Professional,. [Online]. Available: https://www.fer.unizg.hr/_download/repository/Power_Quality_Primer_-_Barry_W._Kennedy.pdf

[32] A. Baggini and Z. Hanzelka, “Voltage and current harmonics quantities – describing voltage and current distortion,” in *Handbook of Power Quality*, Chichester, UK: Wiley & Sons, 2008.

[33] *IEEE Recommended Practice and Requirements for Harmonic Control in Electric Power Systems.* IEEE Std 519™-2014, 2014.

[34] S. Santoso, M. F. McGranaghan, R. C. Dugan, H. W. Beaty, “Fundamentals of harmonics,” in *Electrical Power Systems Quality,* 3rd ed. New York: McGraw-Hill Professional, 2012.

[35] A. E. Emanuel, “Front matter” in *Power Definitions and The Physical Mechanisms of Power Flow,* UK: Wiley & Sons, 2010.

[36] J. D. Glover et al. *(2015). Power system analysis and design*, 4th ed. Thomson Learning. [Online]. Available: https://docs.google.com/file/d/0B8UzJ3PUAuboZ1EzejFYQVcxYmM/view

[37] Z. Hanzelka, “Voltage dips and short supply interruptions,” in *Handbook of Power Quality,* Chichester, UK: Wiley & Sons, 2008.

[38] *IEEE Recommended Practice for Monitoring Electric Power Quality,* IEEE Std 1159-2009, 2009.

[39] D. Chapman. *(2001). Power quality application guide: the cost of poor power quality*, St Albans: Copper Develop. Inst. [Online]. Available: http://admin.copperalliance.eu/docs/librariesprovider5/power-quality-and-utilisation-guide/21-the-cost-of-poor-power-quality.pdf?sfvrsn=4&sfvrsn=4

[40] S. Santoso, M. F. McGranaghan, R. C. Dugan, H. W. Beaty, “Distributed generation and power quality,” in *Electrical Power Systems Quality,* 2nd ed. New York: McGraw-Hill Professional, 2004.

[41] Unknown. (2017, March). *Independent Power Producer Procurement Programme.* [Online]. Available: https://www.ipp-renewables.co.za

[42] H. B. Puttgen, P. R. Macgregor, F. C. Lambert, “Distributed generation: semantic hype or the dawn of a new era?”, *IEEE Power & Energy Magazine*, vol. 99, pp. 22-29, Jan-Feb 2006.

[43] V. V. Thong and J. Driesen, “Distributed generation and power quality,” in *Handbook of Power Quality*, Chichester, UK: Wiley & Sons, 2008, pp. 114-121.

[44] *IEEE Standard for Interconnecting Distributed Resources Within Electric Power Systems,* 1547.2-2008, 2009.

[45] J. J. Burke and A. L. Clapp, “Power Distribution,” in *Standard Handbook for Electrical Engineers,* 16th ed. New York: McGraw-Hill Professional, 2013.

[46] E. Bunge and M. du Preez. *(2010).* “Eskom methodology for network master plans and network development plans, ref. DGL 34-431.” Eskom, Rep. [Online]. Available: https://www.yumpu.com/en/document/view/37358974/dgl-34-431-distribution-technology-home-eskom

[47] F. Vuinovich, A. Sannino, M. G. Ippolito, G. Morana, “Considering power quality in expansion planning of distribution systems,” in *Power Eng. Society General Meeting Proc.*, Denver, CO, 2004. doi: [10.1109/PES.2004.1372896]

[48] R. A. Kelly, “General information and requirements for medium voltage cable systems,” Eskom Distribution, Rep. DST 34-1175, 2008.

[49] K. D. Patil and W. Z. Gandhare, “Threat of harmonics to underground cables,” in *2012 Students Conf. Eng. Syst.,* 2012, pp. 1-6. doi: [10.1109/SCES.2012.6199082].

[50] R. A. Kelly, “Distribution guide – Parts 1 & 22: Planning guideline for medium voltage underground cable systems,” Eskom Distribution, 2009.

[51] D. Suriyamongkol, “Non-technical losses in electrical power systems,” M.Sc. thesis, Faculty Fritz J. Dolores H. Russ College of Eng. and Techn., Ohio Univ., 2002.

[52] M. S. Rad, M. Kazerooni, M. J. Ghorbany, H. Mokhtari , “Analysis of grid harmonics and their impacts on distribution transformers,” in *2012 IEEE Power and Energy Conf.,* Illinois, 2012, pp. 1-5. doi: [10.1109/PECI.2012.6184593].

[53] F. L. Tofoli, A. S. Morais, C. A. Gallo, S. M. R. Sanhueza, A. de Oliveira, “Analysis of losses in cables and transformers under power quality related issues," *Applied Power Electronics Conf. Expo, APEC'04*, Disneyland Hotel, Anaheim, CA, 2004, pp 1521-1526.

[54] A. Baggini *(2007 Feb).* “Power Quality Tutorial,” *Leonardo Energy* [Online]. Available: http://www.leonardo-energy.info/sites/leonardo-energy/files/root/pdf/2007/PQTutorial.pdf

[55] L. Pei, L. Guodong, X. Yonghai, Y. Shujun , “Methods comparation and simulation of transformer harmonic losses,” *Proc. 2010 Asia-Pacific Power Energy Eng. Conf.*, Chengdu, China, 2010, pp. 1-4. doi: [10.1109/APPEEC.2010.5448566]

[56] J. Desmet. *(2009).* "Power quality application guide: harmonics – selection and rating of transformers," *Copper Develop. Assoc.* [Online]. Available: http://admin.copperalliance.eu/docs/librariesprovider5/power-quality-and-utilisation-guide/352-selection-and-rating-of-transformers.pdf?sfvrsn=4&sfvrsn=4

[57] Copper Alliance. *(2000).* "Harmonics, Transformers and K-Factors." *Publication 144. Copper Develop. Assoc.* [Online]. Available: http://copperalliance.org.uk/docs/librariesprovider5/resources/pub-144-harmonics-transformers-k-factors-pdf.pdf?Status=Master&sfvrsn=0

[58] A. M. Blanco, R. Stiegler, J. Meyer, M. Schwenke, "Implementation of harmonic phase angle measurement for power quality instruments," in *2016 IEEE Int. Workshop Applied Measurements Power Syst. (AMPS)*, Aachen, Germany, 2016, pp. 1-6. doi: [10.1109/AMPS.2016.7602811]

[59] B. Peterson, J. Rens, J. Meyer, G. Botha, J. Desmet, "On the assessment of harmonic emission in distribution networks: opportunity for the prevailing harmonic phase angle," in *2016 IEEE Int. Workshop Applied Measurements Power Syst. (AMPS)*, Aachen, Germany, 2016 pp. 1-6. doi: [10.1109/AMPS.2016.7602809]

[60] Unknown. *Electromagnetic compatibility (EMC) – Part 4-30: Testing and measurement techniques – Power quality measurement methods. IEC 61000-4-30,2015.*

[61] J. Meyer, A. M. Blanco, M. Domagk, P. Schegner, "Assessment of prevailing harmonic current emission in public low voltage network," in *IEEE Trans. Power Del.*, vol. PP, no. 99, pp. 1-1, Dec. 2016. doi: [10.1109/TPWRD.2016.2558187]

[62] J. Meyer, "The impact of modern equipment on harmonic emission in low voltage networks," in *SAIEE Bus. Breakfast Presentation,* Aug 6, 2015, unpublished

[63] J. Meyer, "International survey on prevailing harmonic phase angles in residential low voltage grids (ISOPHARES)." Tech. Universitaet Dresden, Germany, August 2015.

[64] S. Muller, F. Moller, J. Meyer, A. J. Collin, A. Z. Djokic, "Characterisation of harmonic interactions between electric vehicle battery chargers and PV inverters," in*16th Int. Conf. Harmonics Quality Power (ICHQP),* Bucharest, Romania, 2014, pp. 645-649. doi: [10.1109/ICHQP.2014.6842842].

[65] J. Meyer, P. Schegner, K. Heidenreich, "Harmonic summation effects of modern lamp technologies and small electronic household equipment," in *CIRED 21st Int. Conf.*

Electricity Distribution, Frankfurt, Germany, 2011. Paper No 0755. [Online]. Available: http://www.cired.net/publications/cired2011/part1/papers/CIRED2011_0755_final.pdf

[66] A. M. Blanco, E. Gasch, J. Meyer, P. Schegner, "Web-based platform for exchanging harmonic emission measurement of electronic equipment," in *2012 IEEE 15th Int. Conf. Harmonics Quality Power,* Hong Kong, China, 2012, pp. 943-948. doi: [10.1109/ICHQP.2012.6381290].

[67] Tlokwe City Council, "Financial report for the quarter ending 30 June 2016," Potchefstroom: Tlokwe City Council Rep., 2016. [Online]. Available: http://www.potch.co.za/pdf2016/FINANCIAL%20REPORT%20FOR%20THE%20MONTH%20ENDING%203O%20JUNE%202016.pdf

[68] International Energy Agency (IEA), "World Energy Outlook 2015," 2015. 718 pp.

[69] J. Rens, T. van Rooyen, F. de Jager, "Where is the power of IEEE 1459-2010?," in *2014 IEEE Int. Workshop Applied Measurements Power Syst. Proc. (AMPS)*, Aachen, Germany, 2014, pp. 1-6 doi: [10.1109/AMPS.2014.6947698]

[70] J. L. Devore and N. R. Farnum, "Bivariate and multivariate data and distributions," in *Applied Statistics for Engineers and Scientists*, Belmont, UK: Thomson Brooks/Cole, 2005, pp. 99-136.

[71] Microsoft. *(2007). Microsoft office support. Choosing the best trend line for your data.* [Online]. Available: https://support.office.com/en-us/article/Choosing-the-best-trendline-for-your-data-1bb3c9e7-0280-45b5-9ab0-d0c93161daa8

[72] H. W. Beaty and D. G. Fink, "Transformers," in *Standard Handbook for Elect. Engineers*, New York: McGraw-Hill Professional, 2013.

[73] Schneider Electric Industries SAS. *(2011). Oil distribution transformers Minera MP – from 5 to 60 MVA, for 7.2 to 123 kV systems.* [Online]. Available: http://download.schneider-electric.com/files?p_Reference=NRJED311273EN&p_EnDocType=Technical%20leaflet&p_File_Id=101823346&p_File_Name=Minera_MP_123kV_FTR_TechnicalLeaflet_EN.pdf

[74] Schneider Electric Industries SAS. *(2015). Power and distribution transformers Minera – up to 3150kV.* [Online]. Available: http://download.schneider-electric.com/files?p_enDocType=Catalog&p_File_Id=1582036895&p_File_Name=NRJED315628EN_%28web%29.pdf&p_Reference=NRJED315628EN

[75] M. Shareghi, B. T. Phung, M. S. Naderi, T. R. Blackburn, E. Ambikairajah, “Effects of current and voltage harmonics on distribution transformer losses,” in *2012 IEEE Int. Conf. Condition Monitoring Diagnosis,* Bali, Indonesia, 2012, pp. 633-636, doi: [10.1109/CMD.2012.6416225

[76] R. D. Henderson and P. J. Rose, “Harmonics: effect on power quality and transformers,” in *IEEE Trans. Ind. Appl.*, vol. 30, pp. 528-532, May-Jun. 1994. doi: [10.1109/28.293695]

[77] *Unknown (2018, April 30). SEBok, Guide to the Systems Engineering body of knowledge. [Online]. Available: http://www.sebokwiki.org/wiki/System_Verification*

[78] Aberdare Cables. *(2008). Paper insulated cables.* [Online]. Available: http://www.aberdare.co.za/download/map?map=sites/default/aberdare_cables/files/brochures/654/brochures_654.pdf

Appendix A – research outputs

Conference proceedings – Energycon 2016

A paper was submitted for the 2016 IEEE Energycon conference held in Leuven, Belgium titled “Evaluation of system losses due to harmonics in medium voltage distribution networks”. The paper was accepted for publication for the conference proceedings and the work presented during an oral presentation. The paper in its entirety is attached.